NASA CR-165138

Development of Procedures for Calculating Stiffness and Damping of Elastomers in Engineering Applications

Part VII

by
A. Rieger and E. Zorzi

Mechanical Technology Incorporated

Prepared for
National Aeronautics and Space Administration

NASA Lewis Research Center
Contract NAS 3-21623

1 Report No	2 Government Accession No	3 Recipient's Catalog No
CR-165138		

4 Title and Subtitle	5 Report Date
Development of Procedures for Calculating Stiffness and Damping of Elastomers in Engineering Applications - Part VII	September 1980
	6 Performing Organization Code
7 Author(s)	8 Performing Organization Report No
A Rieger and E. Zorzi	80TR63
	10 Work Unit No
9 Performing Organization Name and Address	11 Contract or Grant No
Mechanical Technology Incorporated 968 Albany-Shaker Road Latham, New York 12110	NAS 3-21623
	13 Type of Report and Period Covered
12 Sponsoring Agency Name and Address	Contractor Report
NASA-Lewis Research Center Washington, D.C 20546	14 Sponsoring Agency Code

15 Supplementary Notes

Data Report NASA/Lewis Project Manager - Robert E. Cunningham
Structures and Mechanical Technologies

16 Abstract

An elastomer shear damper has been designed, tested, and compared with the performance of the T-55 power turbine supported on the production-engine roller bearing support The Viton-70 shear damper was designed so that the elastomer damper could be interchanged with the production T-55 power-turbine roller bearing support. The results show that the elastomer sheer dampener permitted stable operation of the power turbine to the maximum operating speed of 16,000 rpm

A Mechanical Design Handbook for Elastomers has been prepared under separate cover, NASA CR-165161 This handbook reviews the state of the art in elastomer-damper technology with particular emphasis on the applications of high-speed rotor dampers.

17 Key Words (Suggested by Author(s))		18 Distribution Statement
Viscoelasticity	Critical Speeds	Unclassified - Unlimited
Elastomers	Resonance Testing	
Dynamic Properties	Gas Turbine	
Damping	Strain Effects	
Vibrations		

19 Security Classif (of this report)	20 Security Classif (of this page)	21 No of Pages	22 Price*
Unclassified	Unclassified		

* For sale by the National Technical Information Service, Springfield Virginia 22161

N80-32718 #

This Page Intentionally Left Blank

TABLE OF CONTENTS

This Page Intentionally Left Blank

LIST OF FIGURES

LIST OF FIGURES

ABSTRACT

An elastomer shear damper has been designed, tested, and compared with the performance of the T-55 power turbine supported on the production-engine roller bearing support. The Viton-70 shear damper was designed so that the elastomer damper could be interchanged with the production T-55 power-turbine roller bearing support. The results show that the elastomer shear damper permitted stable operation of the power turbine to the maximum operating speed of 16,000 rpm.

A Mechanical Design Handbook for Elastomers has been prepared under separate cover; NASA CR-165161. This handbook reviews the state of the art in elastomer-damper technology with particular emphasis on the applications of high-speed rotor dampers.

SUMMARY

A program has been undertaken to: (1) determine the effectivness of an elastomer damper for the T-55 power turbine, and (2) provide an Elastomer Design Handbook as a usable guide for engineers designing elastomer dampers for rotating machinery.

The Viton-70 elastomer damper has clearly shown its viability as an effective shear damper on the T-55 power turbine. The elastomer permitted safe operation of the rotor and excellent control of synchronous and nonsynchronous excitation through all phases of testing to 16,000 rpm. The elastomer damping capabilities were predictable with excellent correlation achieved between test data and analysis, and offered no special problems in this rotor application.

The Mechanical Design Handbook for Elastomers has been completed. Its contents include a review of published work of a similar type covering analysis and experimental investigation of dynamic properties of viscoelastic materials and application of elastomeric dampers for high-speed rotating machinery. It has been published under separate cover; NASA Cr-165161.

This Page Intentionally Left Blank

INTRODUCTION

A shaft operating above one or more of its critical speeds is subjected to any number of destabilizing mechanisms. Splines, material hysteresis, aerodynamic forces, and fluid bearings can and do produce rotor loads which encourage instabilities. With the trend towards higher power density gas turbines and more compact power transmission shafting with long unsupported shafts operating at higher speeds, significant expenditures of manpower and facilities are required to insure safe, reliable operation.

Balancing technology has matured to a point at which the control of synchronous vibrations is generally not an inhibiting factor in rotor design. However, the control of nonsynchronous excitations may require additional consideration, such as the use of a hydraulic mount or squeeze film damper to dissipate undesirable vibration and stabilize the rotor-bearing assembly. It is not surprising then to find squeeze film dampers on a wide variety of high-speed rotating machinery. But a squeeze film damper is expensive in a number of ways. Close tolerance machining, oil supply, and associated plumbing are generally required.

It is desirable to find a convenient dry compact damper which offers a wide range of stiffness and damping characteristics and which can achieve the same control of rotor vibrations offered by the squeeze film. However, factors which have inhibited the growth and application of elastomer dampers are the limited availability of design-oriented data on their dynamic performance, environmental stability, and consistency of predictable performance.

For several years, a program has been pursued at Mechanical Technology Incorporated (MTI) whose intent is to quantify dynamic performance of elastomer dampers, provide the capability to design for desired characteristics, evaluate the effects of environment, demonstrate the effectiveness of elastomers in vibration control, and assess problems which may occur in applications to high-speed rotating machinery. References 1, 2, 3, 4, and 5 document previous work under this MTI program.

A powerful test method for determining elastomer component properties has been developed, entitled "The Base Excitation Resonant Mass Method." This test method employs a large electromagnetic shaker on which test specimens are mounted. The test specimens comprise a one-degree-of-freedom spring-mass-damper system in which a variable mass is excited at or near the resonant frequency of that mass mounted on an elastomeric spring. Transmissibility and phase angle across the elastomer spring are measured and, in the region of resonance, allow accurate determination of both stiffness and damping.

Under past test programs the effects of excitation frequency, specimen geometry, environmental temperature, dynamic strain, and material have been tested. Empirical approaches to predicting component properties have evolved and their effectiveness has been evaluated under both translatory and rotating excitation.

MTI has been actively engaged in evaluating the dynamic properties of elastomers as well as evaluating their potential for practical applications. Past testing permitted a comparison of an elastomeric damper with a squeeze-film damper for a power transmission shaft. This program permitted evaluation of a Viton-70 elastomer shear-mount damper for operation on the power turbine spool of the T-55 gas-turbine engine. The design requirements included consideration of practical hardware constraints typical of a gas-turbine environment. Accordingly, the damper was designed to be active in shear to minimize required radial envelope. This is particularly important as many gas turbines are multishafted and radial design flexibility is inhibited. Also the shear-mount design does accommodate axial thrust loading which may be required for this type of damper application on gas-turbine hardware.

As documented, the shear elastomer damper operated successfully to the maximum operating speed of 16,000 rpm. Orbit control was reliable with no severe or large nonsynchronous components of vibration observed. Thermocouple monitoring of the elastomer recorded no temperature in excess of 65°C for all of the testing performed.

As will be shown, the comparison of analytic prediction and measured data for critical speeds, mode shapes, and logarithmic decrement was excellent. The T-55 power-turbine elastomer damper clearly demonstrated its ability to control rotor vibration for safe, reliable operation.

Past program activities have generated much test data for both generic elastomer materials evaluated, using the "Base Excitation Resonant Mass Method," as well as specific elastomer damper designs for rotor evaluation. As a portion of this program, a handbook has been prepared under separate cover, NASA CR-165161, reviewing the general state of the art in elastomer technology with particular emphasis on high-speed rotor elastomer damper design and applications. The handbook covers the general areas of:

- Viscoelasticity
- Test Methods
- Elastomer Material Properties
- Practical Design Considerations
- Fabrication
- Test Results for Rotor Applications.

This Page Intentionally Left Blank

TEST FACILITY

The test facility used for this program was designed and constructed by MTI under NASA Contract NAS 3-20609. It is a prototype high-speed balancing system for the T-55 and T-53 power turbine. This facility, although available at MTI for this test program, is scheduled for delivery and installation by MTI at the Corpus Christi Army Depot (CCAD) for engine balancing.

The major hardware items of the facility are shown in figures 1, 2, and 3 and consist of the following components:

- Drive Motor
- Gearbox/Belt-Drive Speed Increaser
- Vacuum Chamber
- Hydraulic System
- Lube Oil System
- Auxiliary Control
- Computerized Data Acquisition and Balancing System with CRT Display Terminal

Drive Motor

The balancing system is driven by a 44.7 kW (60 hp) variable-speed AC motor. Motor speed is varied from zero to 1700 rpm by a solid-state Silicon-Controlled Rectifier (SCR) circuitry. The motor is a standard-wound rotor, open drip-proof, thermostat-protected motor. The motor controller consists of solid-state circuitry contained in a NEMA 12 enclosure, and an attached bank of enclosed load resistors. Both the motor and controller are supplied by Control Products Company and are standard products sold by that company.

Speed Increaser

The speed increaser provides an approximate 1:12 increase in speed from the drive motor to the power turbine to be balanced. The speed increaser is composed of two components: a standard belt drive and a high-speed gearbox.

Belt Drive. - The belt drive provides a 1:2 step-up in speed, from the output of the motor to the input of the high-speed gearbox. The belt drive consists of two, side-by-side, 3.31 cm (1.5 in.) wide nonsynchronous belts. A belt guard provides a safe enclosure for the belt drive.

High-Speed Gearbox. - The high-speed gearbox provides a 1:6 step-up in speed, from the belt drive to the power turbine to be balanced. The gearbox, a standard Sunstrand Model LMV 311, is a totally enclosed unit. The low-speed shaft is enclosed by the belt guard described above. A high-speed coupling guard provides a safe enclosure for the output shaft and coupling.

Vacuum Chamber

The vacuum chamber provides a totally enclosed container that insures safe high-speed operation of the power turbine to be balanced. The nominal chamber wall thickness (1.27 cm (0.5 in.) low-carbon steel) is augmented in a plane around the power turbine stages by 2.54 cm (1.0 in.) thick aluminum plate.

Hydraulic System

The hydraulic system raises and lowers the vacuum chamber cover and consists of an off-the-shelf Enerpac Model PEM-1541L electric-motor-powered hydraulic pump with associated cylinders, piping hoses, and safety valves. The hydraulic cylinders are double acting and maintain position when the pump is de-energized. An additional safety feature consists of a support rod that supports the vacuum chamber cover in the open position.

Lube Oil System

The lube oil system supplies lubricating oil to the power-turbine bearings and consists of an off-the-shelf Tri-Line oil system, composed of an electric-motor-powered pump with associated reservoir, piping, fluid controls and safety valves, guards and covers. The oil system also contains a scavenge pump that returns oil from a sump tank inside the vacuum chamber to the reservoir. The reservoir contains a low-level switch which activates an audio and visual alarm at the operator stations.

Vacuum System

The vacuum system evacuates the vacuum chamber. This reduces windage and allows the power turbine to be driven with a low-power drive system. The vacuum system is an off-the-shelf Kinney Model KDH-80, consisting of an electric-motor-powered, dual-piston, high-vacuum pump with associated piping, controls and safety valves, covers and guards. The vacuum system is capable of 3 torr absolute pressure.

Control System

Operator Stations. - The balancing system incorporates two operator stations. One station is located on the balancing stand itself and provides the operator an indication of the mechanical status of the balancing system, as well as the capability to rotate the power turbine at low speeds. The second operator station is located in the control room as part of the computer console. This second station also indicates mechanical status, but allows the operator to run the power turbine at all speeds.

Speed Control. - Power-turbine speed is controlled by a potentiometer. The potentiometer at the balance stand operator station is limited to a maximum of 1000 rpm power-turbine speed. This low-speed capability allows the operator to "slow roll" the power turbine to make certain that all systems are operating properly. The vacuum chamber cover may be open at these low speeds to make visual checks of the power turbine.

The speed control at the control room operator station accommodates all power turbine speeds to 22,000 rpm.

Status Display Panels. - The status display sections of each operator station indicate when the following parameters are out-of-spec.:

- Low Lube Oil Pressure
- High Lube Oil Temperature
- Low Lube Oil Level
- Low Vacuum
- High Vacuum Chamber Air Temperature
- Vacuum Chamber Door Open
- High Vibration.

ROTOR OPTIMIZATION STUDIES

The CCAD balancing rig has successfully operated the T-55 power turbine to the speed of 16,000 rpm on its production hardware bearing supports. Since attaining maximum speed, a number of power turbines have been successfully balanced. Even though minor modifications and adjustments to the balancing rig have altered the response characteristics, the typical response is as shown in figure 4. This figure is a trace of the synchronous response of an acceleration pattern for a 90° pair of probes (vertical and horizontal) at approximately midshaft location. The two dominant features are the peaks at approximately 4,000 and 6,000 rpm. It is significant that the horizontal peak at 4,000 rpm occurs when the vertical probe response is minimum. The vertical peak at 6,000 rpm shows similarity in the lack of response of the horizontal probe. This highly elliptical horizontal orbit, rapidly changing to a dominant vertical ellipse, is typical of characteristics of a retrograde and forward precession encouraged by asymmetric support characteristics. The response of the turbine end at these two speeds is dominant whereas the roller bearing end (cold end) shows little activity, indicating a strong precession of the turbine such as a rigid body conical mode shape. A subsequent set of peaks occurs in the 8,000 to 9,000 rpm speed range, with all probe sets along the shaft indicating motion. The activity at this speed has not been predicted analytically, but is generally subordinate to the two main peaks at 4,000 and 6,000 rpm.

To assess possible rotor modes and the acceptability of the proposed rotor-dynamic model, a small exciter was attached to the CCAD rig to excite the nonrotating T-55 power turbine. Swept sine-wave excitation, figure 5, indicated three possible structural modes:

- 115 Hz bounce mode of turbine
- 210 Hz bending mode of shaft
- 600 Hz bending mode of shaft

Figure 6 indicates the location of these structural frequencies when compared to a tuned analytical model of the T-55 (whirl speed marked by "X" at zero spin speed axis). This analytic model also predicted a first retrograde

(backward) precision turbine conical mode at 4,500 rpm, a first forward mode at 6,000 rpm and a first bending (2nd critical) at 21,000 rpm. The production engine support rigidity needed to provide this model was reasonable, with a roller bearing stiffness of 8.75×10^7 N/m (500,000 lb/in.) and a ball bearing (turbine) pedestal stiffness of 1.40×10^7 N/m (80,000 lb/in.).

Thus it is reasonable to predict the modes at 4,000 to 6,000 rpm yet not encounter the bending mode with operation to 16,000 rpm. Gyroscopic forces affect the speed of the first backward and forward modes so that a minimum of asymmetry is necessary to induce excitation of both the 4,500 rpm and 6,000 rpm peak.

Further evidence that the location of the second mode for baseline T-55 configuration was above the operating speed of 16,000 rpm was obtained from observing the supersynchronous excitation of the small 2/rev component of motion throughout a normal acceleration pattern to maximum speed. The 2/rev peaked while operating at 7,100 rpm indicating the presence of a mode. This is shown as a circled dot located on the dashed line extending from the lower left to the upper middle of figure 6. The dashed line represents a whirl speed of twice the corresponding spin speed (2/rev excitation).

Therefore, from observation of rotor synchronous response, static shaker excitation data and observation of the 2/rev vibration, the rotor-dynamics model (figure 7) was considered as acceptable for analytic examination of possible elastomeric-damper designs.

Previous elastomer material testing of shear specimens (ref. 1) using the MTI Ling Shaker was reviewed for candidate elastomer material selection. From figures 8 through 10, the Viton-70 data at 32°C showed the largest measured value of loss coefficient for the entire range of frequencies. As the loss coefficient is a measurement of the ratio of material damping to stiffness, a higher value of loss coefficient reflects an increased capacity to dissipate energy. Temperature increases make the selection of material for damping somewhat arbitrary as the loss coefficient for all materials, Buna-N, EPDM, Neoprene and Viton ranges between 0.1 and 0.2 (figure 10) for the

entire frequency range. Therefore the decision to use Viton as the damping material was based upon the following:

- Viton-70 shows superior damping properties compared to the other materials tested for 32°C or 66°C operation (figure 8 and 9).
- Viton-70's dissipation characteristics are as good as any of the other materials tested for operation at 88°C (figure 10).
- Viton-70 was previously used as a damper in successful testing of high-speed rotor dampers (references 1 and 5).
- Unused Viton material was available from MTI elastomer test activity under NASA Program NAS 3-18546.

The range of loss coefficient from data obtained from shear specimen shaker testing of Viton-70 (ref.5) indicated that a range of loss coefficients from 0.15 to 0.75 was reasonable for the 0-16,000 rpm operation of the CCAD balancing rig. Accordingly, the T-55 power-turbine rotor-dynamics model was modified to determine the optimal damper design (figures 11 and 12). All system damping was assumed to be due to the elastomer damper, consequently no structural damping was modeled for the turbine or gearbox bearing. The two disk pack couplings were included as elastic elements which offered a minimum of bending rigidity but offered full shear restraint. Figure 7 indicates these couplings at stations 8 and 19 of the rotor model.

From the rotor damper optimization studies (figures 11 and 12) a number of facts surfaced regarding the design of the elastomeric damper:

- The first critical speed is a conical precession of the turbine. The nodal point is extremely close to the elastomer damper test bearing location. Accordingly, the first critical speed offers little damping and is insensitive to the elastomer damper stiffness or damping characteristics.

- The second and third mode shapes offer significant activity of the elastomeric damper. Consequently, the critical speed location and log decrement of those critical speeds are sensitive to damper selection.
- A best, or optimal, tradeoff between the second and third mode is obtained by a Viton-70 elastomeric damper of between 5.25×10^6 - 7.0×10^6 N/m (30,000-40,000 lb/in.)
- It is expected with this value of stiffness, the T-55 rotor mounted on the elastomeric damper would traverse the second critical, which is not within the operational range of the roller-bearing mounted production T-55 configuration (figure 6).
- The range of log decrement expected for the second critical speed is between 0.2 to 1.1 dependent upon the loss coefficient (temperature of operation) for the elastomer damper.

ELASTOMERIC DAMPER DESIGN AND FABRICATION

Past damper designs at MTI have consisted of button configurations. One of the first applications used a power-turbine simulator as shown in figures 13 and 14. In that program (ref. 1), the rig was used to evaluate Polybutadiene and Viton as rotor dampers. The design selected consisted of a cartridge insert (figure 15) which could easily be interchanged to evaluate different materials. This rig proved to be excellent for evaluating synchronous rotor response. A later MTI button design was developed (ref. 5) for elastomeric-damper testing on a power-transmission shaft with an existing squeeze film (figures 16 and 17). The design constraints were different as interchangeability of material was not essential, but interchangeability of operation between the squeeze film or elastomer without shaft disassembly was required for comparison of response characteristics (figures 18 and 19). Both the button design selected for the power-turbine simulator and the button design selected for the power-transmission rig performed very well.

The T-55 design offered uniquely challenging problems. This damper configuration was to be more compatible with actual gas-turbine design technology and constraints. Buttons require additional radial envelope and are not necessarily a desirable geometry for a bearing which may also be required to tolerate thrust. Most gas turbines do not have large amounts of radial envelope available, particularly if they are multishaft turbofan or turboshaft engines, such as the T-55. Design maneuverability and flexibility are generally less restricted in the axial direction. The design must also accommodate possible thrust loading (although the T-55 roller-bearing mount does not take thrust) in combination with radial loads and be capable of controlled preload. These requirements were satisfied by a shear damper configuration.

Figure 20 illustrates the concept used for the elastomer damper mount on the roller-bearing support for the T-55. Two Viton-70 shear rings mounted along the entire circumference satisfied all requirements. Axial preload was accommodated by controlled machining of the outer flanges which attached to the housing by twelve equally spaced socket head cap screws. An overload protector was installed by using an O-ring with a prescribed clearance of

0.254 mm (0.010 in.) to avoid interference with normal operation of the damper. It was designed to be a back-up protection if the shear damper failed. (As all testing proved successful, the O-ring was never required to dampen rotor vibrations.)

To obtain Viton-70 shear damper with the required stiffness, the results of previous MTI shear specimen data were used (ref. 5). Using the values for material properties and characteristic temperatures for Viton-70, and the unified design curves from reference 5, as shown in figure 21, the analysis showed that an ID of 6.98 cm (2.75 in.) and an OD of 9.52 cm (3.75 in.) for 3.175 mm (0.125 in.) thick Viton specimen would produce a stiffness in shear of approximately 6.12×10^6 - 7.0×10^6 N/m (35,000 to 40,000 lb/in.) depending upon strain amplitude experienced in operation.

Construction of the elastomeric damper (figure 22) consisted of machining the aluminum-bearing supports and shear restraining plates, bonding the Viton using REN H998 hardener with a RP-138 resin adhesive, and inserting four thermocouples and two capacitance probes into the assembly. The overload protection O-ring was also attached using the REN adhesive. As shown in figure 23, the damper was split radially into two halves for ease of assembly and replacement with the production T-55 support (which is shown on the left of figure 24). Prior to installation of the damper on the CCAD rig, the elastomer was subjected to static loading for calibration purposes. Figure 25 presents the static data for shear loading on the damper. The static values of stiffness determined were between 6.12×10^6 and 6.47×10^6 N/m (35,000 and 37,000 lb/in.). Static loads were applied and held for up to 5 minutes. No reduction in load was observed on the pressure load gauge (figure 26). For the purpose of shear loading, a mandrel was machined to support the inner block on a "V"-block setup (figure 27). In addition to shear loading, a static compression load was applied to the two 3.175 mm (0.125 in.) elastomer pads. An axial compression stiffness of 1.26×10^7 N/m (72,000 lb/in.) was determined (figure 28). Again holding the load for a period of up to 5 minutes did not produce measurable load relaxation.

TEST SETUP AND SEQUENCE

With fabrication of the elastomer damper complete, the CCAD balancing rig with a balanced T-55 power turbine was made available for this test (figure 29). Figure 30 illustrates the location and designation of the proximity probes which were active throughout this testing. In addition, phase reference was provided through a Spectral Dynamics Fiber-Optics Tachometer. A Digital Equipment Corporation PDP 11/03 microcomputer with 32K of memory, associated A/D conversion and interface components, and a RXV11 dual floppy disk drive for mass storage were used for testing. The AVT52 video terminal provided system input/output to the operator. A monitoring oscilloscope also provided a visual display of incoming signals from the vibration sensors. All data were recorded on a Sangamo Sabre VI recorder. The test sequence was as follows:

- Run T-55 power turbine supported on production roller-bearing mount to 16,000 rpm to establish baseline vibration data
- Remove engine roller-bearing housing and install elastomer-damper housing
- Hook-up thermocouple and capacitance probes #7 and #8 (figure 30)
- Run T-55 on elastomer damper to 16,000 rpm
- Induce imbalance by the following weight sets:
  - 3 gm at 300° on balance plane #2
  - 2 gm at 300° on balance plane #1 and 2 gm at 120° on balance plane #3
  - 3 gm at 300° on balance plane #1
- Run with each weight set to 16,000 rpm
- Remove all imbalance weights and remove elastomer damper; install T-55 roller bearing mount
- Run T-55 to 16,000 rpm and reconfirm baseline performance of rotor.

The installed elastomer damper with the two additional probes (probes #7 and #8) is shown in close-up in figure 31.

This Page Intentionally Left Blank

TEST RESULTS

The baseline run of the T-55 power turbine supported on the production roller-bearing housing showed the characteristics previously noted in figure 4. Figures 32-34 show the runout compensated synchronous response for probes #1 through #6. The data from figure 32, for probes #1 and #2, indicates that the 4,000 and 6,000 rpm peaks are very small. These occur in figure 34 for probes #5 and #6 and are larger amplitudes, indicating strong precessing of the turbine end. The intermediate peaks occur for all probes in the 8,000-9,000 rpm range. It is noteworthy that, for the production T-55 engine power turbine operating in the CCAD rig, no critical speeds have ever been observed above the peaks recorded in the 8,000-9,000 rpm range, regardless of the imbalance conditions. The data obtained from the baseline operation indicates:

- Turbine rigid body processional modes at 4,000 and 6,000 rpm. This compares favorably with the baseline rotor analysis as shown in figure 6. The twin peaks at 4,000 and 6,000 rpm are predictable if slight bearing support asymmetry is present
- Little activity of the roller bearing end occurs at the 4,000 and 6,000 rpm peaks (figure 32)
- The 8,500 to 9,000 rpm peaks are not confirmed analytically but results clearly indicated that motion occurs along the entire shaft (figures 32 through 34).

The T-55 roller-bearing housing was removed and the elastomer-damper housing was installed. Two of the four thermocouples monitored elastomer temperatures whereas the other two thermocouples monitored outer race bearing metal temperatures. The two additional probes (probe #7 and #8 of figure 30) were installed with output recorded on the Sangamo Sabre VI tape recorder. The T-55 power turbine was then operated to 16,000 rpm. The filtered synchronous vibration response obtained is documented in figures 35 through 37. Comparative results from the baseline T-55 run (figures 32 through 34) and the elastomer-damper test results (figures 35 through 37) are provided for probes #1 and #5 in figures 38 and 39. From these results a number of facts emerge:

- Figures 38 and 39 indicate that a substantial reduction in synchronous response occurs for the 6,000 and 8,000 rpm peaks with the elastomer operation
- Figure 39 shows that a reduction in vibration occurs for the entire 16,000 rpm operational range for probe #5
- Probe #1, figure 38, shows a definite peak occurring in the 13,500-14,000 rpm range which has provided an increase in rotor vibration with the elastomer damper operational.

The increase in rotor vibration documented for 13,500 to 14,000 rpm range appeared to indicate a new mode was being traversed. Accordingly, unbalance weights were added to balance planes #1, #2, and #3 (figure 30) to determine the sensitivity of this peak and to determine if this peak was indeed the second bending mode which was predicted to occur in this speed range by the rotor analysis (figures 11 and 12):

- Figures 40 through 42 show response for an imbalance of 3 gm at 300° added to balance plane #1
- Figures 43 through 45 shows response for an imbalance of 2 gm at 300° added to plane #1 and an imbalance of 2 gm at 120° added to balance plane #3
- Figures 46 through 48 shows rotor response for an imbalance of 3 gm at 300° added to plane #2.

These tests, and in particular the response of probes #7 and #8 of figure 48, clearly indicate the presence of a critical speed at 13,500 rpm. Thermocouple readings on the elastomer indicated a temperature of approximately 65°C $\pm$ 5.5°C (150°F $\pm$ 10°F) was typical for operation of this damper. This temperature was consistently within 3°C of the bearing metal temperature. Further, changes in axial thrust load of the thrust bearing did not alter the response characteristic of the rotor significantly.

A comparison of the analysis performed for the elastomer-damper supported system with the measured data provides good correlation for mode shapes (figure 49). The following table provides a comparison of critical speeds and logarithmic decrements for the two criticals observed.

TABLE I

	Analysis		Measured	
	Speed (rpm)	Log Decrement	Speed (rpm)	Log Decrement
First Critical	6,022	0.001	6,007	0.090*
Second Critical	13,535	0.201	13,666	0.206*

*Average value for all data obtained.

There is excellent correlation in whirl speed, but the first critical's log decrement is significantly different in value between test and analysis. This is due to the fact that analysis has indicated a node at the damper for the first critical. Slight changes in rigidity of the shaft or location of roller-bearing support would alter the analytically predicted value of log decrement for the first critical appreciably. Further, consideration of structural damping which occurs at the turbine end bearing (which is heavily participating in the first critical, figure 49) was not included in the anaysis. Therefore, the analysis does not reflect this form of parasitic damping which can greatly effect the log decrement of the first critical speed.

Typical measured response indicated dominant 1/rev excitation of the rotor through the testing with the elastomer damper active. Figure 50 presents a typical frequency spectrum from probe #5 at 13,000 rpm. As shown, relatively minor subsynchronous and supersynchronous excitations were experienced and the operation of the T-55 power turbine was as predicted throughout the entire test phase.

This Page Intentionally Left Blank

CONCLUSIONS/RECOMMENDATIONS

- The shear elastomeric damper designed for the T-55 power turbine has proved to be a predictable, reliable dry compact rotor damper.
- Excellent correlation of analysis with experimental data was obtained for this series of tests for both critical speeds traversed.
- The elastomeric damper was easily installed and presented no special problems for operation to 16,000 rpm on the T-55 power turbine.
- Thermocouples indicated that the temperature of the shear damper remained in the vicinity of 65°C for all testing.
- Elastomer dampers have proved to be a viable damper that can easily be incorporated in any existing gas-turbine engine design with minimum modifications to existing hardware design and at low cost.
- Effort should be made to find an elastomer that can sustain a temperature higher than 200°C, rotor transients and the effects of oil and fuel contamination.
- A compact low-cost elastomer configuration, suitable to high-technology advanced rotor designs, should be evaluated on engines such as for the cruise missile mission.

This Page Intentionally Left Blank

APPENDIX A

FIGURES

This Page Intentionally Left Blank

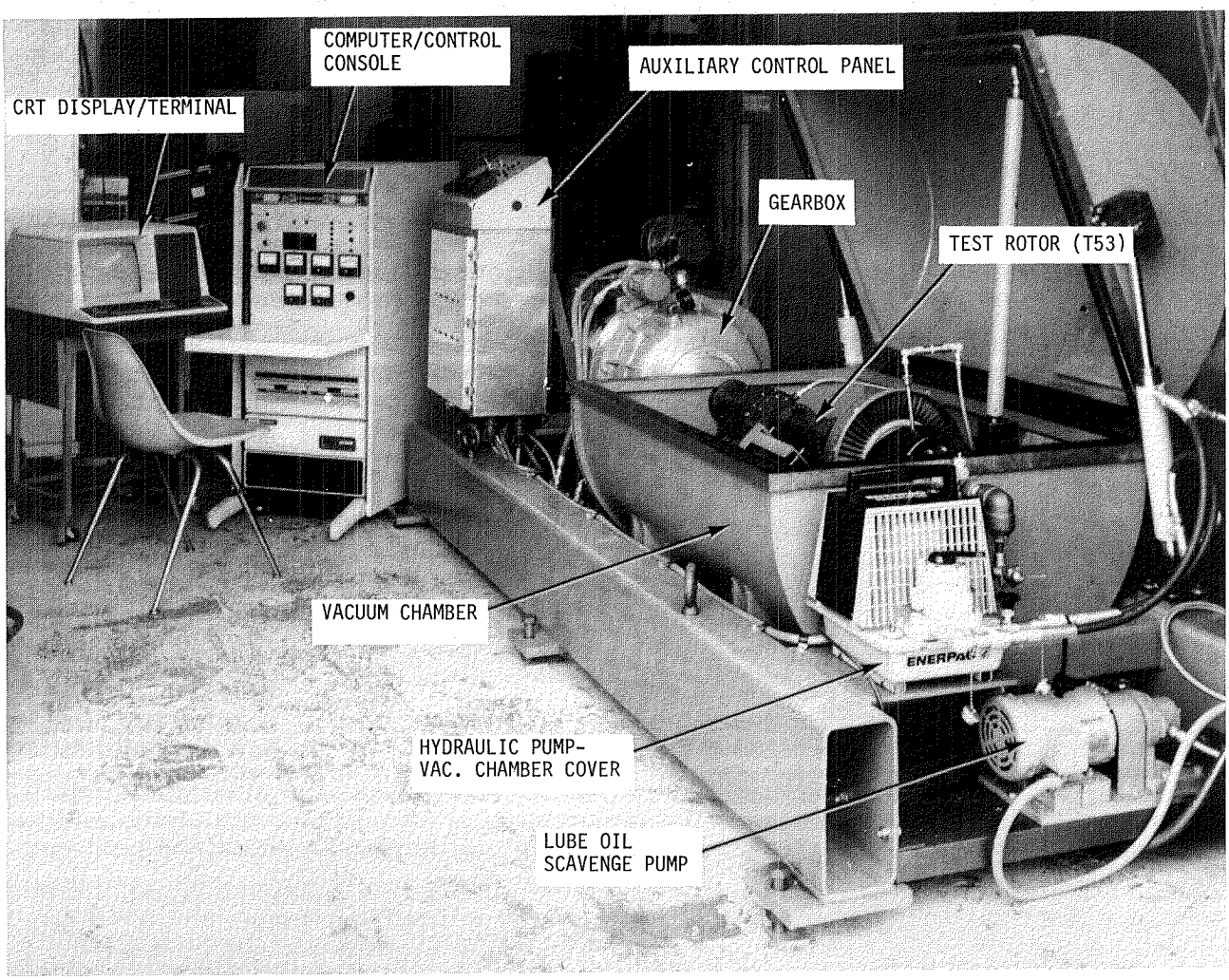

Fig. 1 CCAD Balancing Rig

MTI-19257

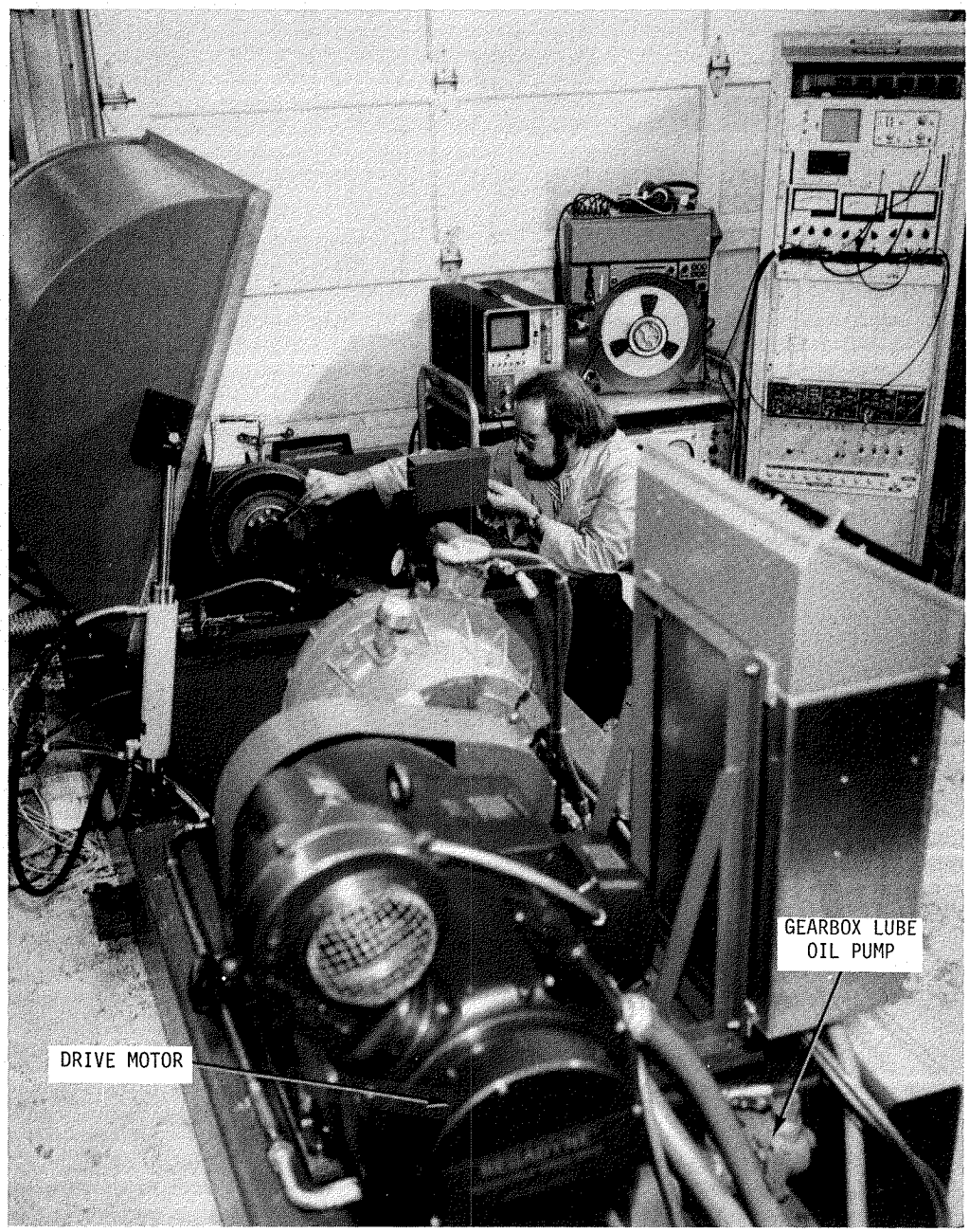

Fig. 2 CCAD Balancing Rig - Vacuum Chamber

Fig. 3 CCAD Balancing Rig - Data Acquisition and Balancing System

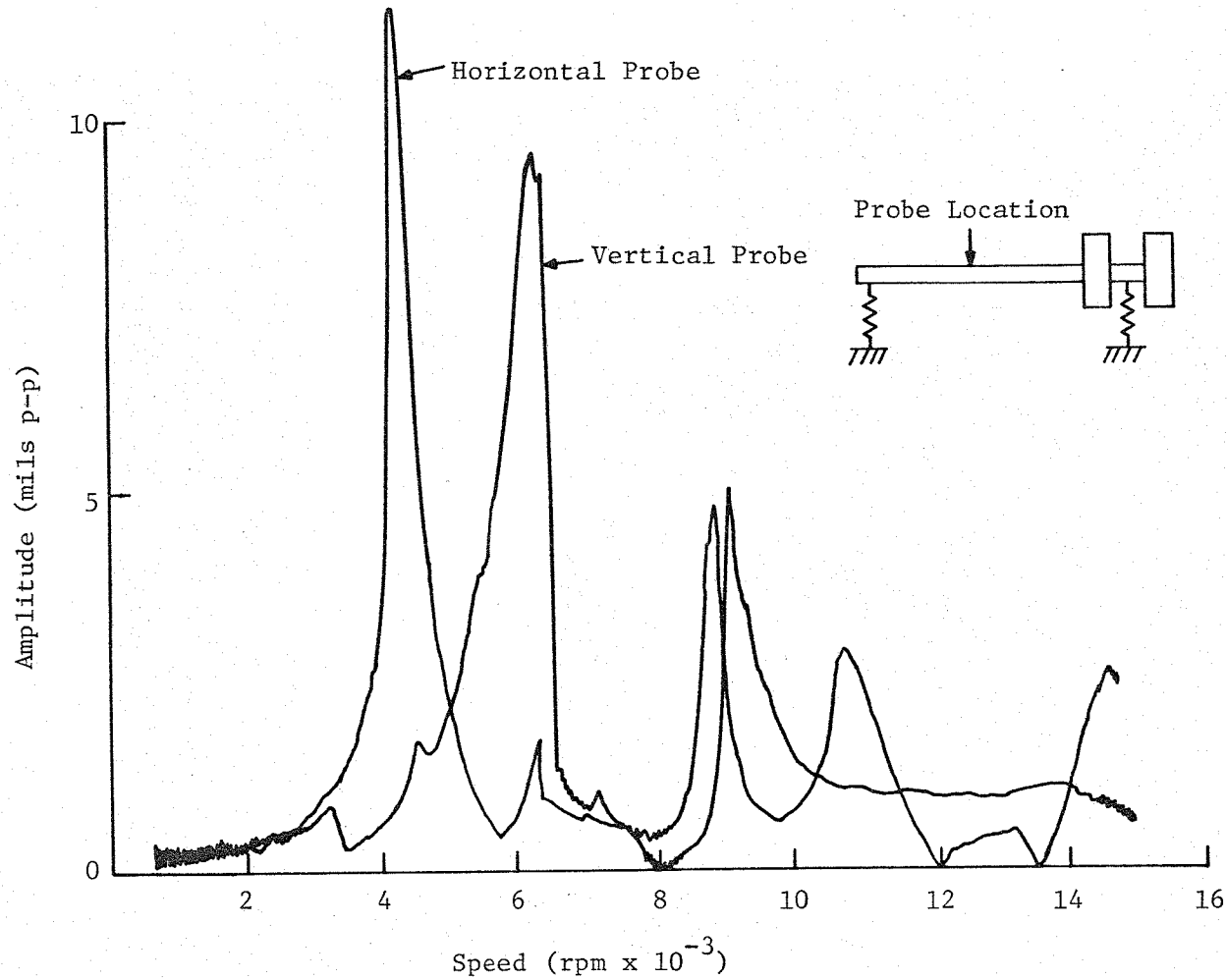

Fig. 4 Synchronous Response of T-55 on CCAD Rig

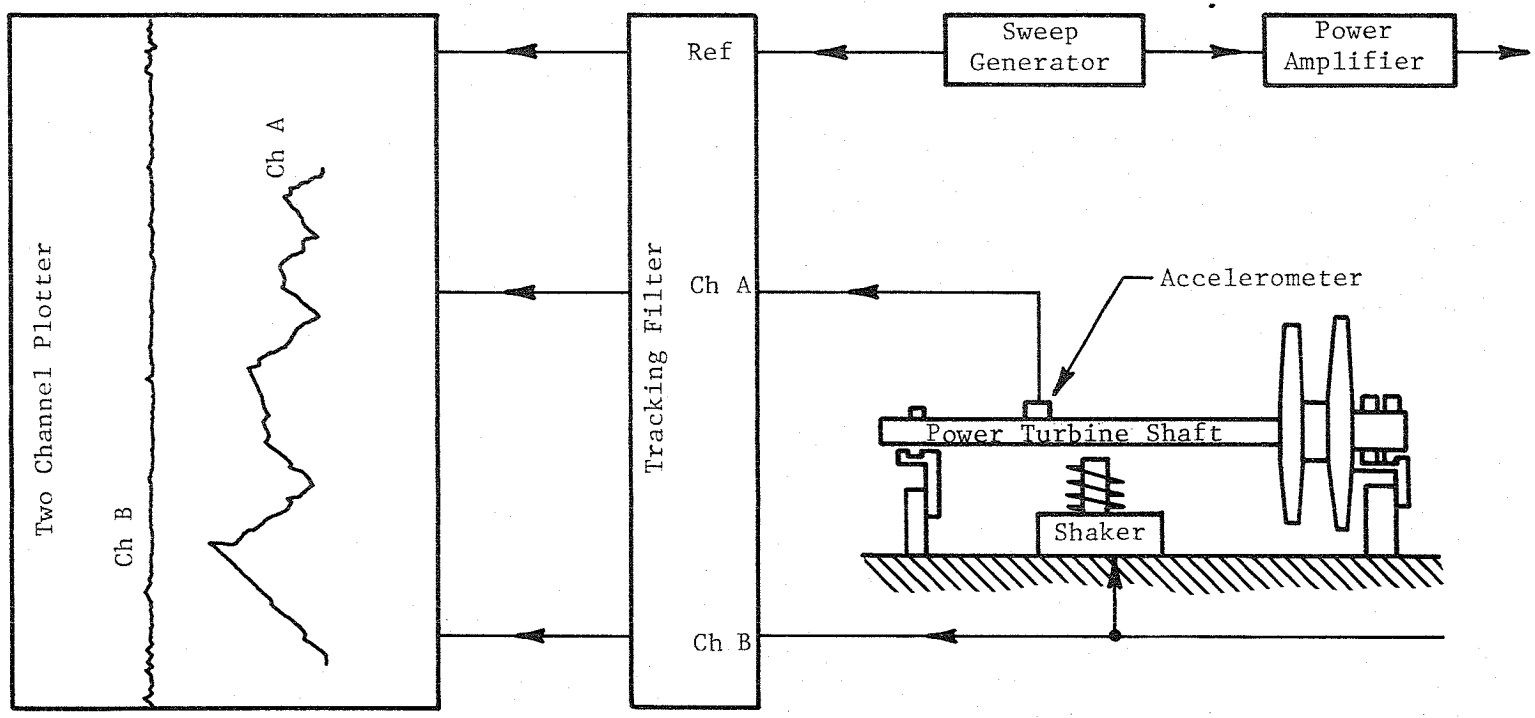

Fig. 5 Sine Swept Shaker Test Set-Up

802738

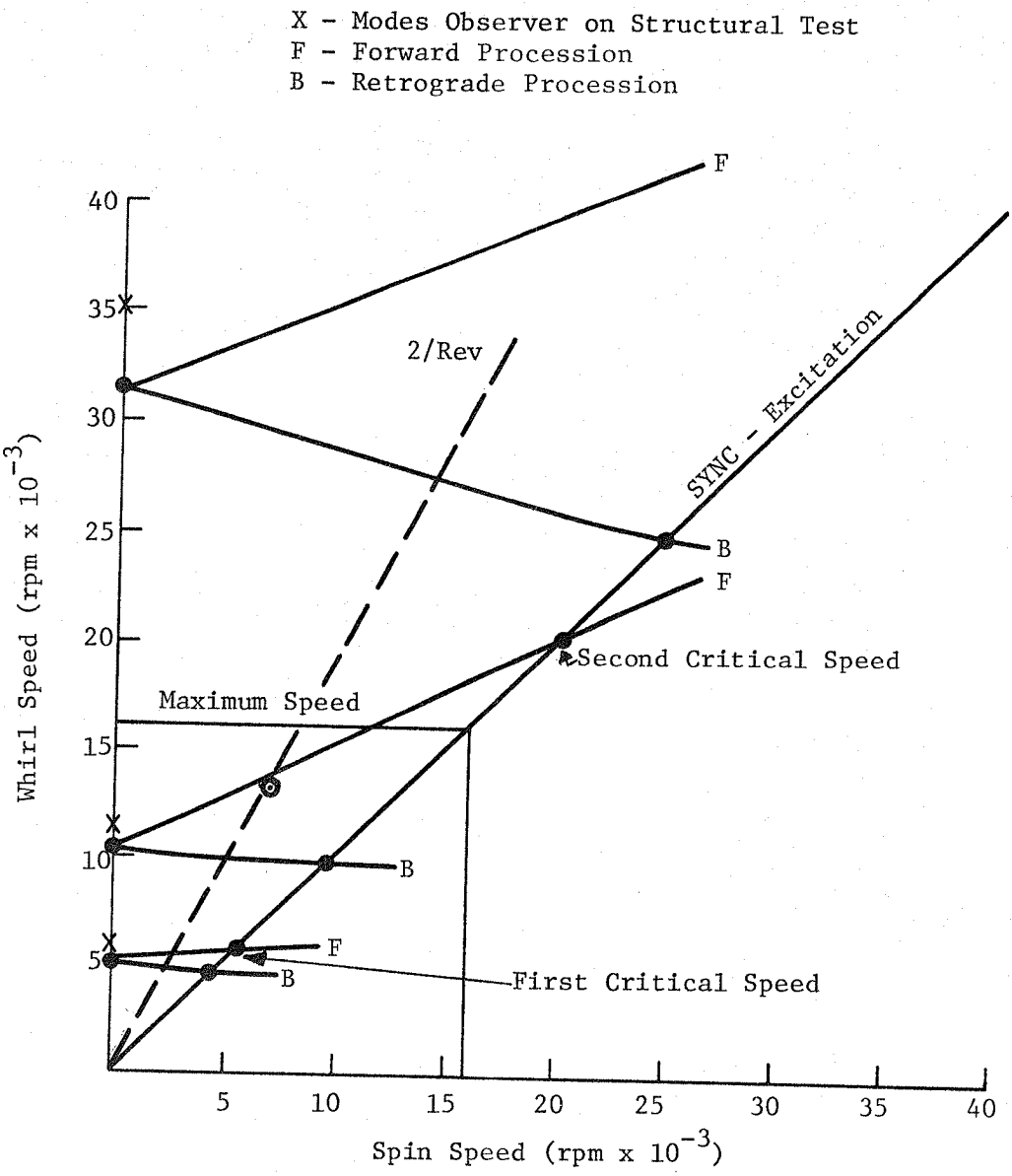

Fig. 6 Whirl Speed versus Spin Speed

80829

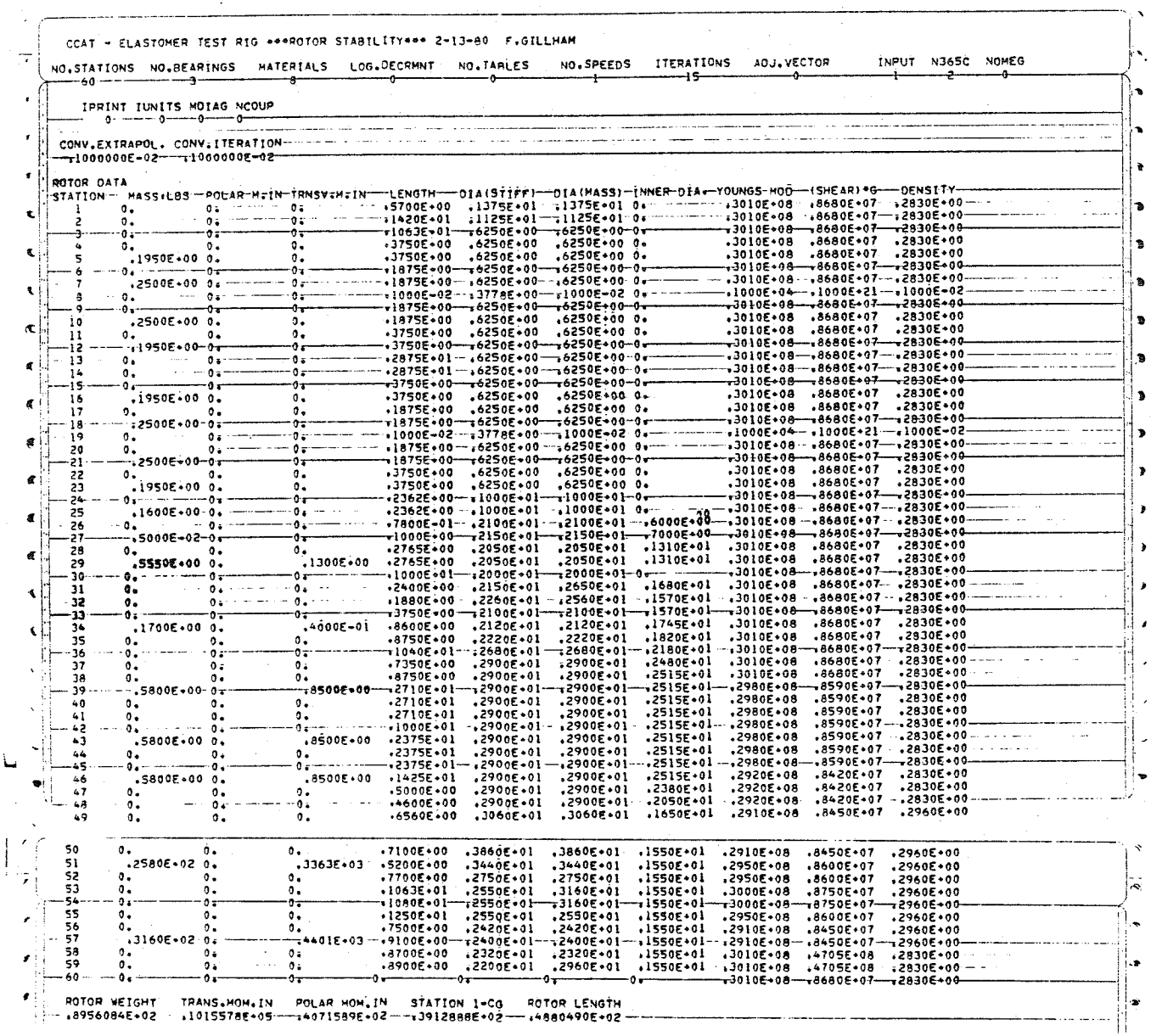

CCAT - ELASTOMER TEST RIG ***ROTOR STABILITY*** 2-13-80 F.GILLHAM

NO.STATIONS	NO.BEARINGS	MATERIALS	LOG.DECRMNT	NO.TABLES	NO.SPEEDS	ITERATIONS	ADJ.VECTOR	INPUT	N365C	NOMEG
60	3	8	0	0	1	15	0	1	2	0

IPRINT	IUNITS	MDIAG	NCOUP
0	0	0	0

CONV.EXTRAPOL.	CONV.ITERATION
.1000000E-02	.1000000E-02

ROTOR DATA

STATION	MASS.LBS	POLAR-M.IN	TRNSV.M.IN	LENGTH	DIA(STIFF)	DIA(MASS)	INNER DIA	YOUNGS MOD	(SHEAR)*G	DENSITY
1	0.	0.	0.	.5700E+00	.1375E+01	.1375E+01	0.	.3010E+08	.8680E+07	.2830E+00
2	0.	0.	0.	.1420E+01	.1125E+01	.1125E+01	0.	.3010E+08	.8680E+07	.2830E+00
3	0.	0.	0.	.1063E+01	.6250E+00	.6250E+00	0.	.3010E+08	.8680E+07	.2830E+00
4	0.	0.	0.	.3750E+00	.6250E+00	.6250E+00	0.	.3010E+08	.8680E+07	.2830E+00
5	.1950E+00	0.	0.	.3750E+00	.6250E+00	.6250E+00	0.	.3010E+08	.8680E+07	.2830E+00
6	0.	0.	0.	.1875E+00	.6250E+00	.6250E+00	0.	.3010E+08	.8680E+07	.2830E+00
7	.2500E+00	0.	0.	.1875E+00	.6250E+00	.6250E+00	0.	.3010E+08	.8680E+07	.2830E+00
8	0.	0.	0.	.1000E-02	.3778E+00	.1000E-02	0.	.1000E+04	.1000E+21	.1000E-02
9	0.	0.	0.	.1875E+00	.6250E+00	.6250E+00	0.	.3010E+08	.8680E+07	.2830E+00
10	.2500E+00	0.	0.	.1875E+00	.6250E+00	.6250E+00	0.	.3010E+08	.8680E+07	.2830E+00
11	0.	0.	0.	.3750E+00	.6250E+00	.6250E+00	0.	.3010E+08	.8680E+07	.2830E+00
12	.1950E+00	0.	0.	.3750E+00	.6250E+00	.6250E+00	0.	.3010E+08	.8680E+07	.2830E+00
13	0.	0.	0.	.2875E+01	.6250E+00	.6250E+00	0.	.3010E+08	.8680E+07	.2830E+00
14	0.	0.	0.	.2875E+01	.6250E+00	.6250E+00	0.	.3010E+08	.8680E+07	.2830E+00
15	0.	0.	0.	.3750E+00	.6250E+00	.6250E+00	0.	.3010E+08	.8680E+07	.2830E+00
16	.1950E+00	0.	0.	.3750E+00	.6250E+00	.6250E+00	0.	.3010E+08	.8680E+07	.2830E+00
17	0.	0.	0.	.1875E+00	.6250E+00	.6250E+00	0.	.3010E+08	.8680E+07	.2830E+00
18	.2500E+00	0.	0.	.1875E+00	.6250E+00	.6250E+00	0.	.3010E+08	.8680E+07	.2830E+00
19	0.	0.	0.	.1000E-02	.3778E+00	.1000E-02	0.	.1000E+04	.1000E+21	.1000E-02
20	0.	0.	0.	.1875E+00	.6250E+00	.6250E+00	0.	.3010E+08	.8680E+07	.2830E+00
21	.2500E+00	0.	0.	.1875E+00	.6250E+00	.6250E+00	0.	.3010E+08	.8680E+07	.2830E+00
22	0.	0.	0.	.3750E+00	.6250E+00	.6250E+00	0.	.3010E+08	.8680E+07	.2830E+00
23	.1950E+00	0.	0.	.3750E+00	.6250E+00	.6250E+00	0.	.3010E+08	.8680E+07	.2830E+00
24	0.	0.	0.	.2362E+00	.1000E+01	.1000E+01	0.	.3010E+08	.8680E+07	.2830E+00
25	.1600E+00	0.	0.	.2362E+00	.1000E+01	.1000E+01	0.	.3010E+08	.8680E+07	.2830E+00
26	0.	0.	0.	.7800E-01	.2100E+01	.2100E+01	.6000E+00	.3010E+08	.8680E+07	.2830E+00
27	.5000E-02	0.	0.	.1000E+00	.2150E+01	.2150E+01	.7000E+00	.3010E+08	.8680E+07	.2830E+00
28	0.	0.	0.	.2765E+00	.2050E+01	.2050E+01	.1310E+01	.3010E+08	.8680E+07	.2830E+00
29	.5550E+00	0.	.1300E+00	.2765E+00	.2050E+01	.2050E+01	.1310E+01	.3010E+08	.8680E+07	.2830E+00
30	0.	0.	0.	.1000E+01	.2000E+01	.2000E+01	0.	.3010E+08	.8680E+07	.2830E+00
31	0.	0.	0.	.2400E+00	.2150E+01	.2650E+01	.1680E+01	.3010E+08	.8680E+07	.2830E+00
32	0.	0.	0.	.1880E+00	.2260E+01	.2560E+01	.1570E+01	.3010E+08	.8680E+07	.2830E+00
33	0.	0.	0.	.3750E+00	.2100E+01	.2100E+01	.1570E+01	.3010E+08	.8680E+07	.2830E+00
34	.1700E+00	0.	.4000E-01	.8600E+00	.2120E+01	.2120E+01	.1745E+01	.3010E+08	.8680E+07	.2830E+00
35	0.	0.	0.	.8750E+00	.2220E+01	.2220E+01	.1820E+01	.3010E+08	.8680E+07	.2830E+00
36	0.	0.	0.	.1040E+01	.2680E+01	.2680E+01	.2180E+01	.3010E+08	.8680E+07	.2830E+00
37	0.	0.	0.	.7350E+00	.2900E+01	.2900E+01	.2480E+01	.3010E+08	.8680E+07	.2830E+00
38	0.	0.	0.	.8750E+00	.2900E+01	.2900E+01	.2515E+01	.3010E+08	.8680E+07	.2830E+00
39	.5800E+00	0.	.8500E+00	.2710E+01	.2900E+01	.2900E+01	.2515E+01	.2980E+08	.8590E+07	.2830E+00
40	0.	0.	0.	.2710E+01	.2900E+01	.2900E+01	.2515E+01	.2980E+08	.8590E+07	.2830E+00
41	0.	0.	0.	.2710E+01	.2900E+01	.2900E+01	.2515E+01	.2980E+08	.8590E+07	.2830E+00
42	0.	0.	0.	.1000E+01	.2900E+01	.2900E+01	.2515E+01	.2980E+08	.8590E+07	.2830E+00
43	.5800E+00	0.	.8500E+00	.2375E+01	.2900E+01	.2900E+01	.2515E+01	.2980E+08	.8590E+07	.2830E+00
44	0.	0.	0.	.2375E+01	.2900E+01	.2900E+01	.2515E+01	.2980E+08	.8590E+07	.2830E+00
45	0.	0.	0.	.2375E+01	.2900E+01	.2900E+01	.2515E+01	.2980E+08	.8590E+07	.2830E+00
46	.5800E+00	0.	.8500E+00	.1425E+01	.2900E+01	.2900E+01	.2515E+01	.2920E+08	.8420E+07	.2830E+00
47	0.	0.	0.	.5000E+00	.2900E+01	.2900E+01	.2380E+01	.2920E+08	.8420E+07	.2830E+00
48	0.	0.	0.	.4600E+00	.2900E+01	.2900E+01	.2050E+01	.2920E+08	.8420E+07	.2830E+00
49	0.	0.	0.	.6560E+00	.3060E+01	.3060E+01	.1650E+01	.2910E+08	.8450E+07	.2960E+00
50	0.	0.	0.	.7100E+00	.3860E+01	.3860E+01	.1550E+01	.2910E+08	.8450E+07	.2960E+00
51	.2580E+02	0.	.3363E+03	.5200E+00	.3440E+01	.3440E+01	.1550E+01	.2950E+08	.8600E+07	.2960E+00
52	0.	0.	0.	.7700E+00	.2750E+01	.2750E+01	.1550E+01	.2950E+08	.8600E+07	.2960E+00
53	0.	0.	0.	.1063E+01	.2550E+01	.3160E+01	.1550E+01	.3000E+08	.8750E+07	.2960E+00
54	0.	0.	0.	.1080E+01	.2550E+01	.3160E+01	.1550E+01	.3000E+08	.8750E+07	.2960E+00
55	0.	0.	0.	.1250E+01	.2550E+01	.2550E+01	.1550E+01	.2950E+08	.8600E+07	.2960E+00
56	0.	0.	0.	.7500E+00	.2420E+01	.2420E+01	.1550E+01	.2910E+08	.8450E+07	.2960E+00
57	.3160E+02	0.	.4401E+03	.9100E+00	.2400E+01	.2400E+01	.1550E+01	.2910E+08	.8450E+07	.2960E+00
58	0.	0.	0.	.8700E+00	.2320E+01	.2320E+01	.1550E+01	.3010E+08	.4705E+08	.2830E+00
59	0.	0.	0.	.8900E+00	.2200E+01	.2960E+01	.1550E+01	.3010E+08	.4705E+08	.2830E+00
60	0.	0.	0.	0.	0.	0.	0.	.3010E+08	.8680E+07	.2830E+00

ROTOR WEIGHT	TRANS.MOM.IN	POLAR MOM.IN	STATION 1=CG	ROTOR LENGTH
.8956084E+02	.1015578E+05	.4071589E+02	.3912888E+02	.4880490E+02

Fig. 7 Rotor Dynamics Model Details

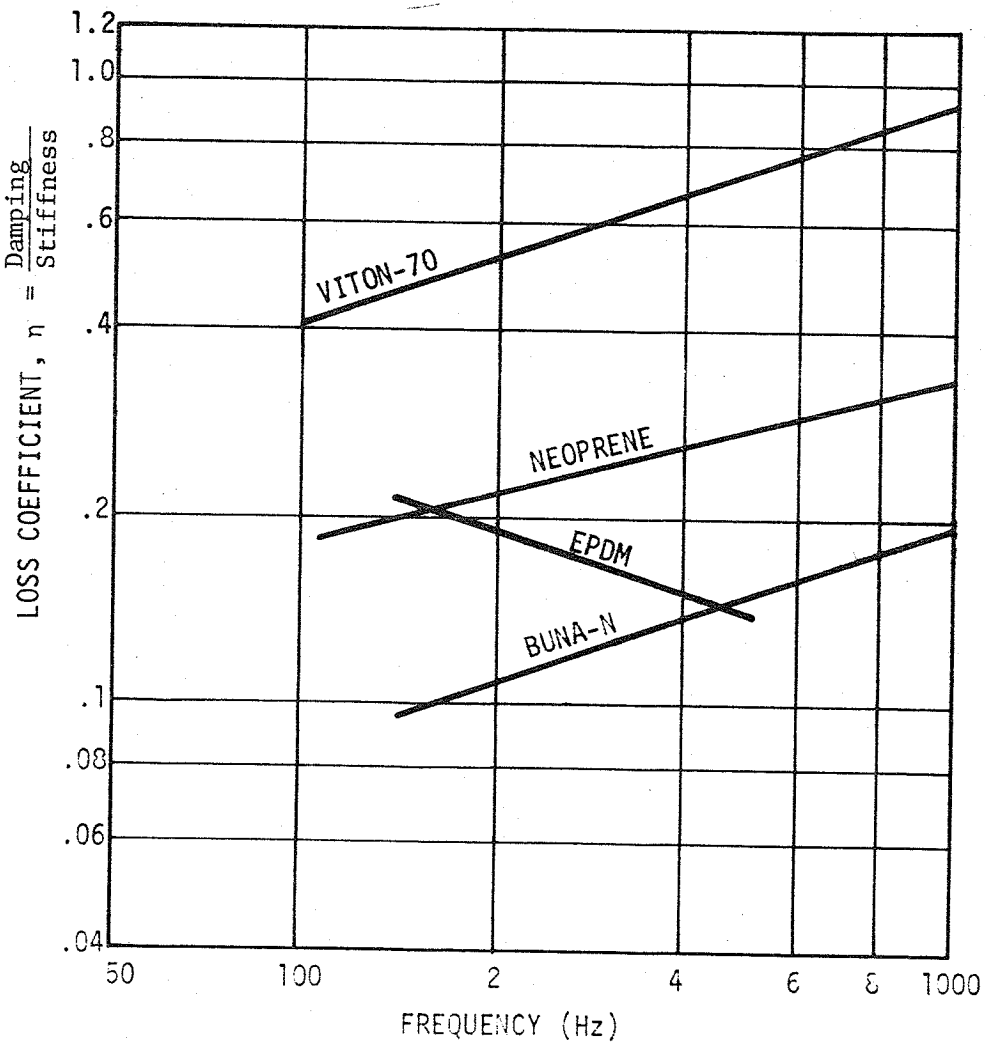

Fig. 8 Shear Specimen Data at 32°C

793479

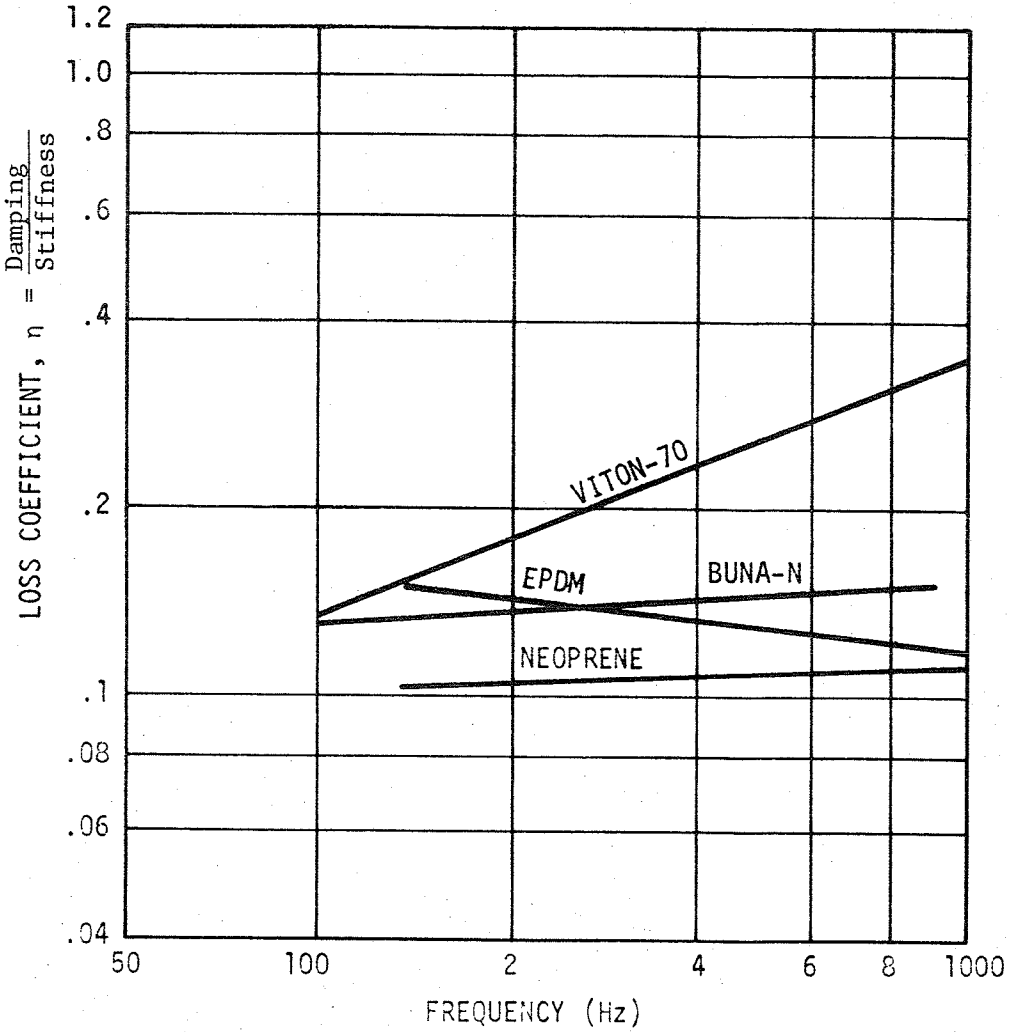

Fig. 9 Shear Specimen Data at 66°C

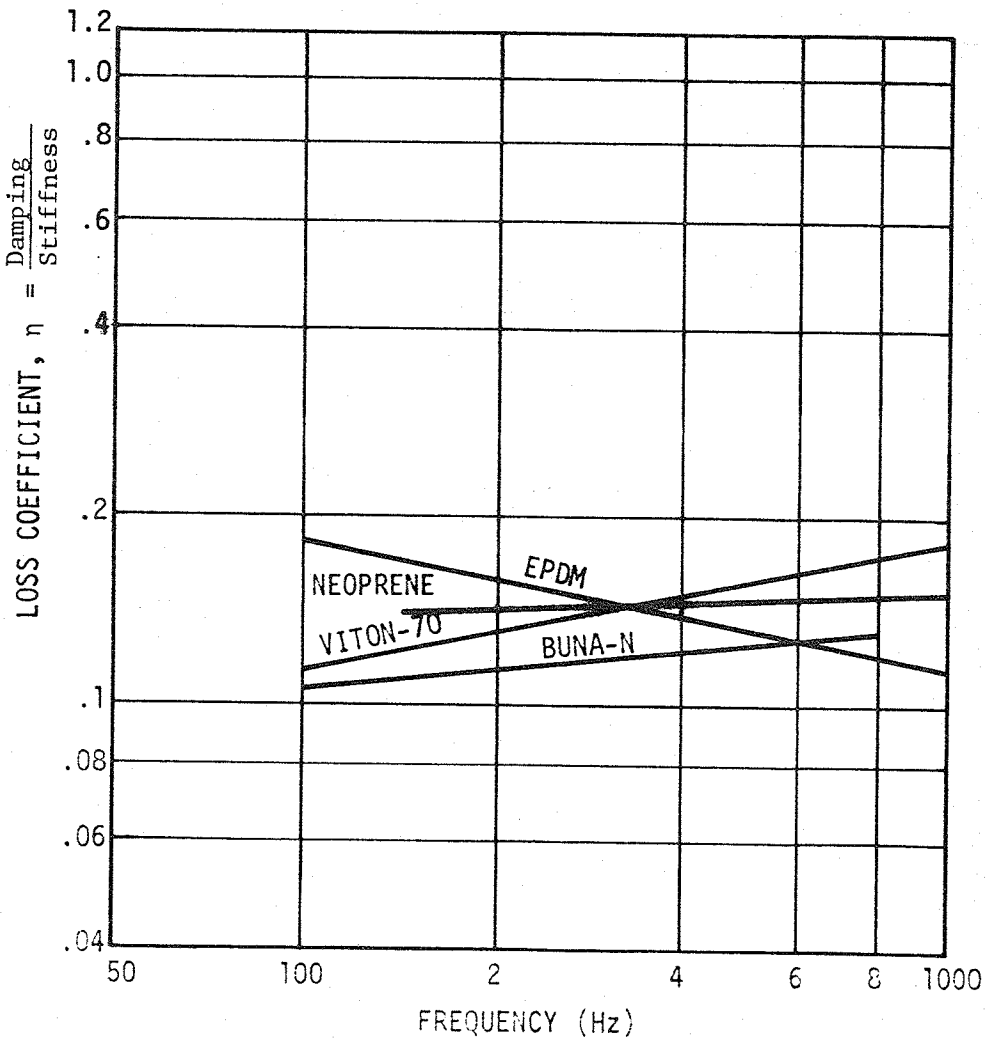

Fig. 10 Shear Specimen Data at 80°C

793477

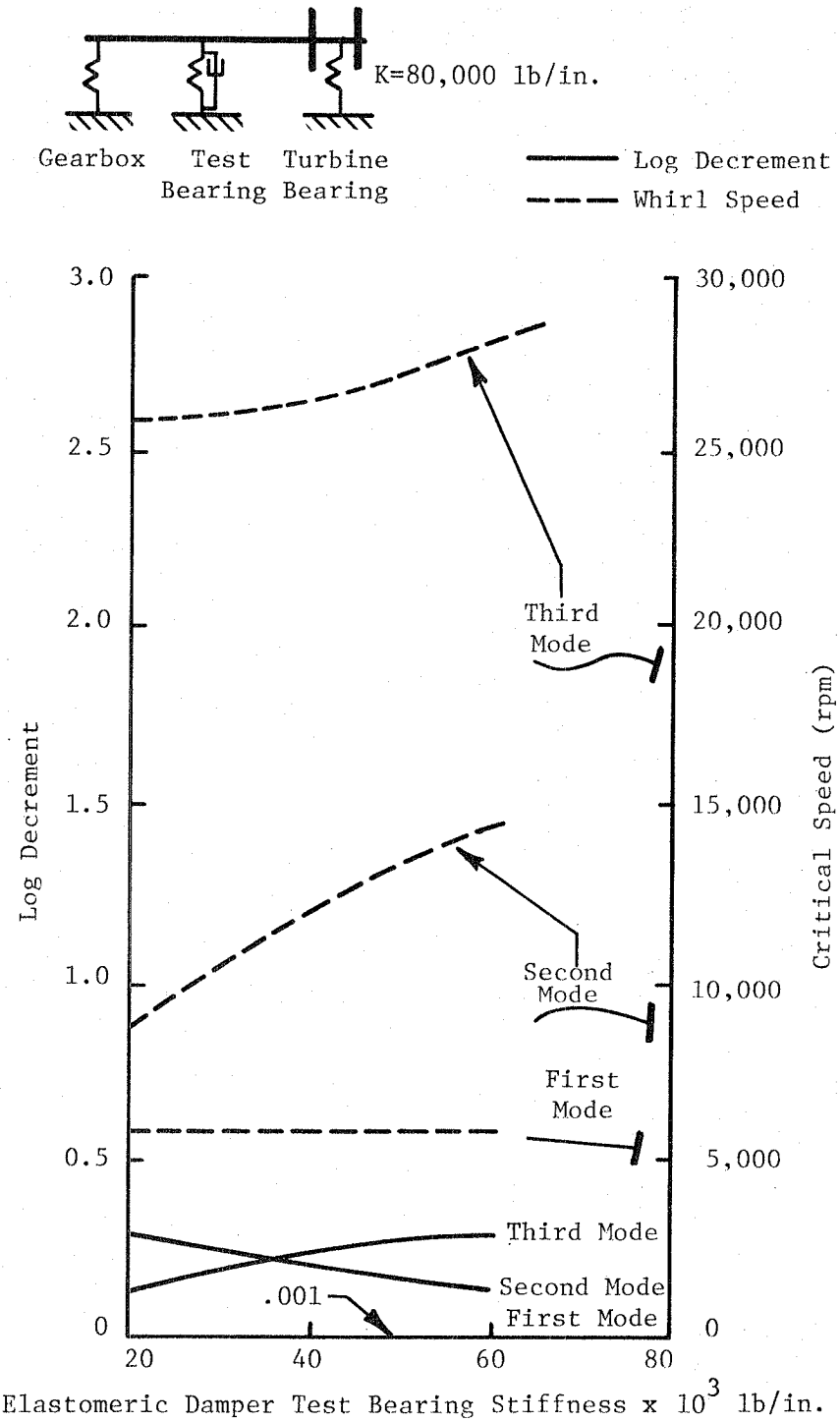

Fig. 11 T-55 Power Turbine - Critical Speeds and Log Decrement vs. Bearing Stiffness for Viton-70 Elastomeric Damper (η = 0.15)

802332

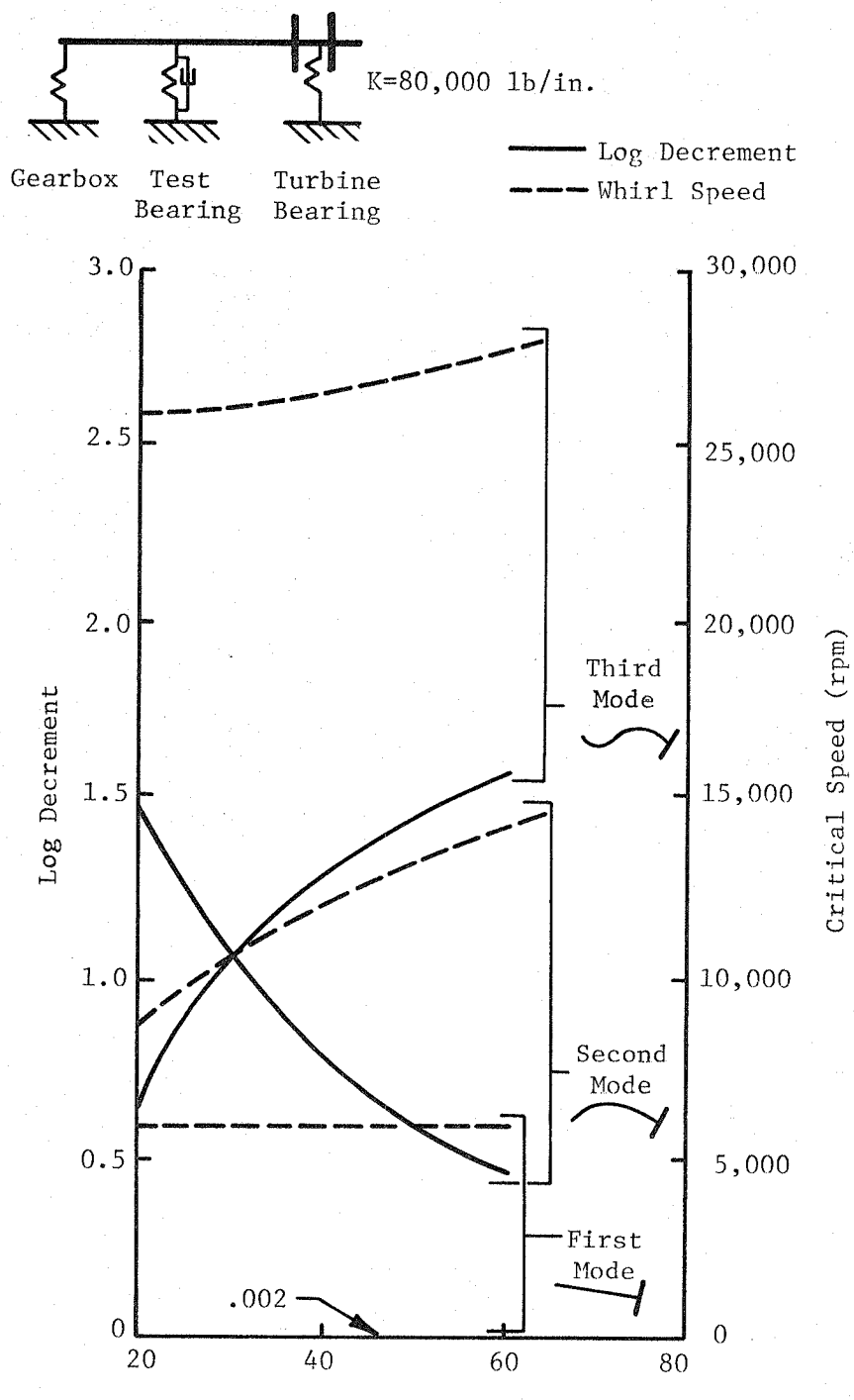

Fig. 12 T-55 Power Turbine - Critical Speeds and Log Decrement vs. Bearing Stiffness for Viton-70 Elastomeric Damper (η = 0.75)

802352

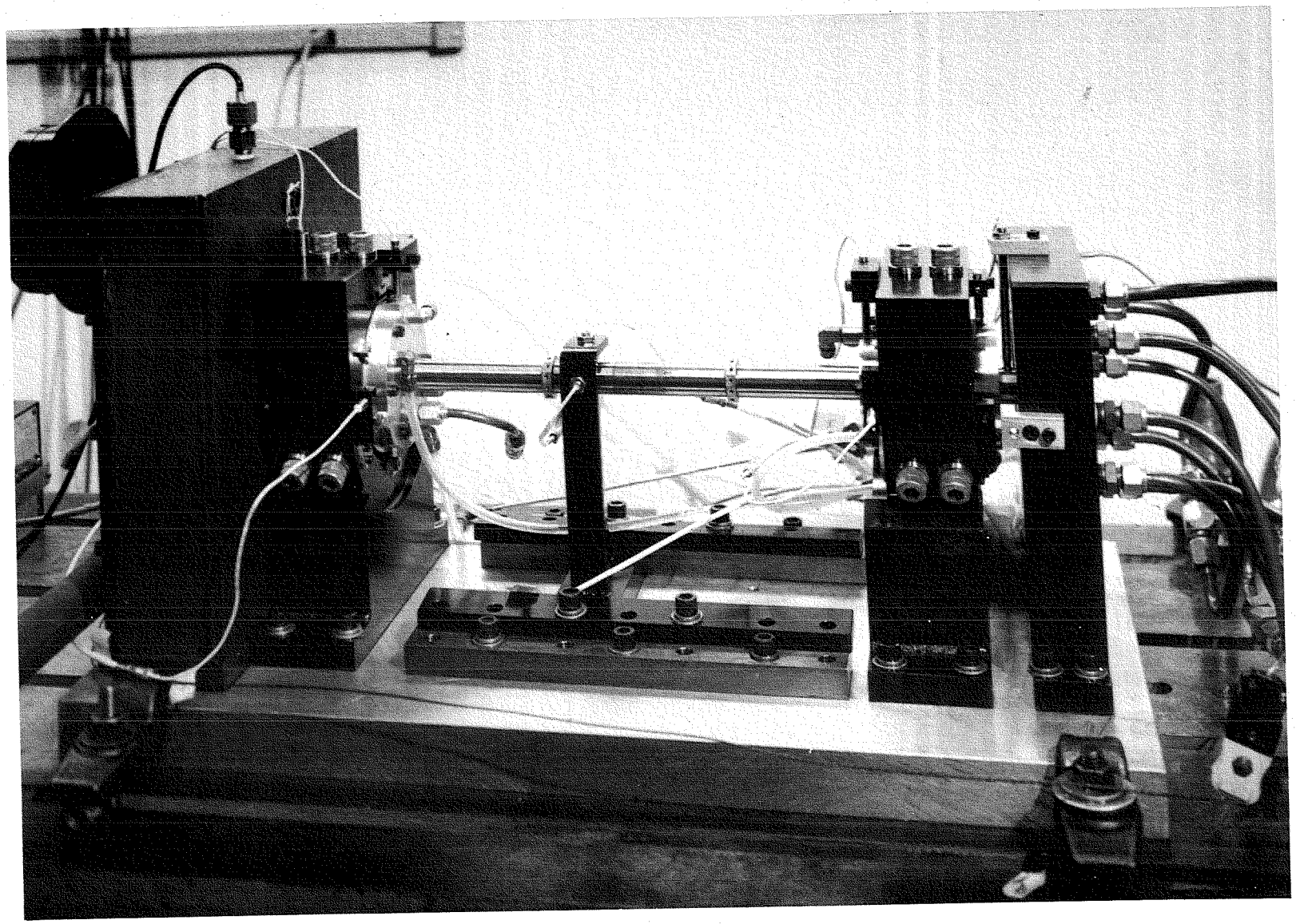

Fig. 13 Assembled Test Rig

MTI-18370

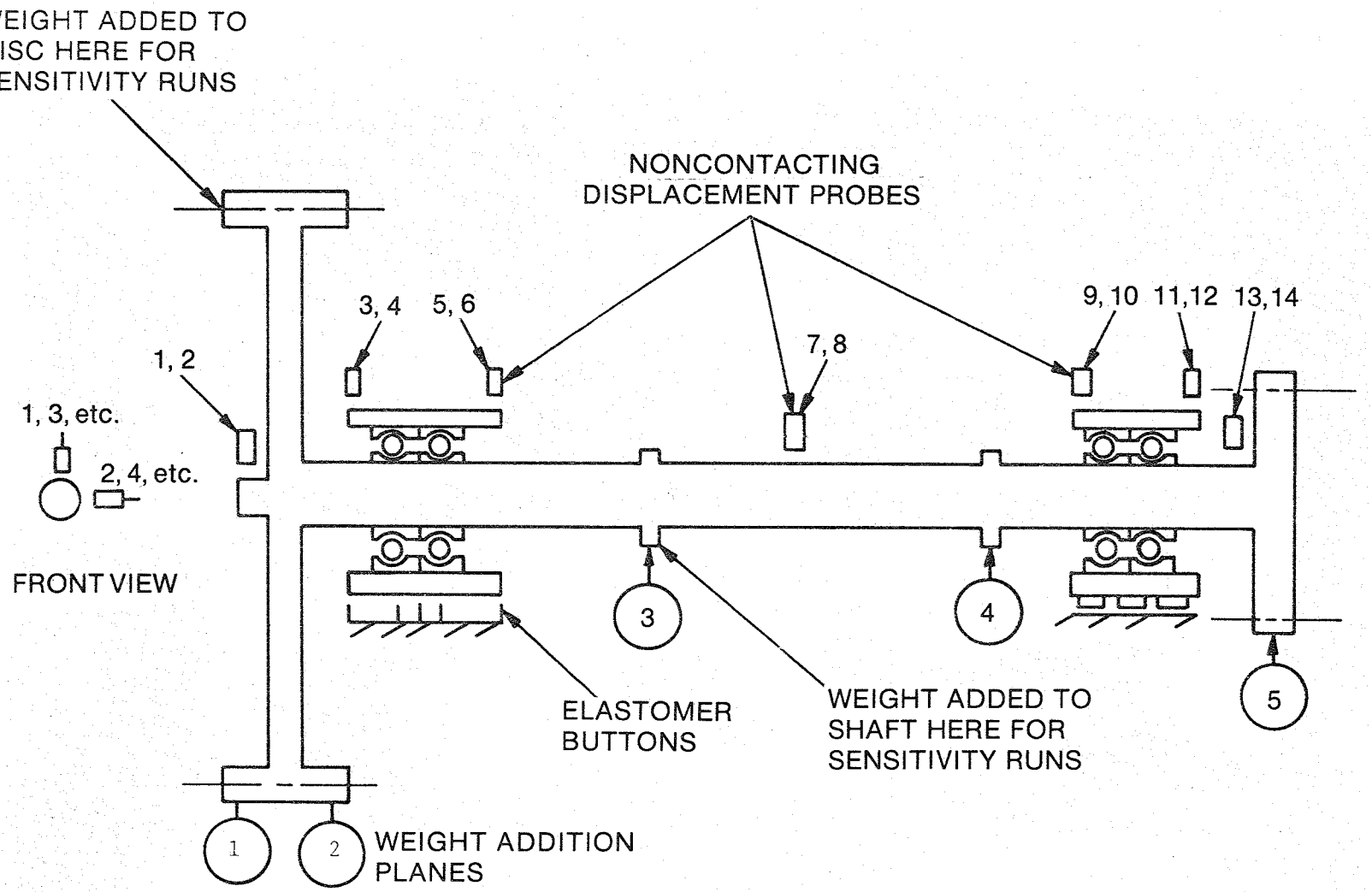

Fig. 14 Schematic Drawing of Rotor System Showing Weight Addition Planes and Displacement Probe Locations

791195-I

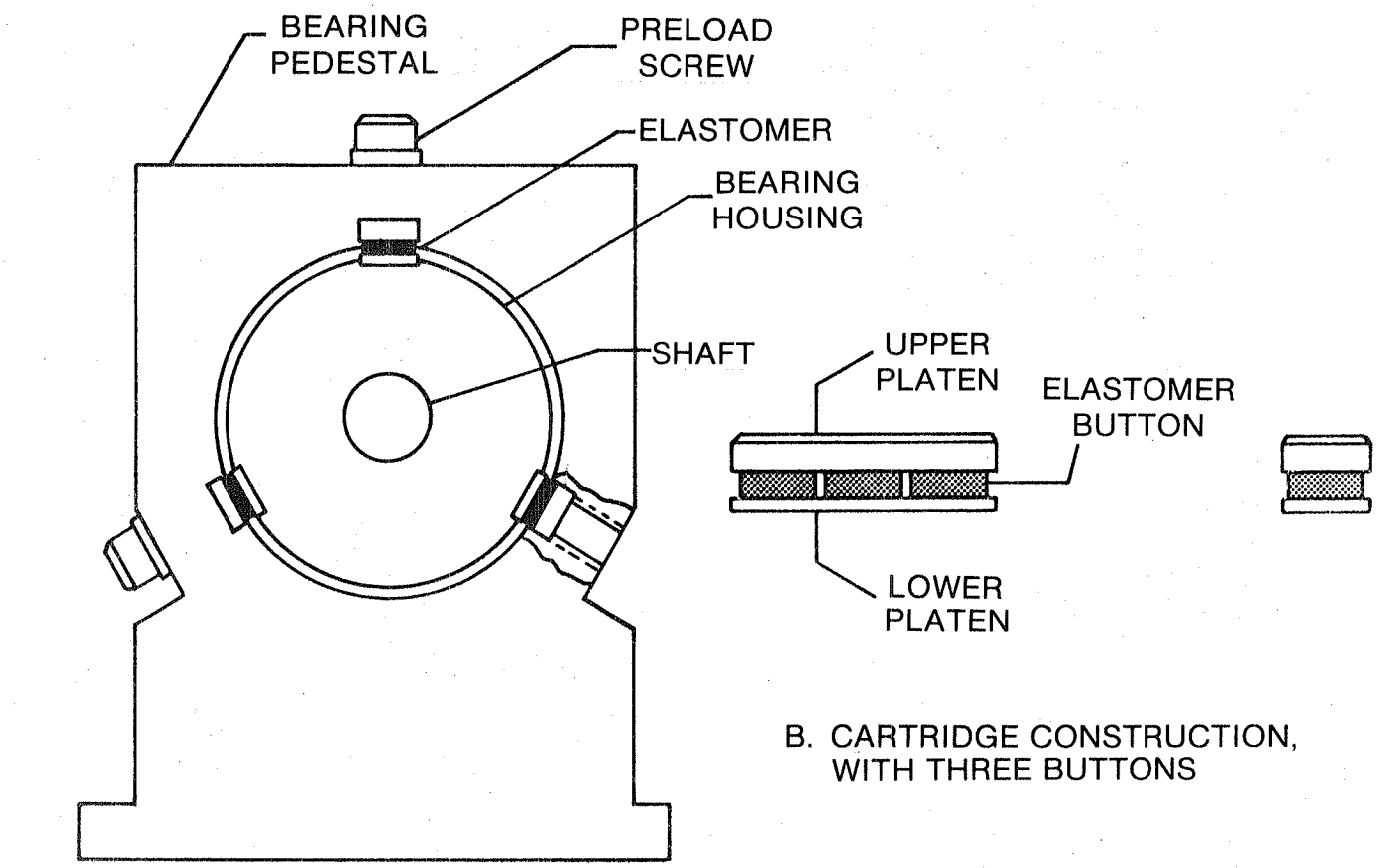

Fig. 15 Method of Supporting Test Rig Rotor on Elastomers

801497-1

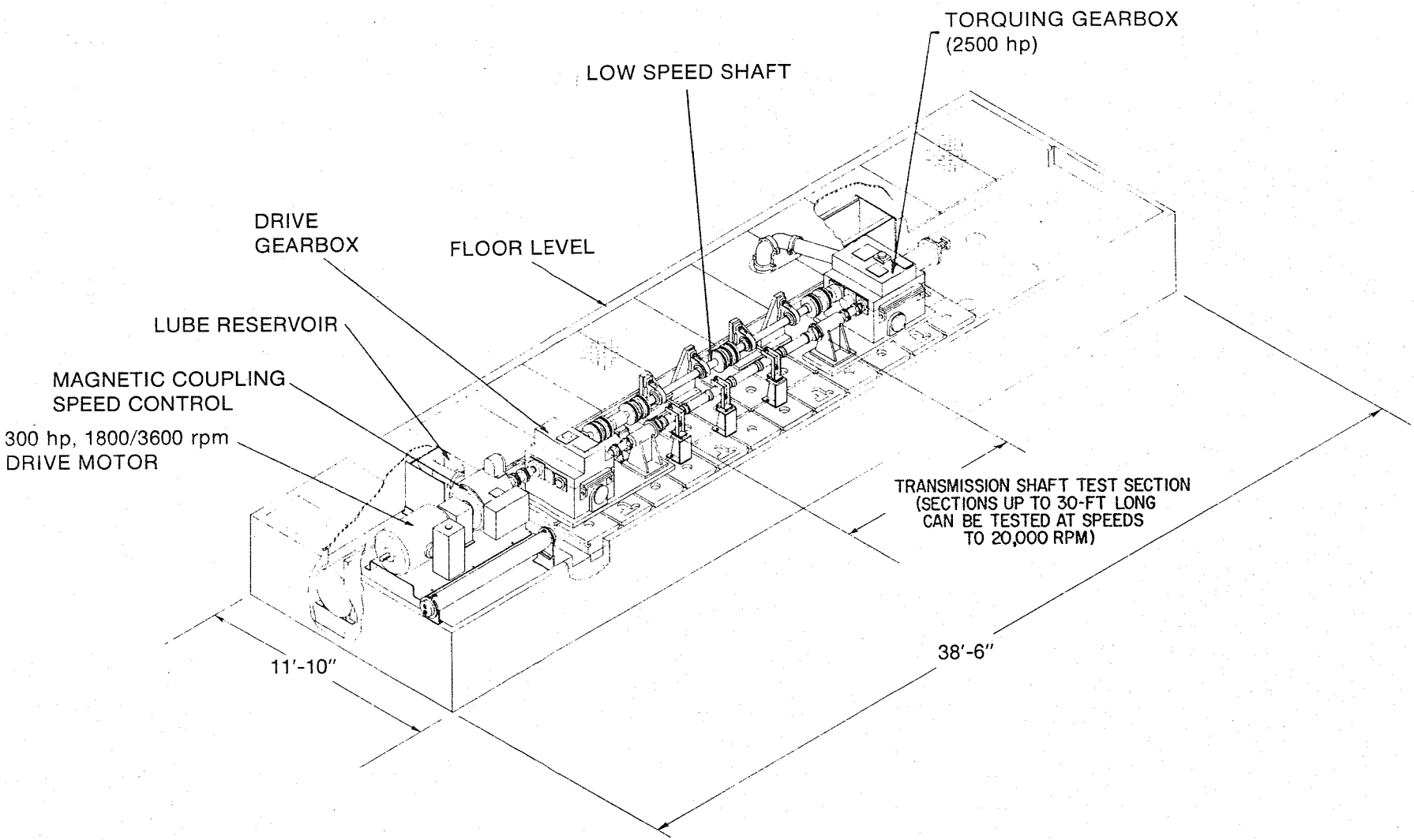

Fig. 16 Drive Train Dynamics Technology Test Rig Configuration for High-Speed Shaft Balancing

801533-1

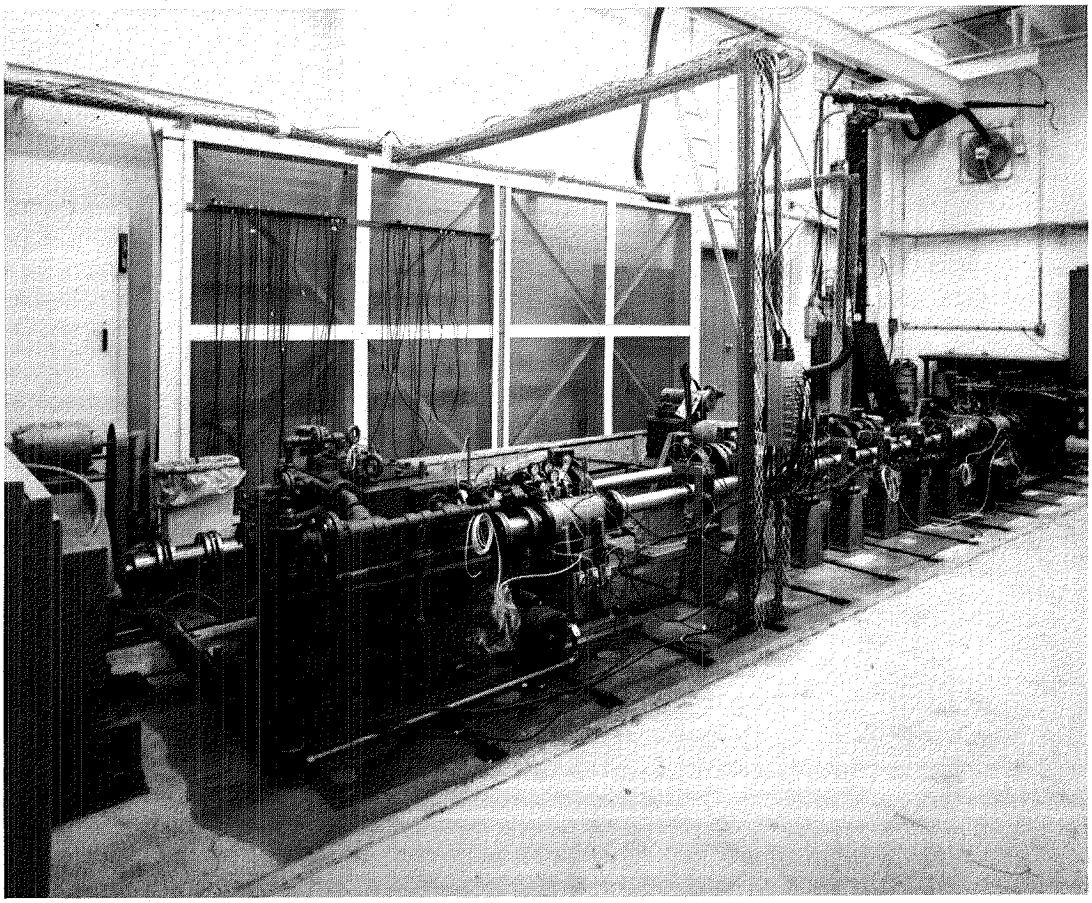

Fig. 17 View of Completely Assembled Test Rig Showing High-Speed Side from Drive Gearbox End

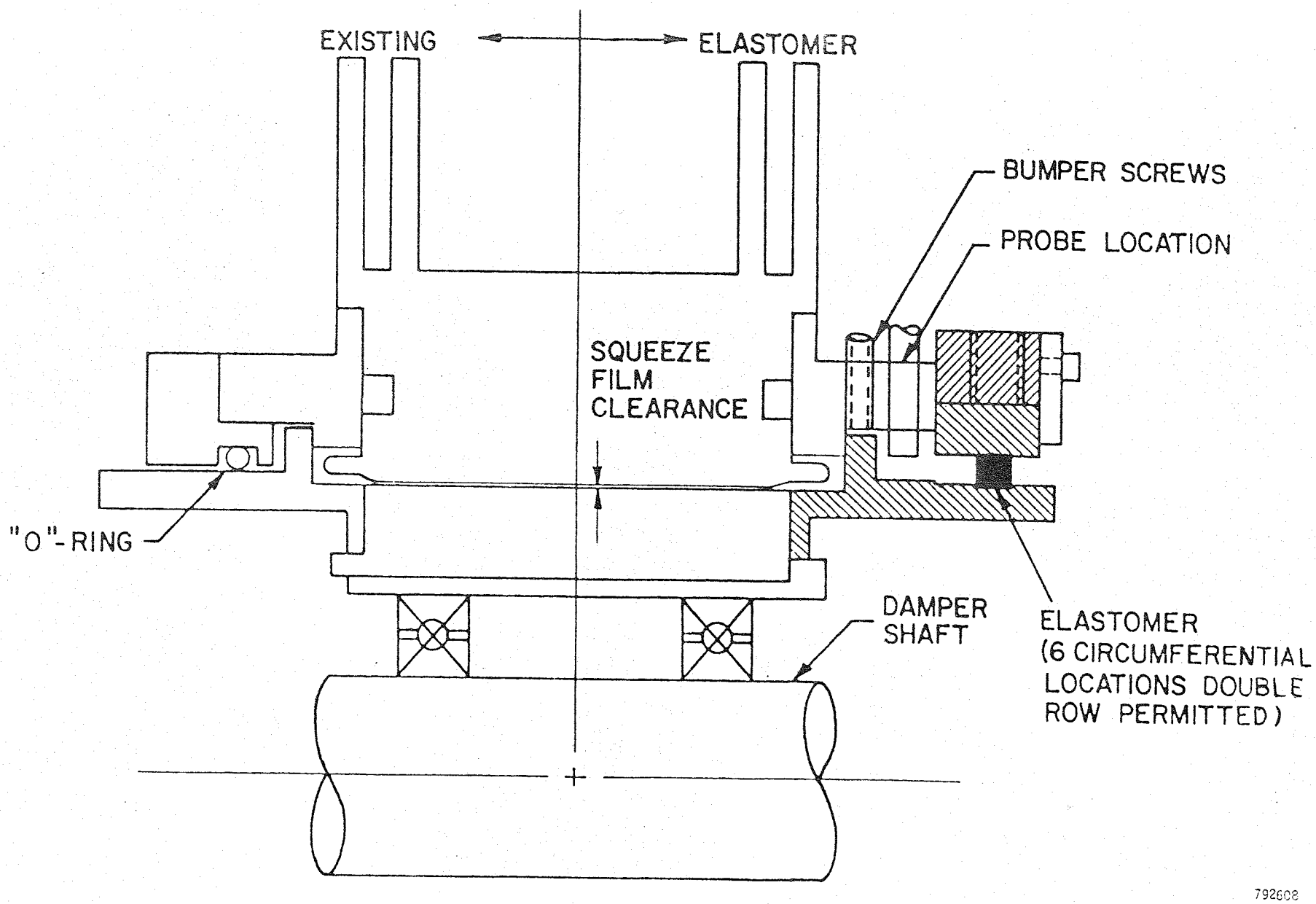

Fig. 18 Elastomer Damper/Squeeze-Film Damper Schematic

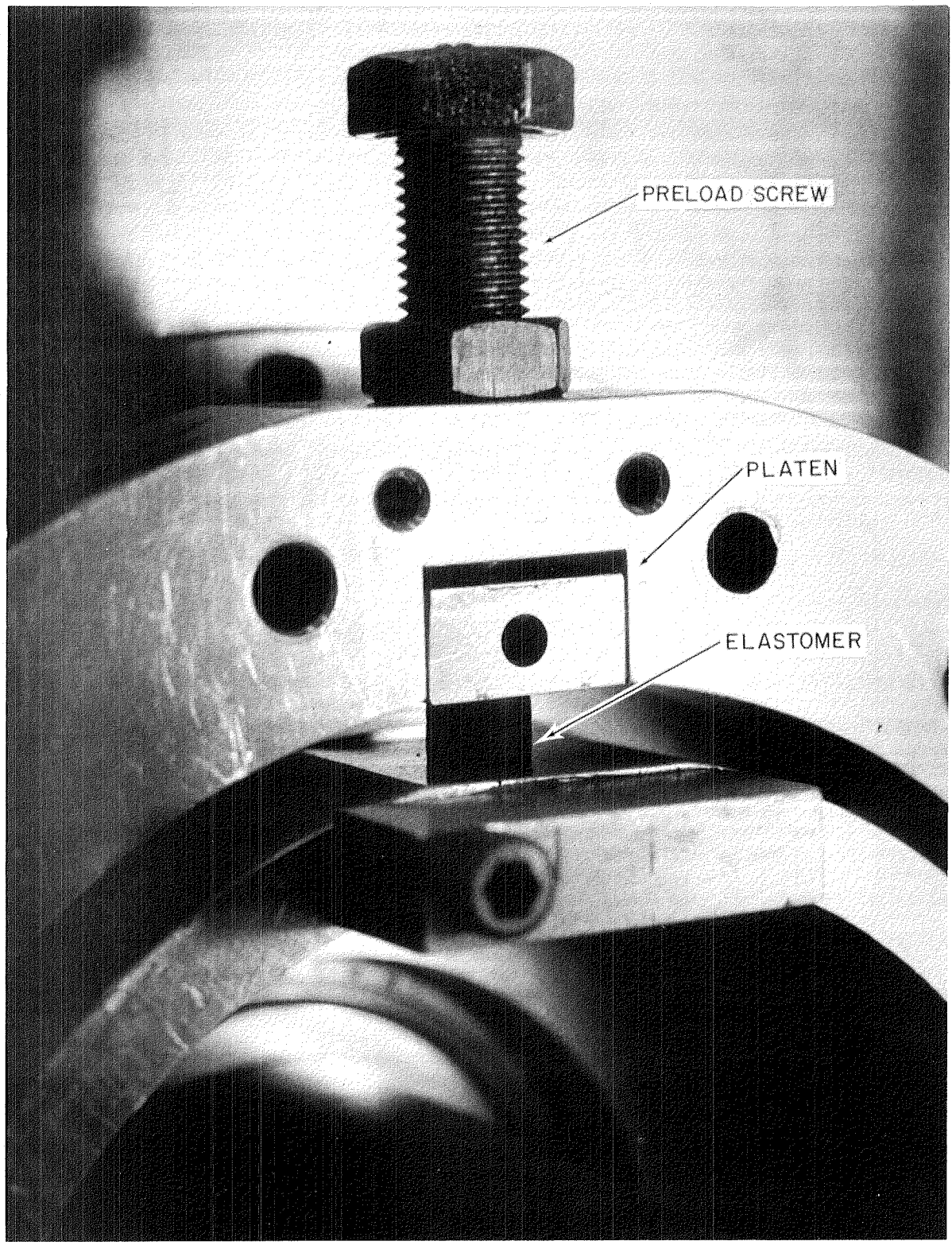

Fig. 19 Elastomer Damper Installed in Rig

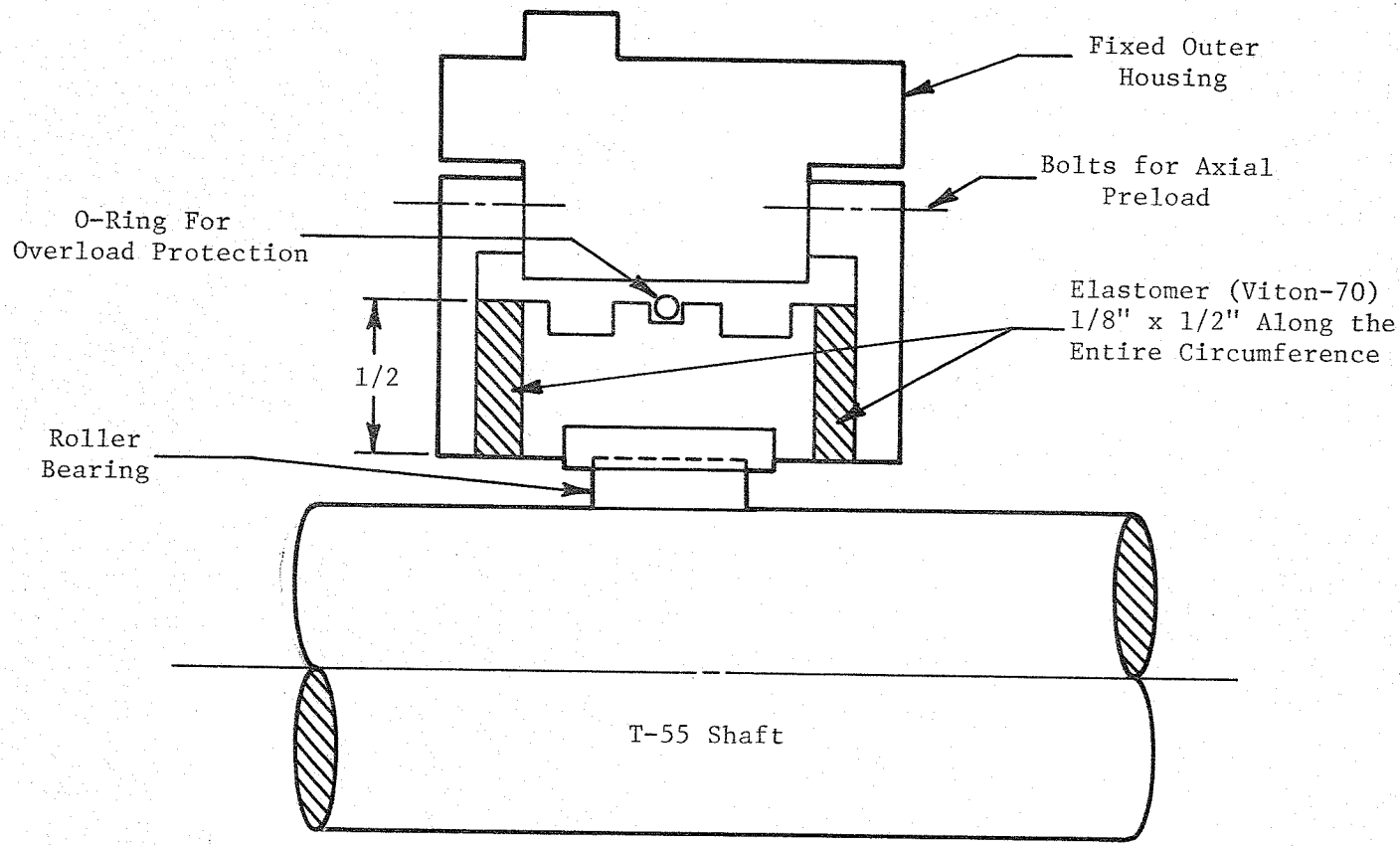

Fig. 20 T-55 Elastomer Supported Roller Bearing Cartridge

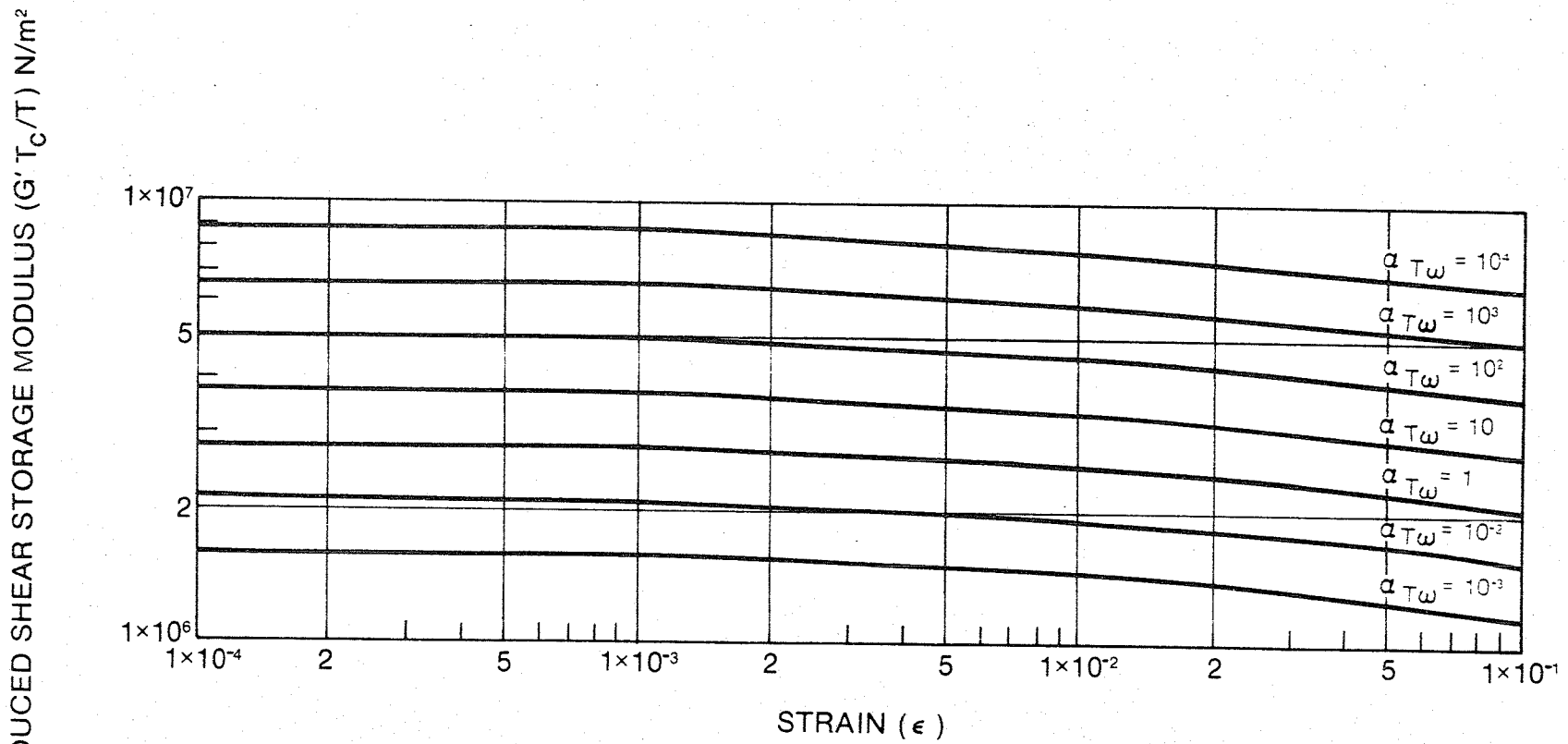

Fig. 21 Viton-70 Design Curves from Reference 5

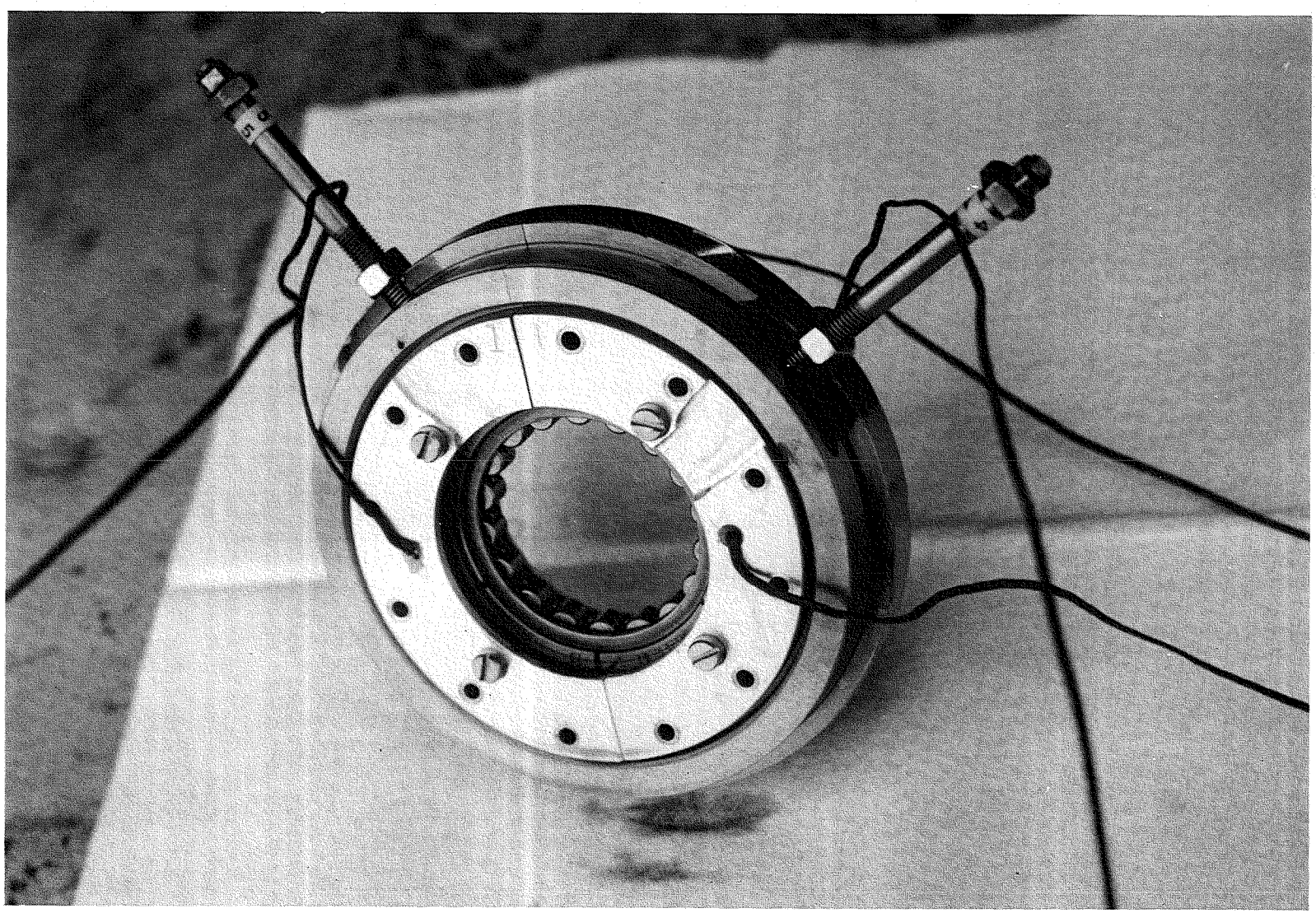

Fig. 22 Assembled T-55 Power Turbine Elastomeric Damper

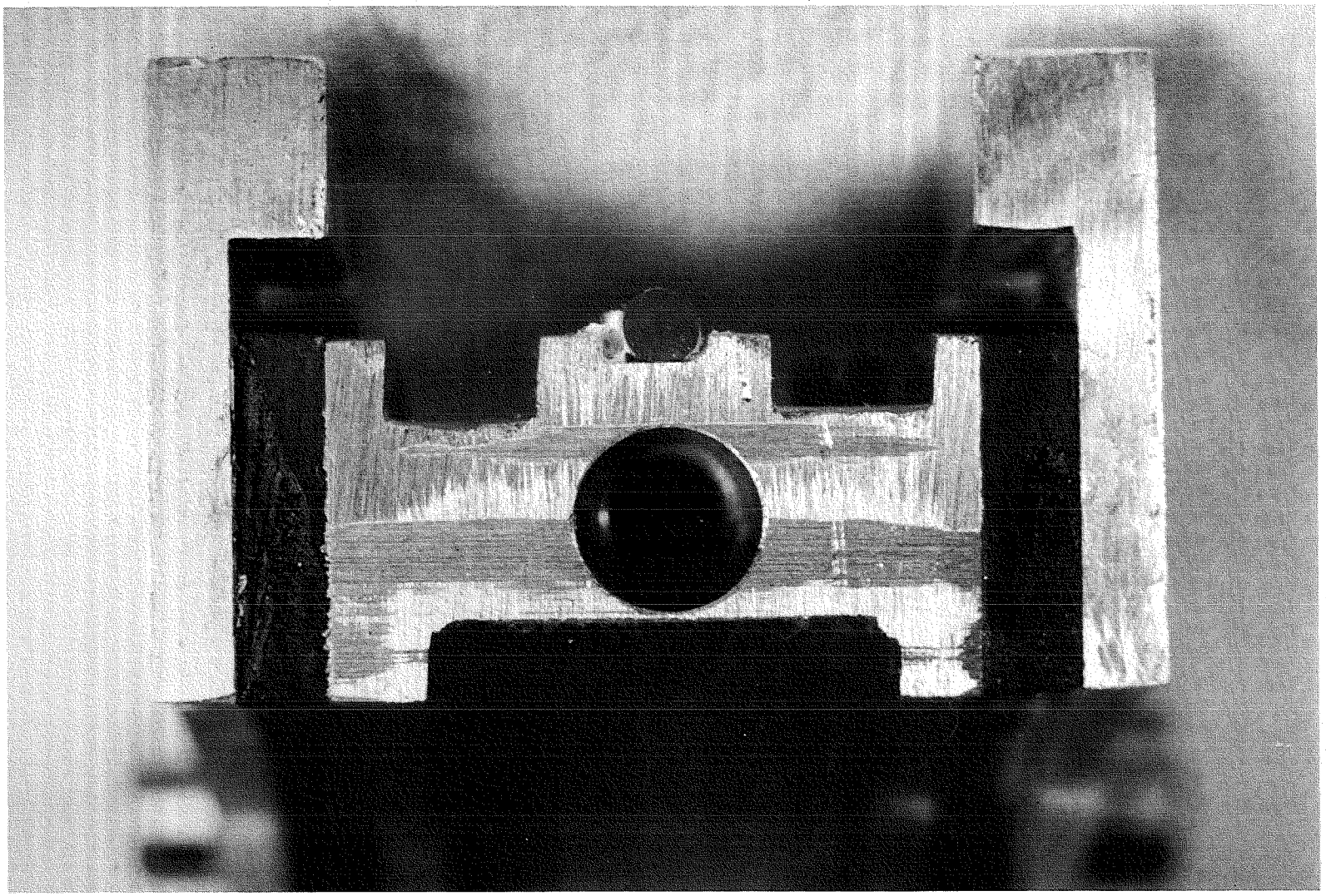

Fig. 23 Cross Section of the T-55 Elastomer Damper

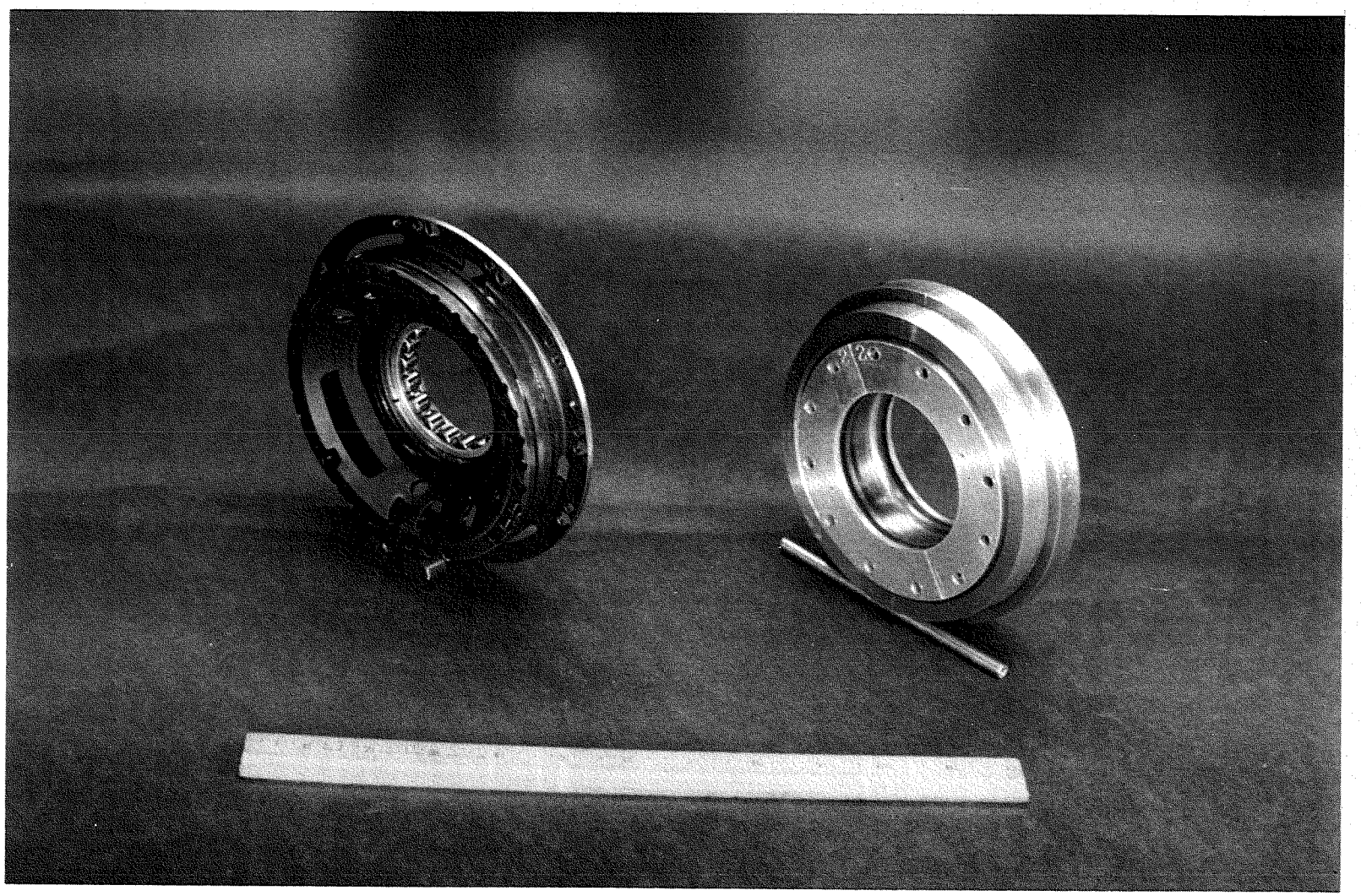

Fig. 24 The Production T-55 Roller Bearing Support and the Replacement Elastomer Damper

MTI-20123

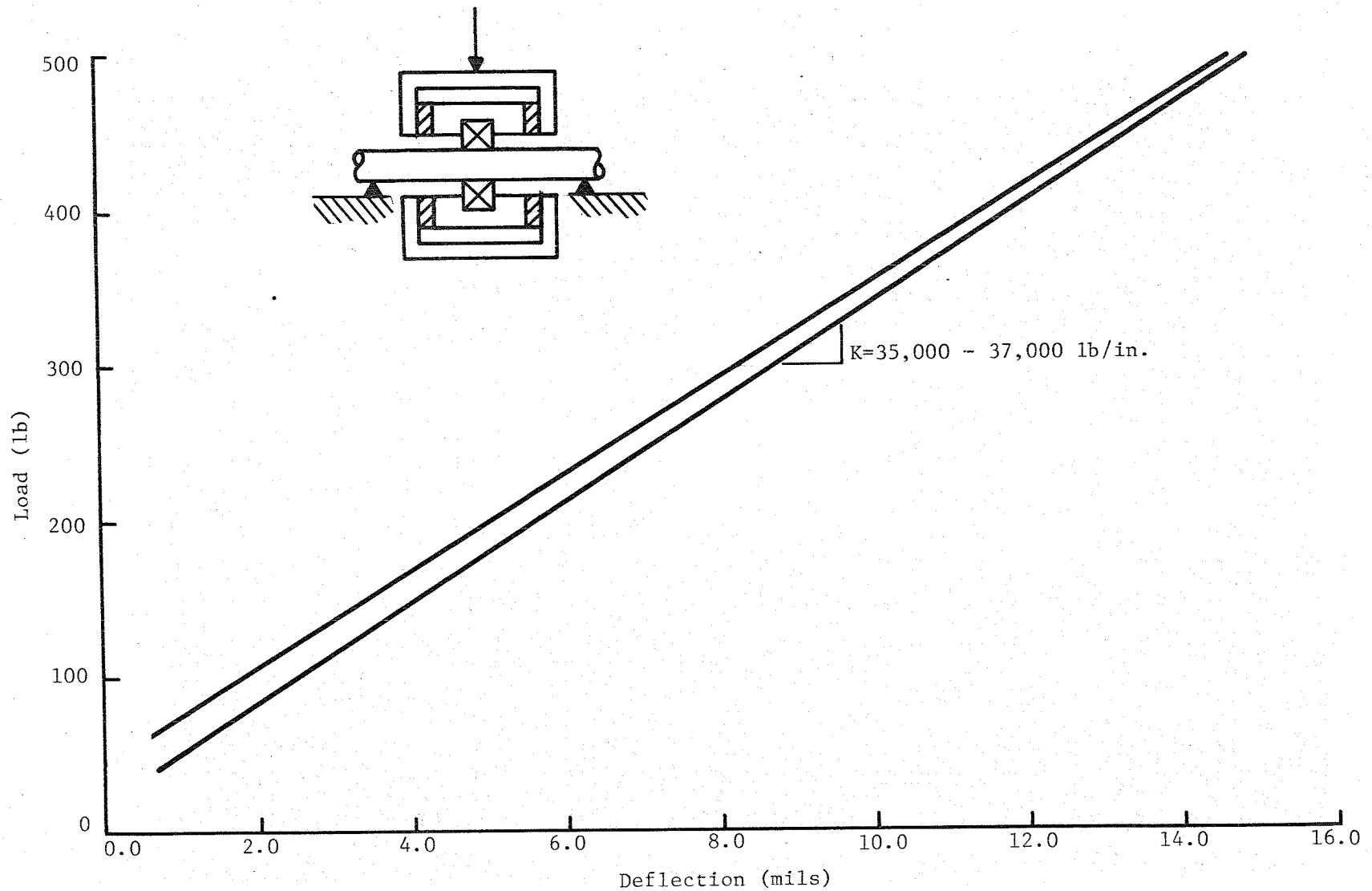

Fig. 25 Static Shear Loading of Viton-70 T-55 Elastomer Mount

802331

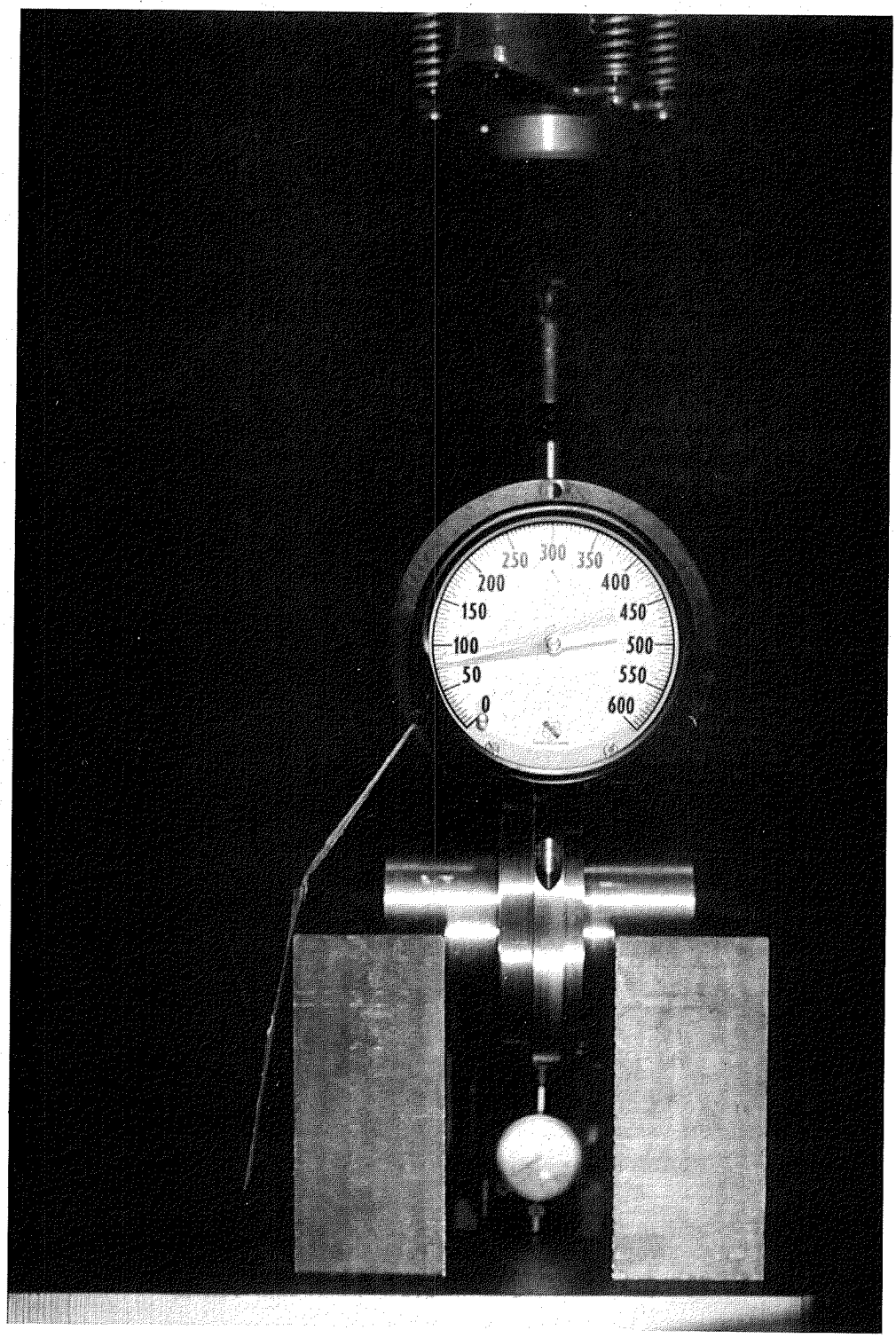

Fig. 26 Static Shear Load Test Set-Up for T-55 Elastomer Damper

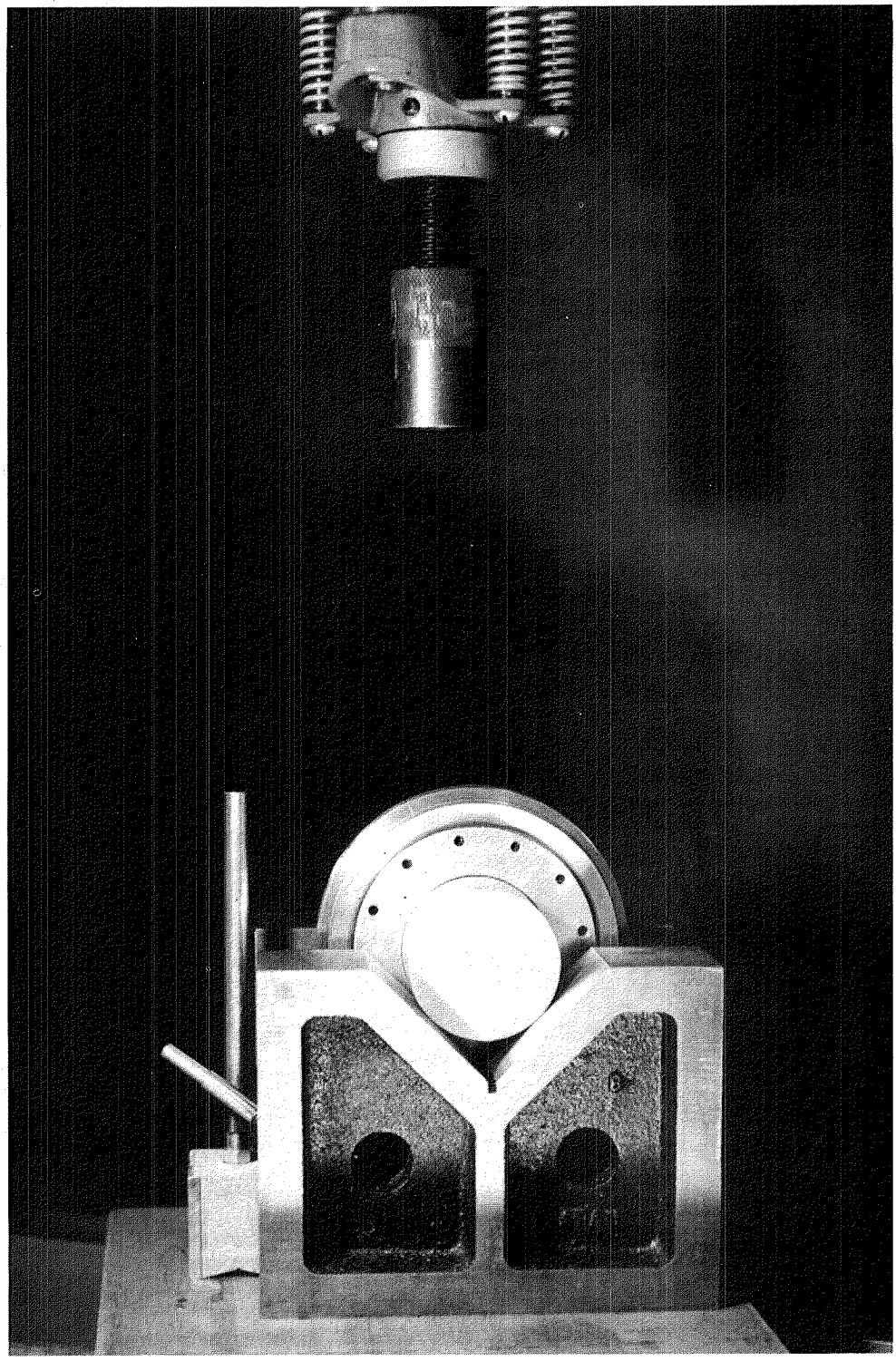

Fig. 27 "V"-Block Set-Up for Static Shear Testing

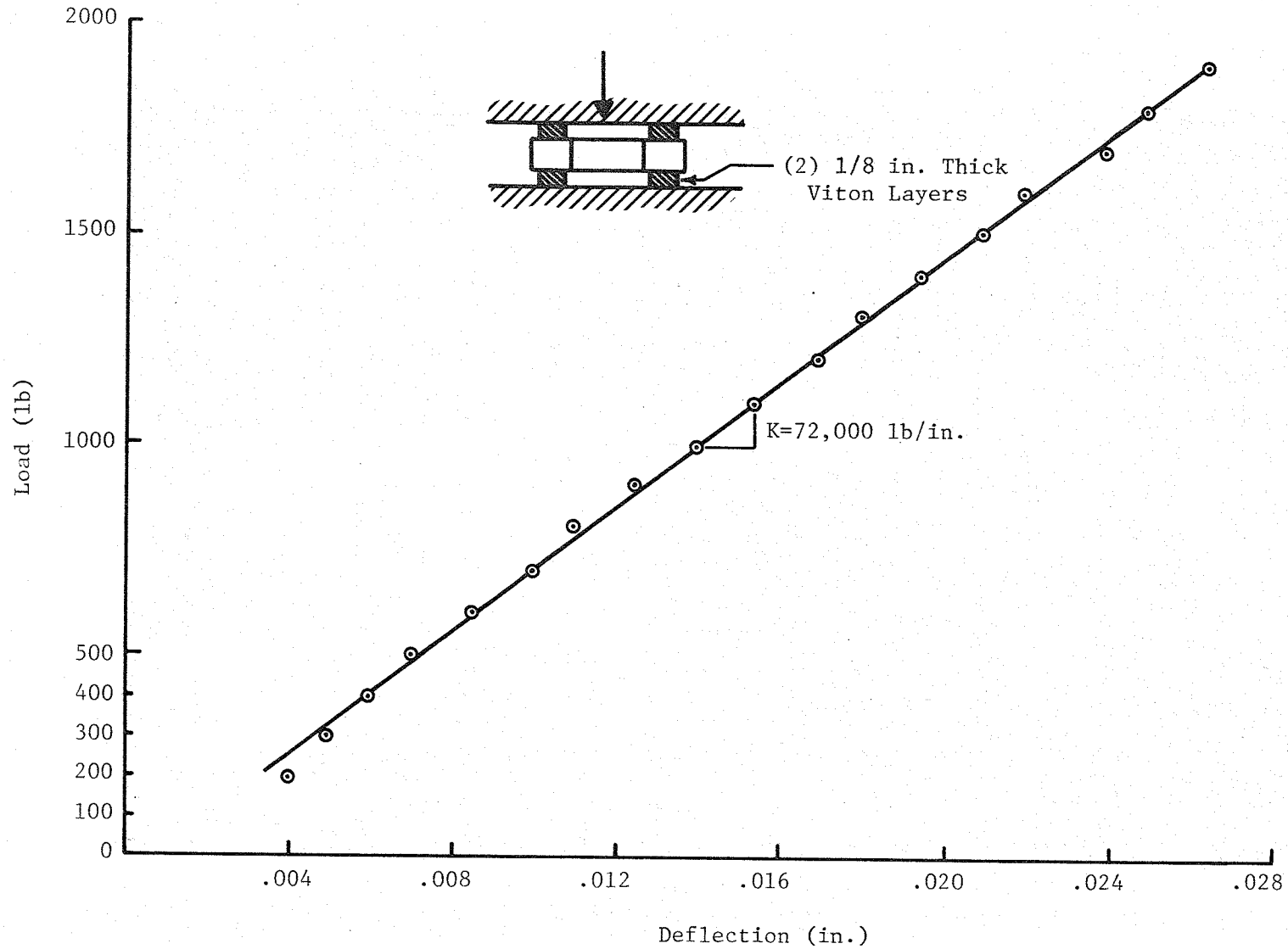

Fig. 28 Axial Static Loading of Viton-70 T-55 Elastomer Mount

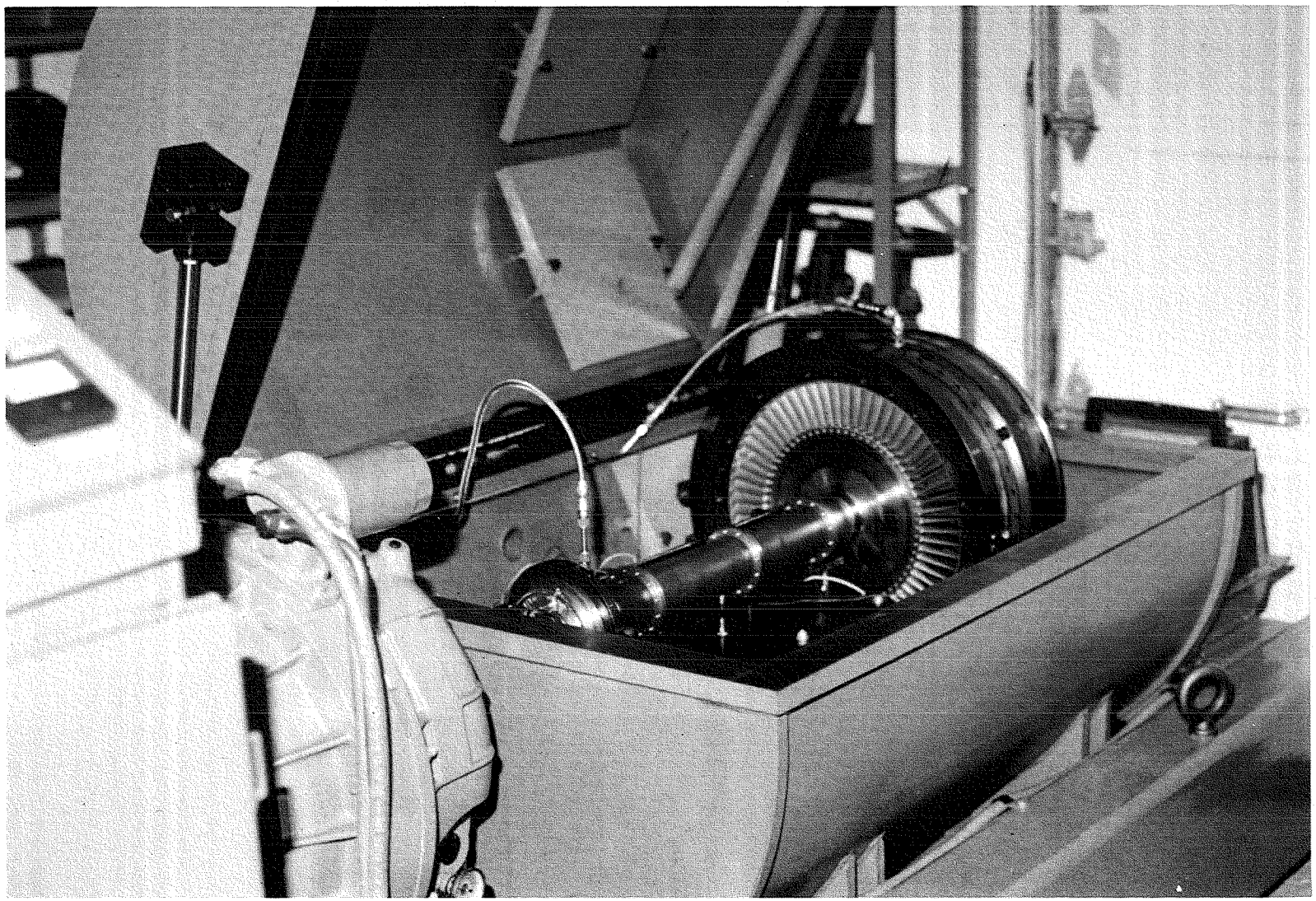

Fig. 29 CCAD Test Rig with T-55 Power Turbine and Elastomer Damper Installed

MTI-20124

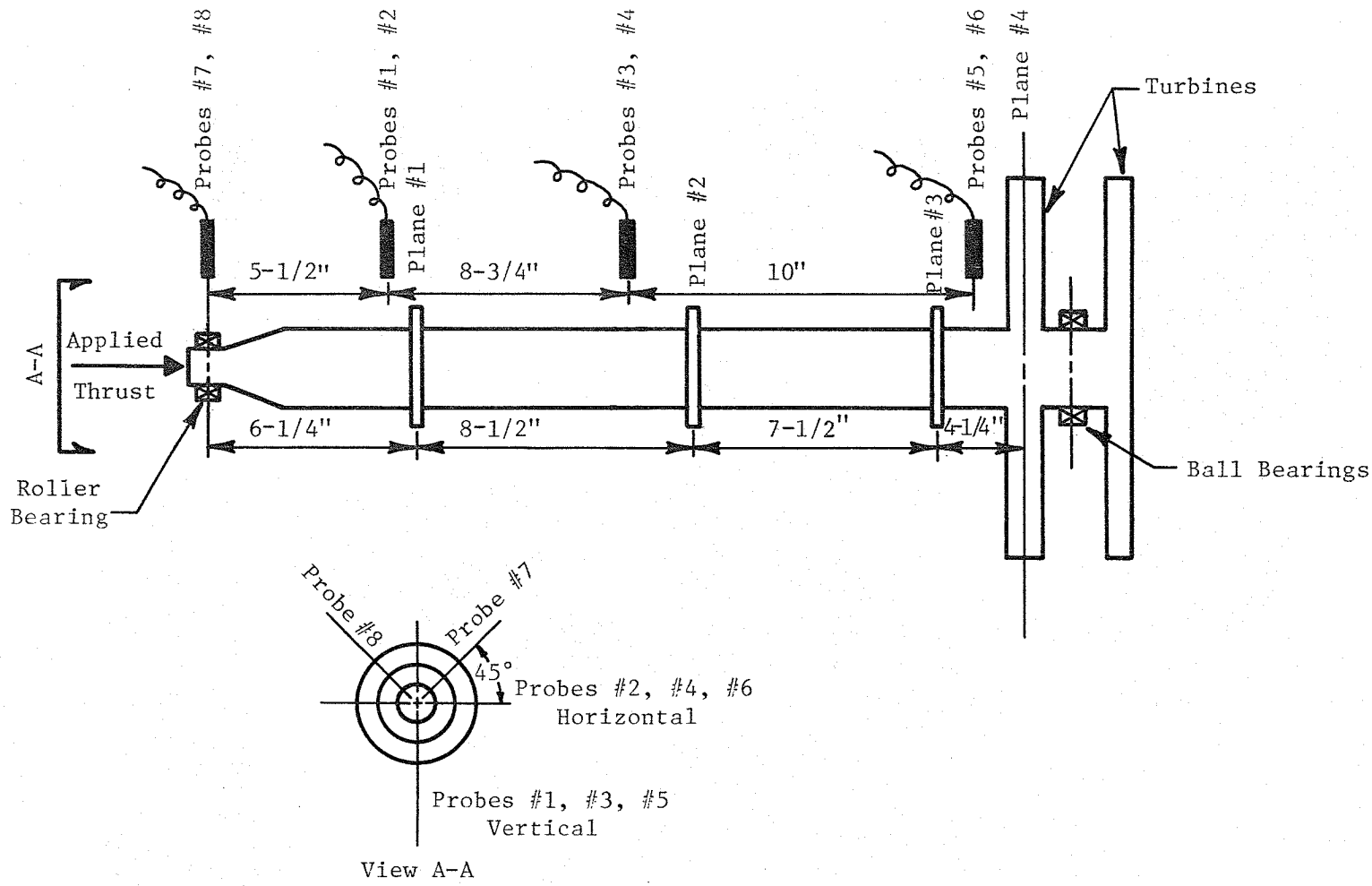

Fig. 30 T-55 Power Turbine Rotor in CCAD Rig

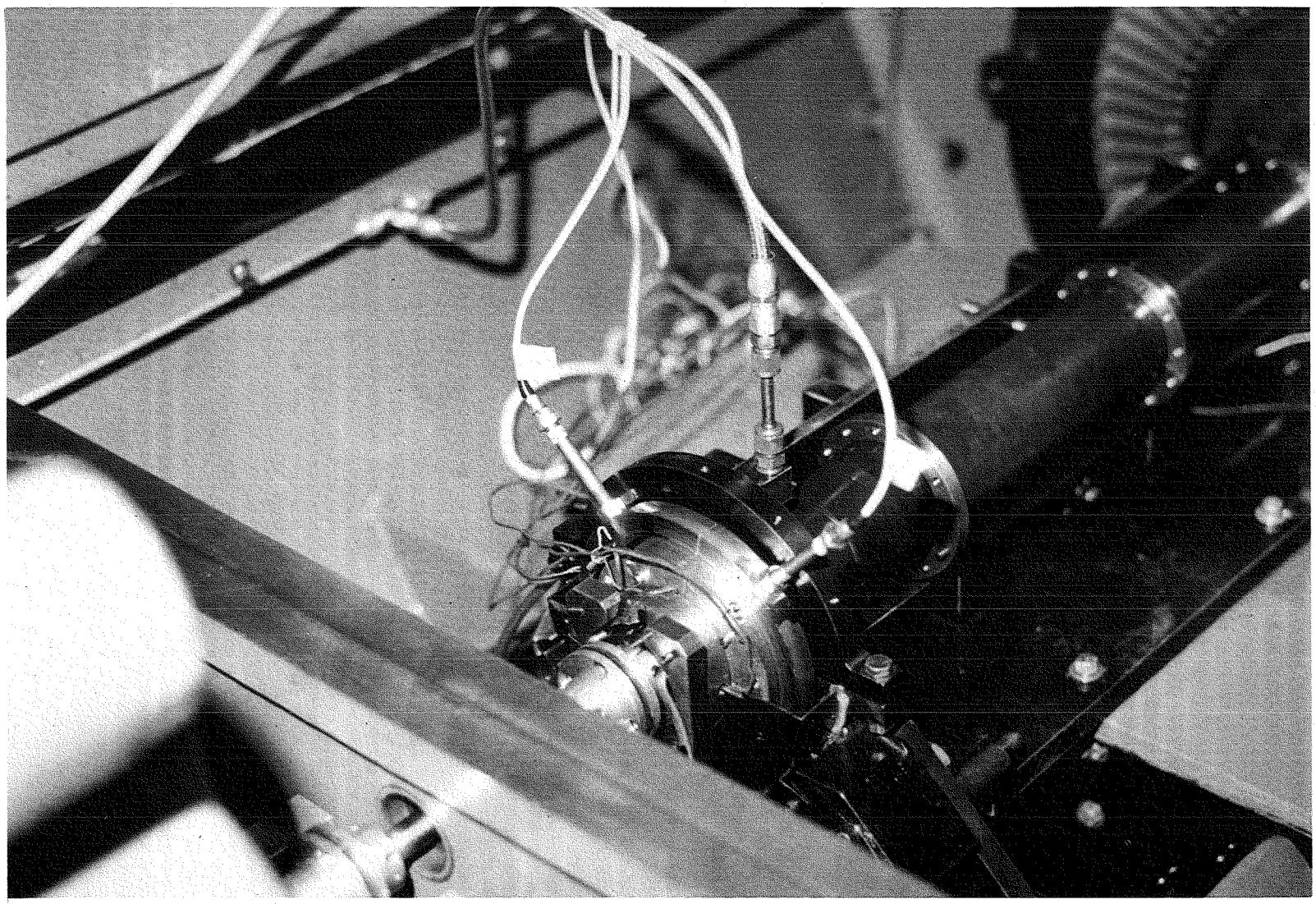

Fig. 31 Close-Up of Elastomeric-Damper Support for T-55 Power Turbine in CCAD Rig

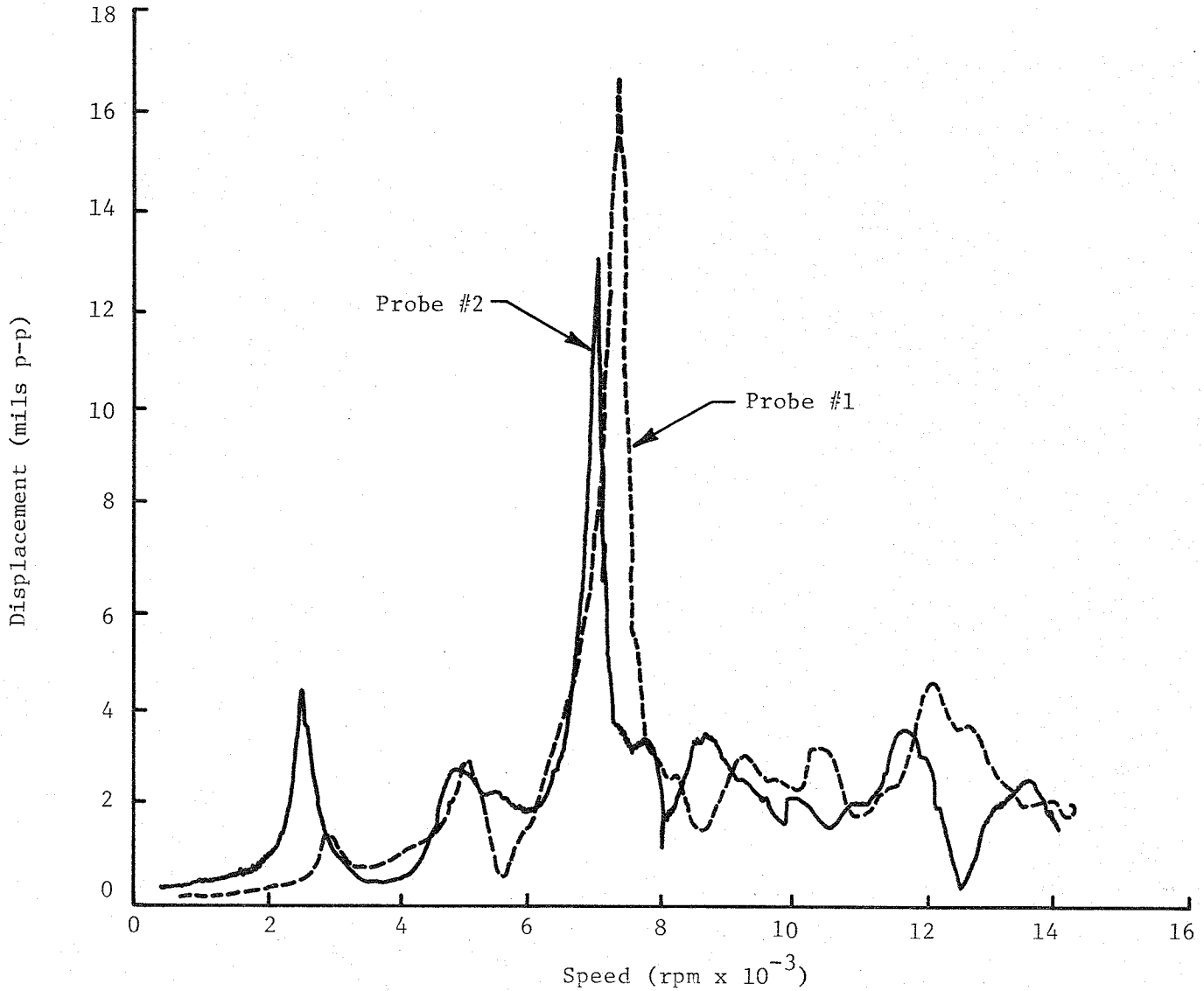

Fig. 32 T-55 Production Power Turbine Baseline Data - Probes #1 and #2

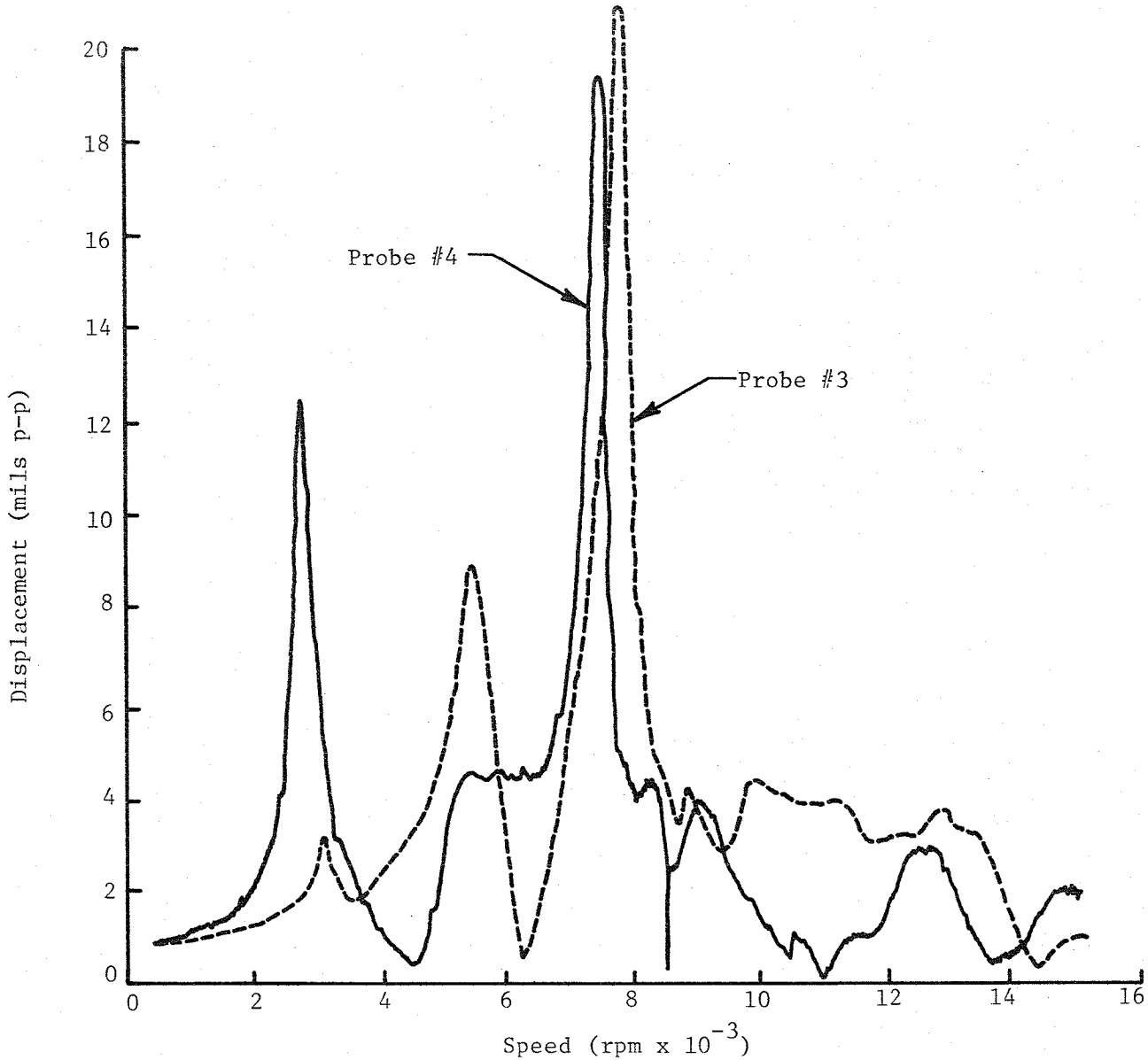

802346

Fig. 33 T-55 Power Turbine Baseline Data - Probes #3 and #4

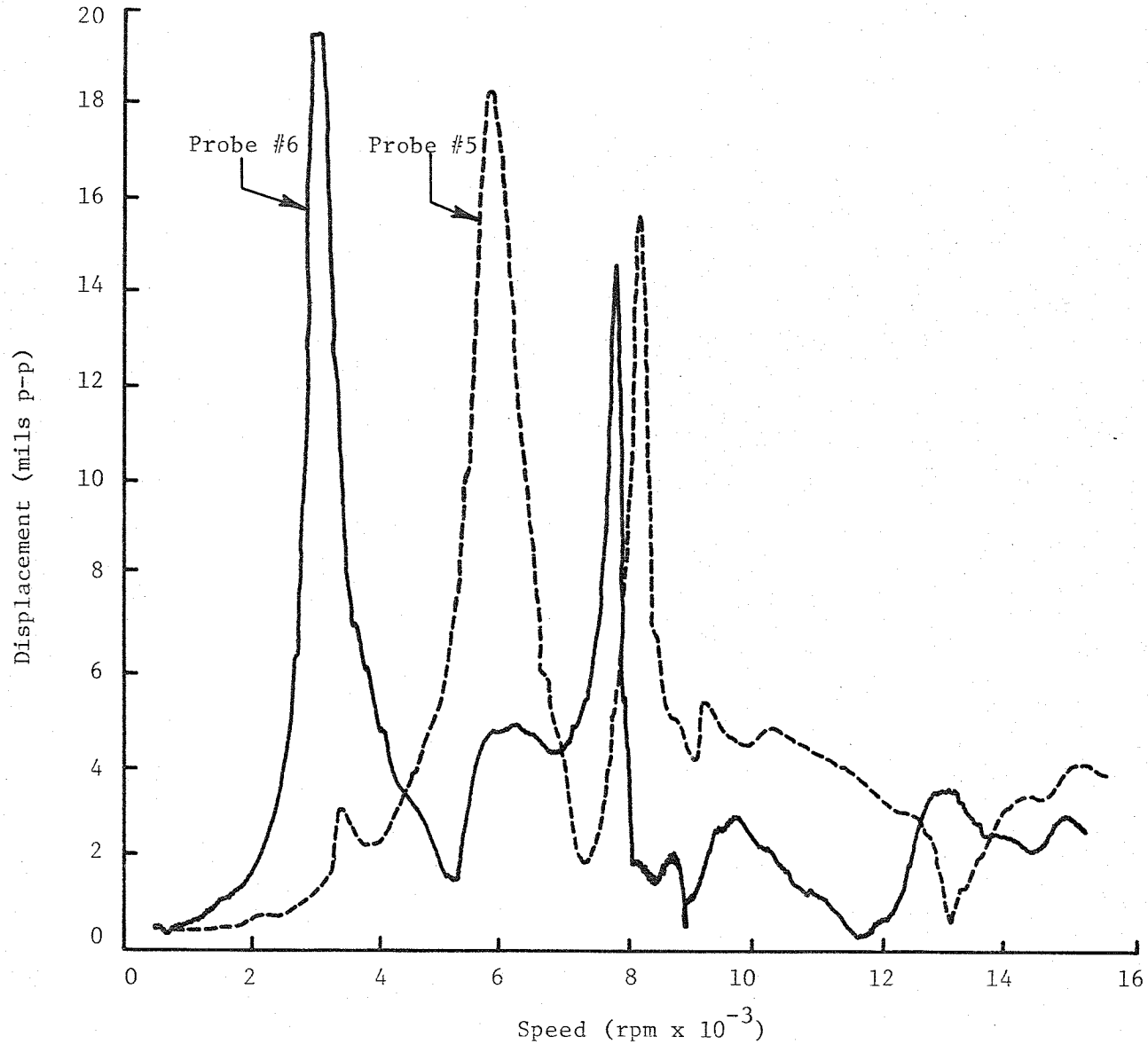

Fig. 34 T-55 Power Turbine Baseline Data - Probes #5 and #6

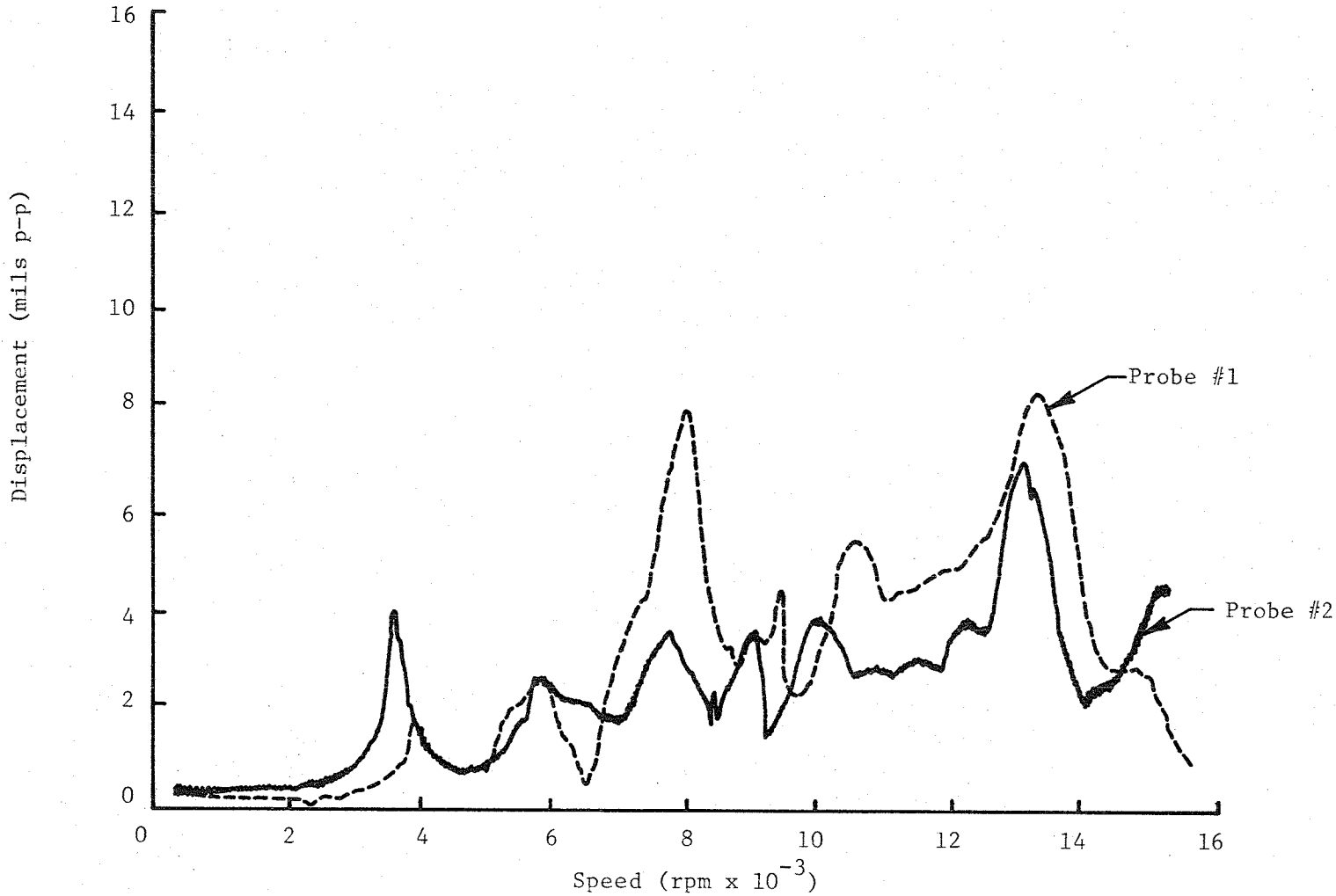

802345

Fig. 35 T-55 Elastomeric Damper Baseline Data - Probes #1 and #2

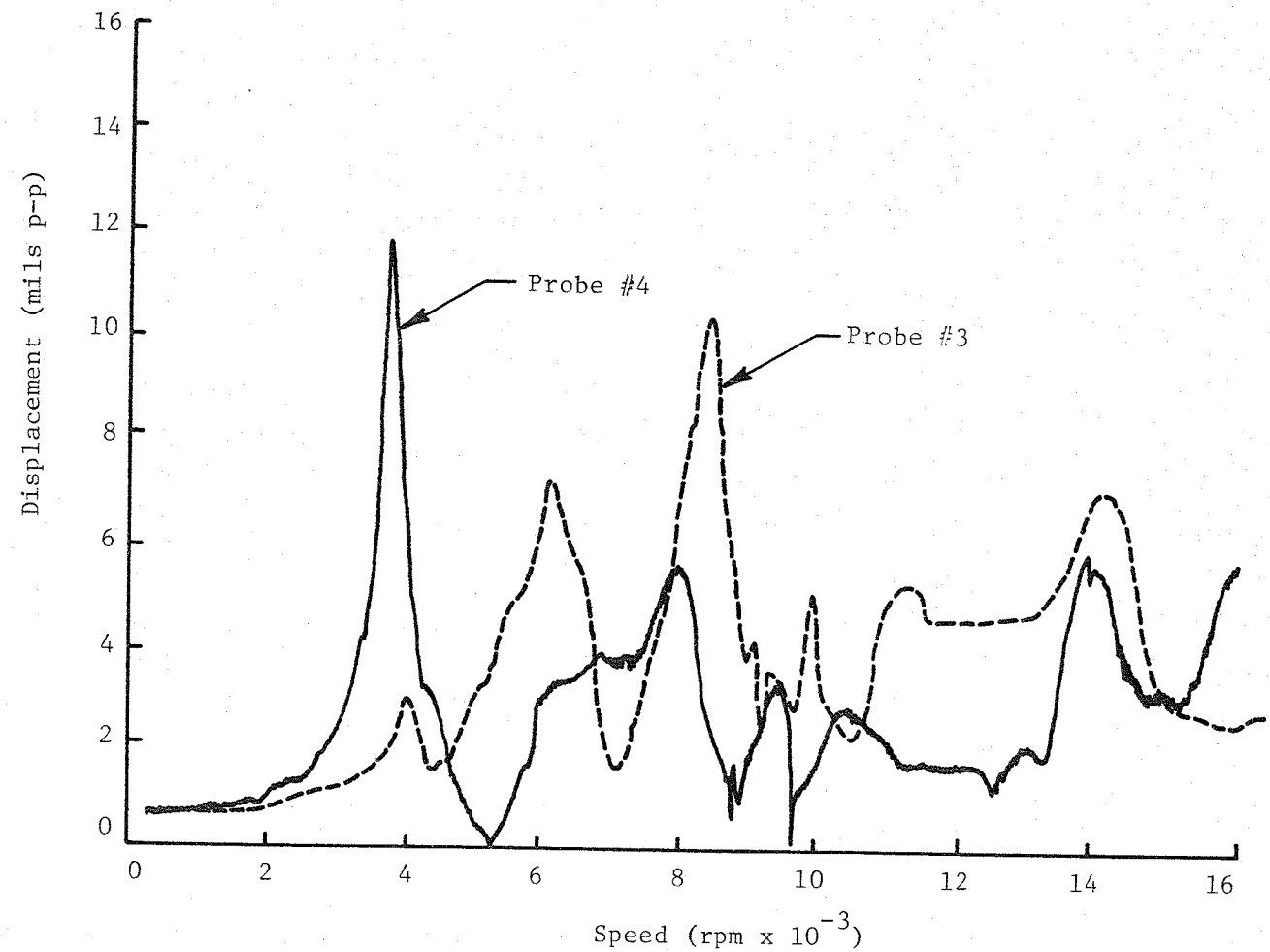

Fig. 36 T-55 Elastomeric Damper Baseline Data - Probes #3 and #4

802344

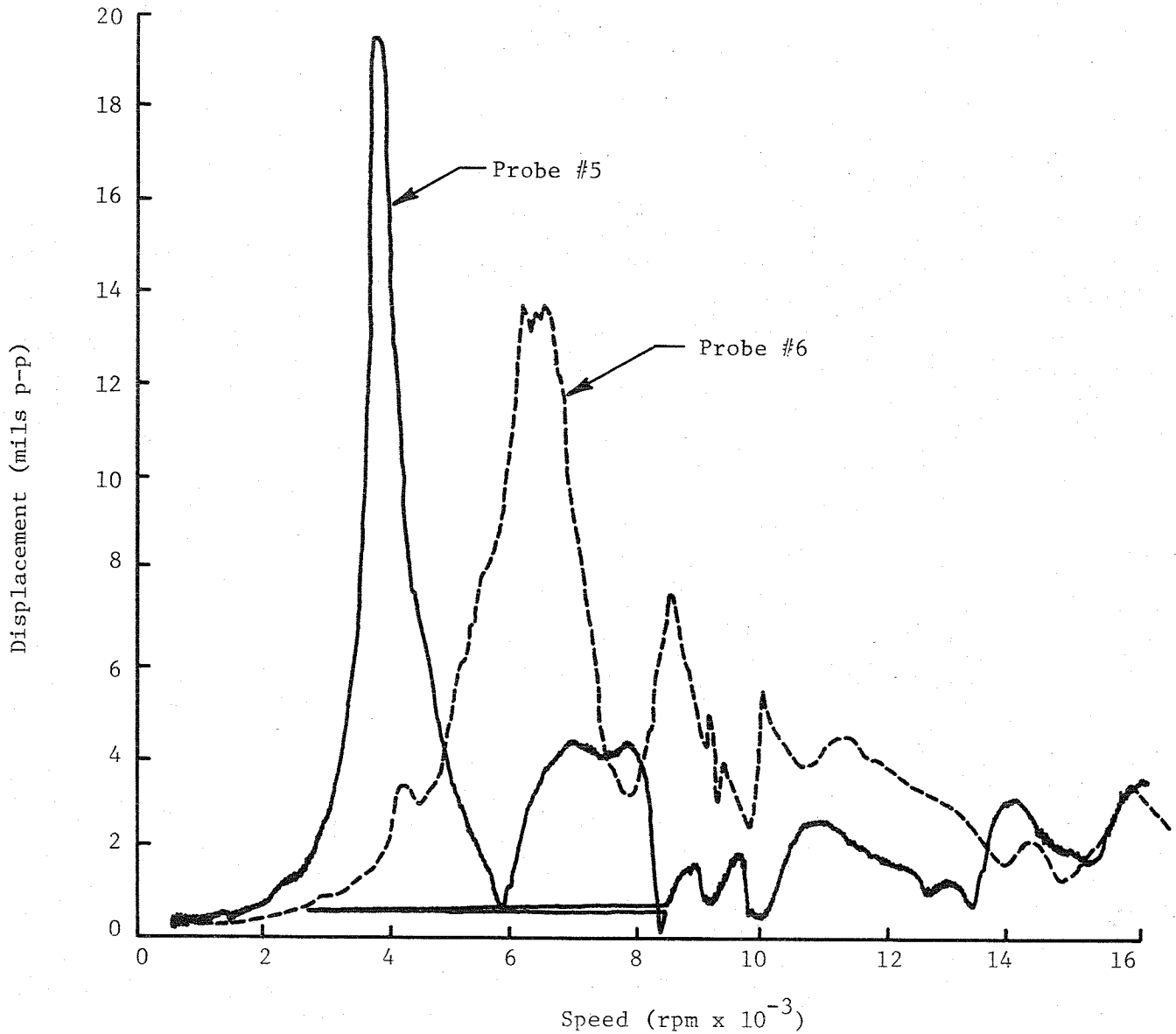

Fig. 37 T-55 Elastomeric Damper Baseline Data - Probes #5 and #6

802343

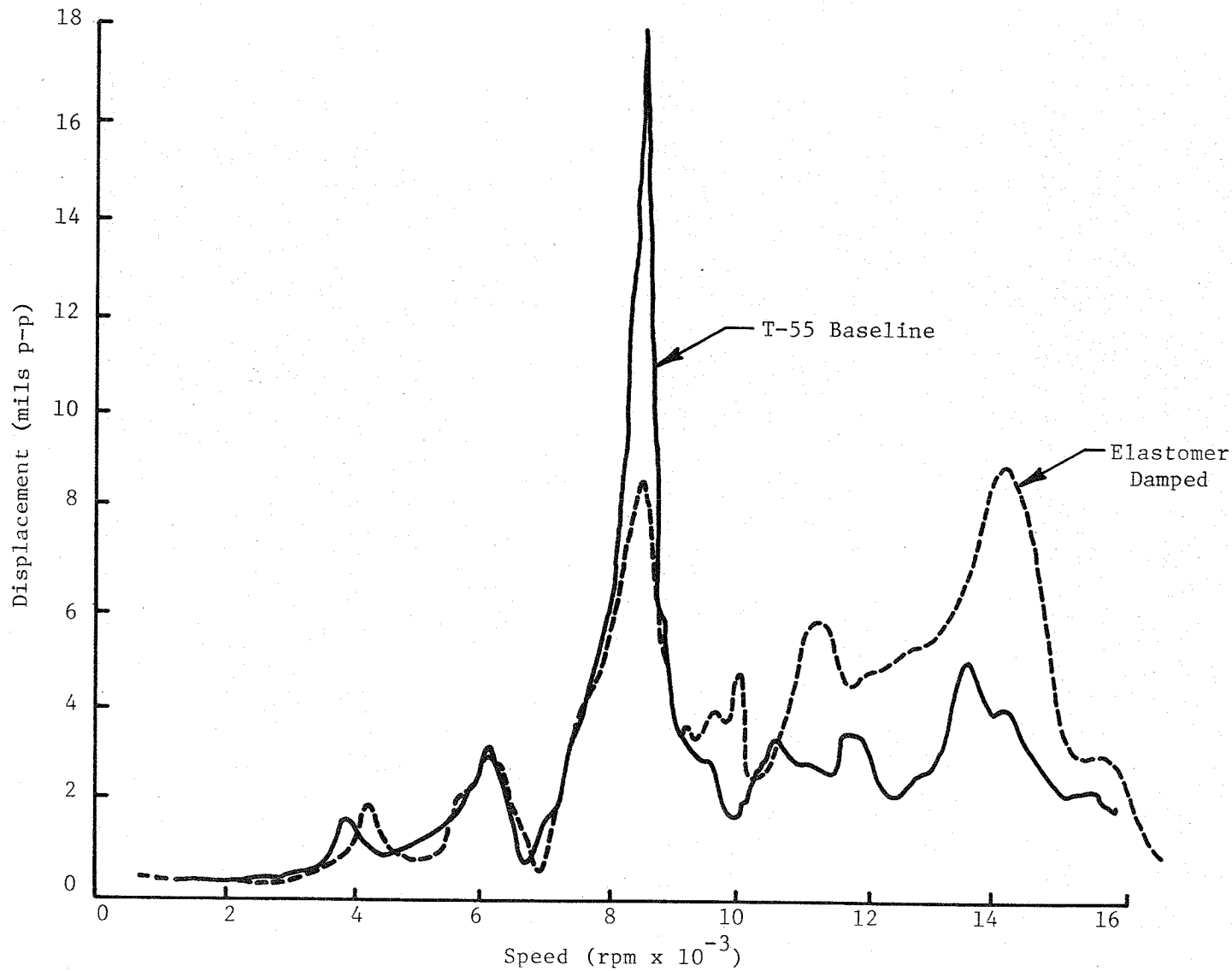

Fig. 38 Vibration Plot Comparing Baseline and Elastomer Mounted Rotor Response at Probe 1

802342

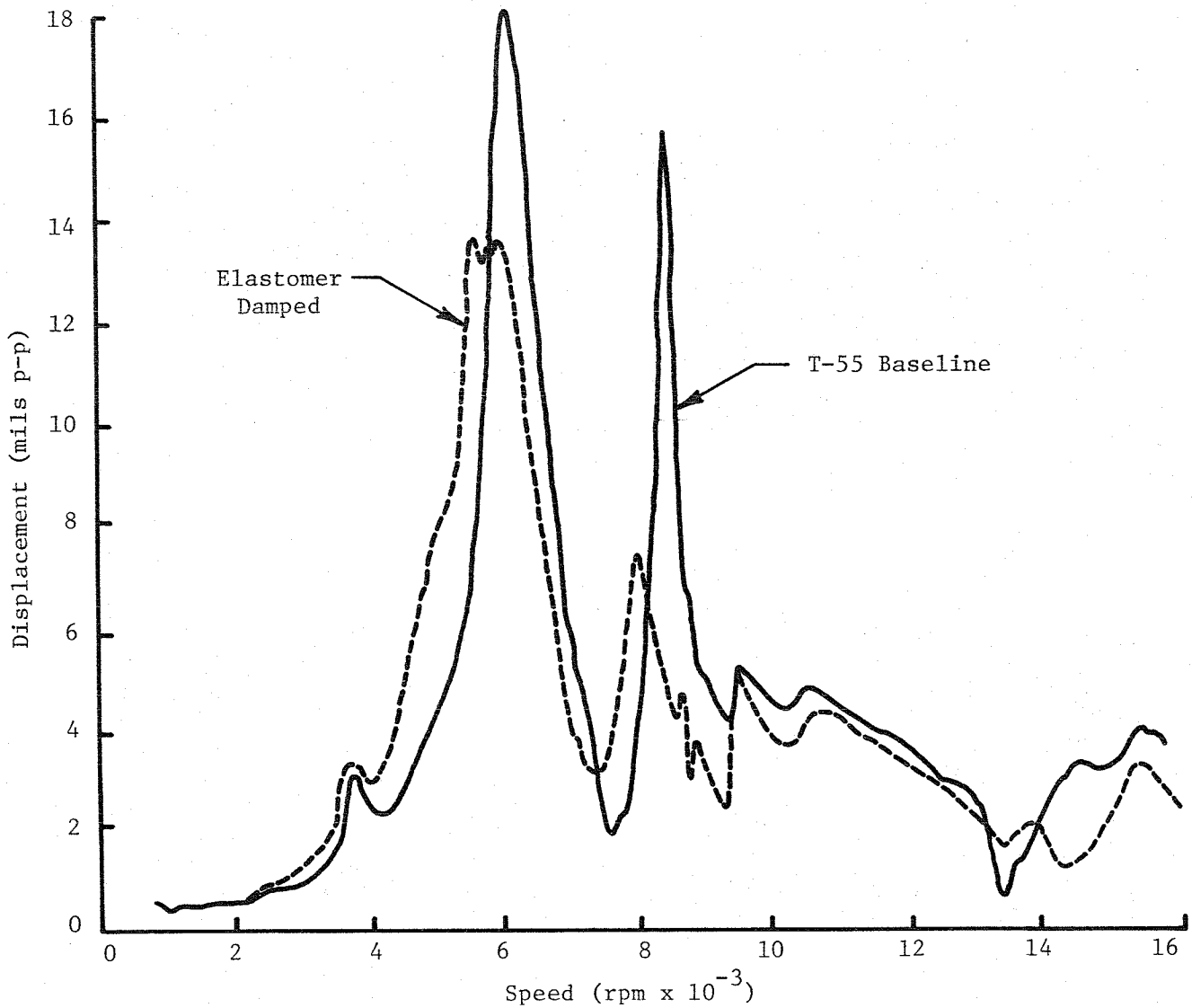

Fig. 39 Vibration Plot Comparing Baseline and Elastomer Mounted Rotor Response at Probe 5

802341

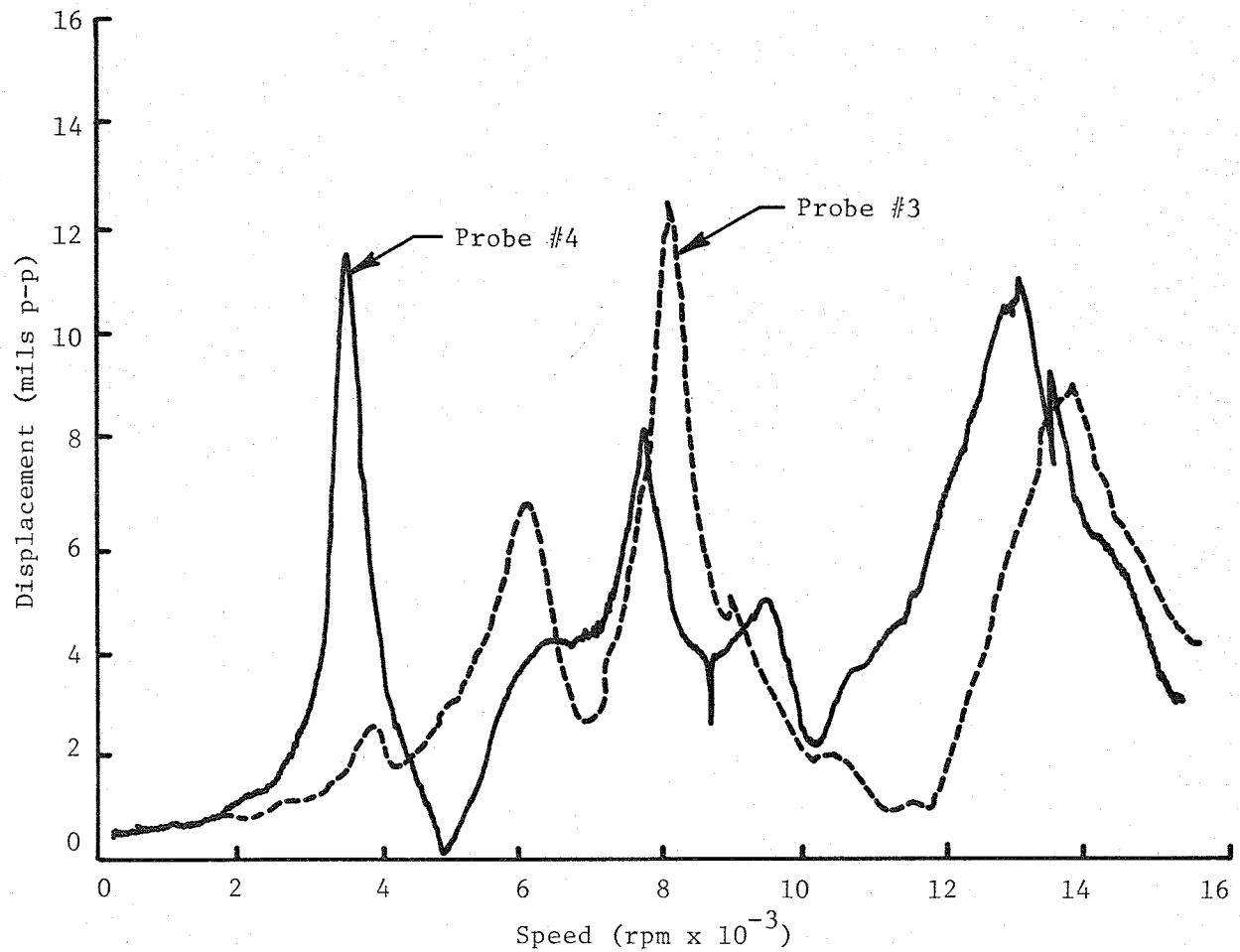

Fig. 40 T-55 Elastomer Damped; 3 gm @ 300° Plane #1

802340

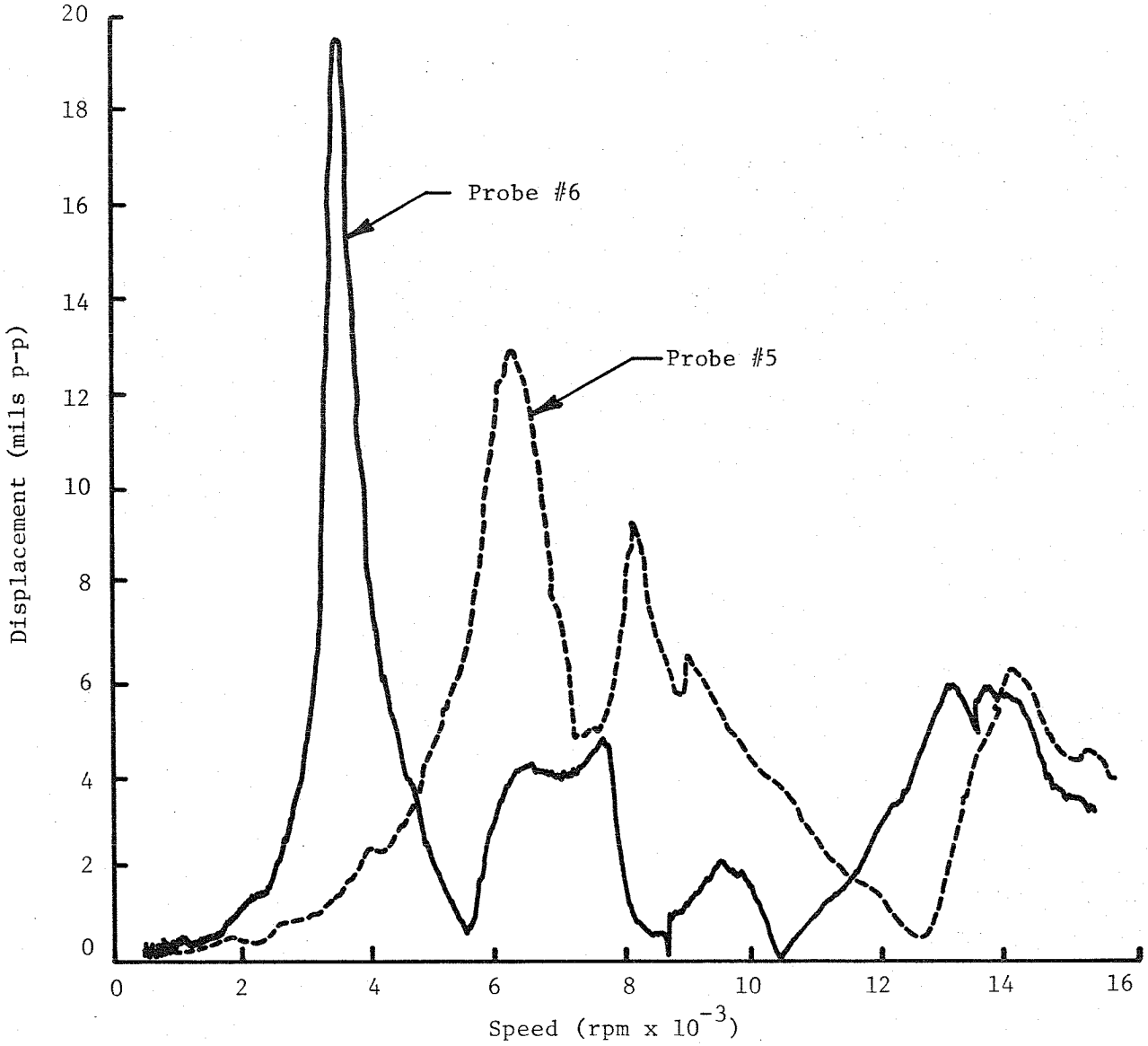

Fig. 41 T-55 Elastomer Damped; 3 gm @ 300° Plane #1

802339

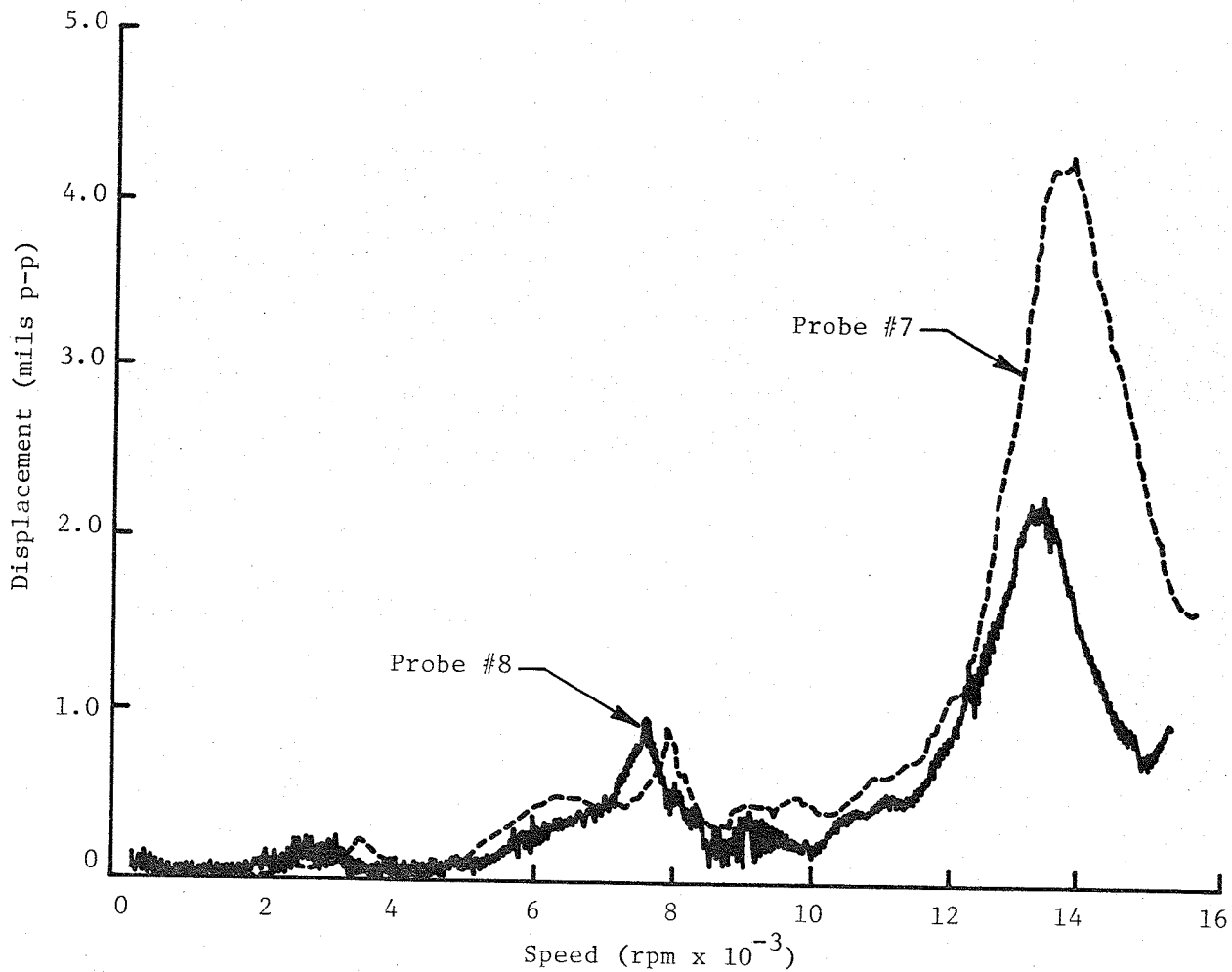

Fig. 42 T-55 Elastomer Damped; 3 gm @ 300° Plane #1

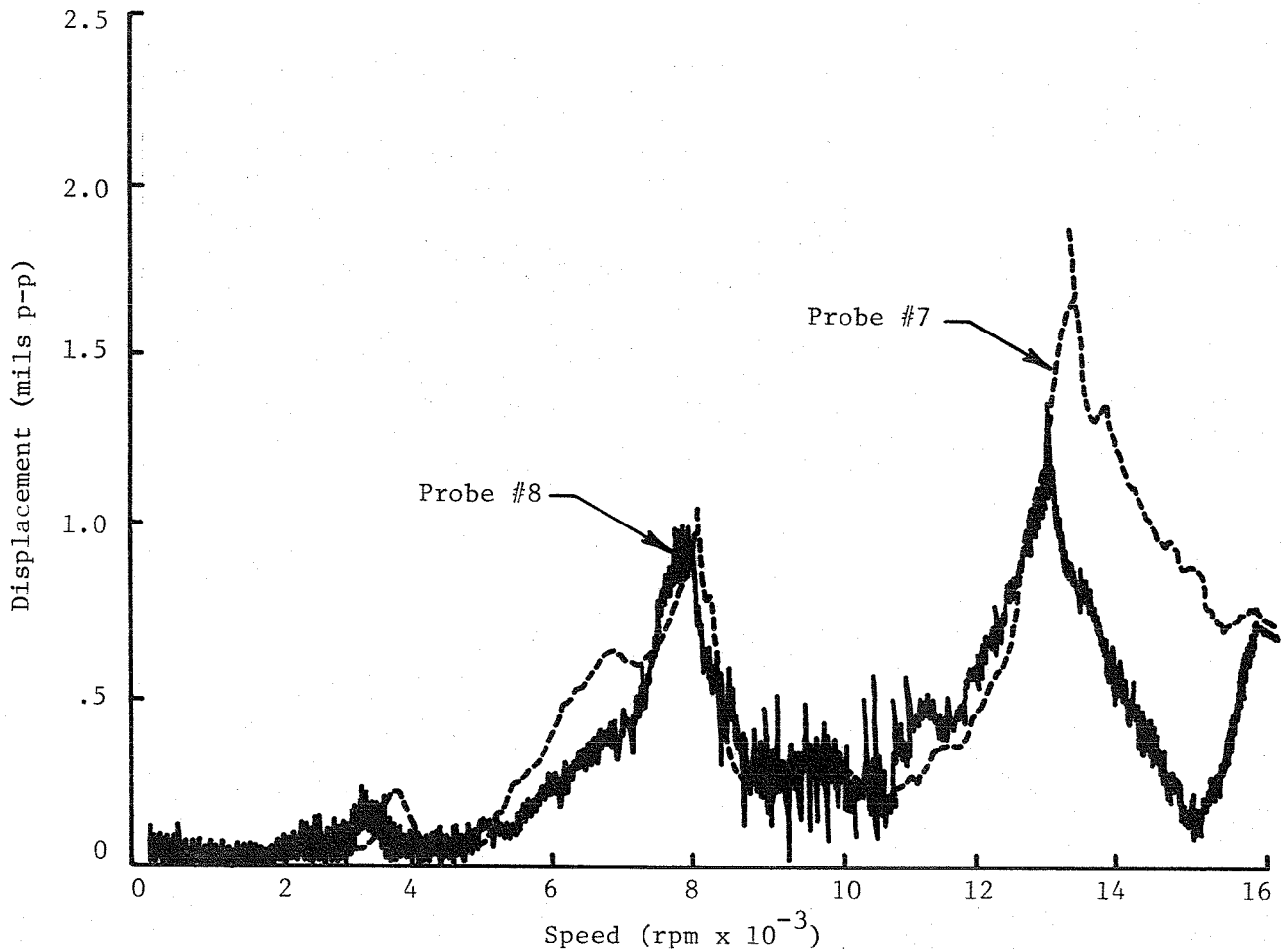

Fig. 43 T-55 Elastomer Damped; 2 gm @ 300° Plane #1, 2 gm @ 120° Plane #3

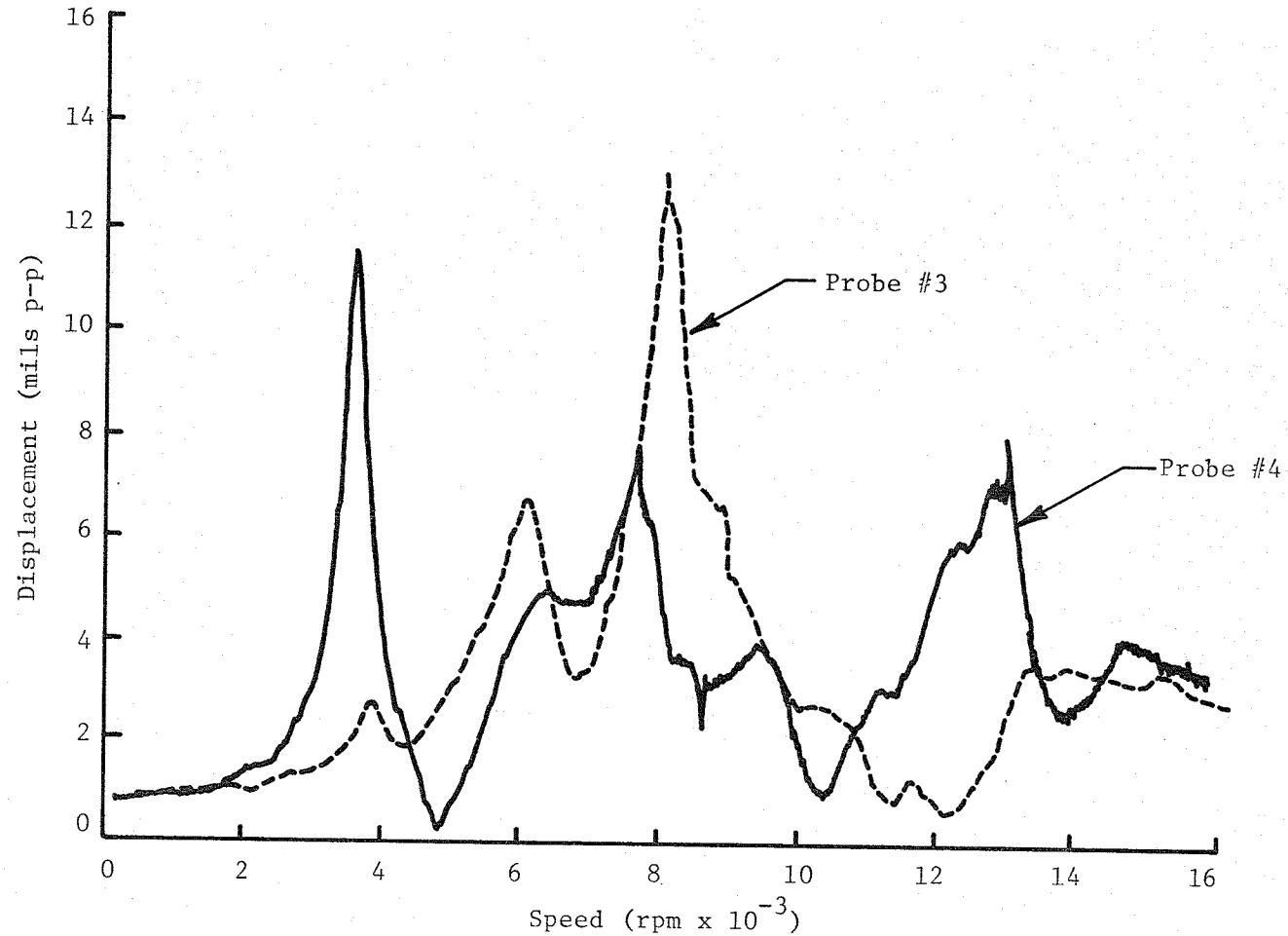

Fig. 44 T-55 Elastomer Damped; 2 gm @ 300° Plane #1, 2 gm @ 120° Plane #3.

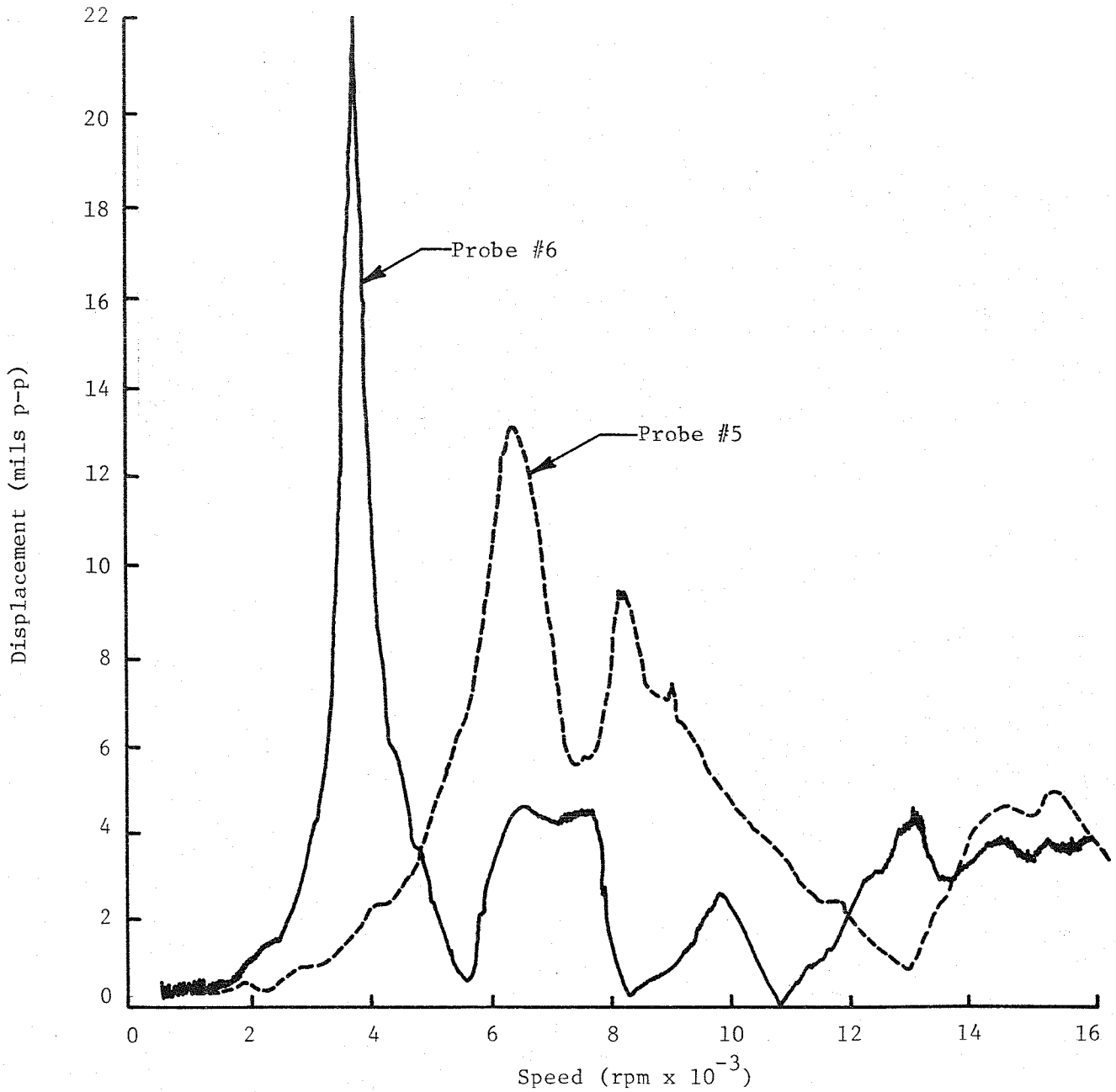

Fig. 45 T-55 Elastomer Damped; 2 gm @ 300° Plane #1, 2 gm @ 120° Plane #3

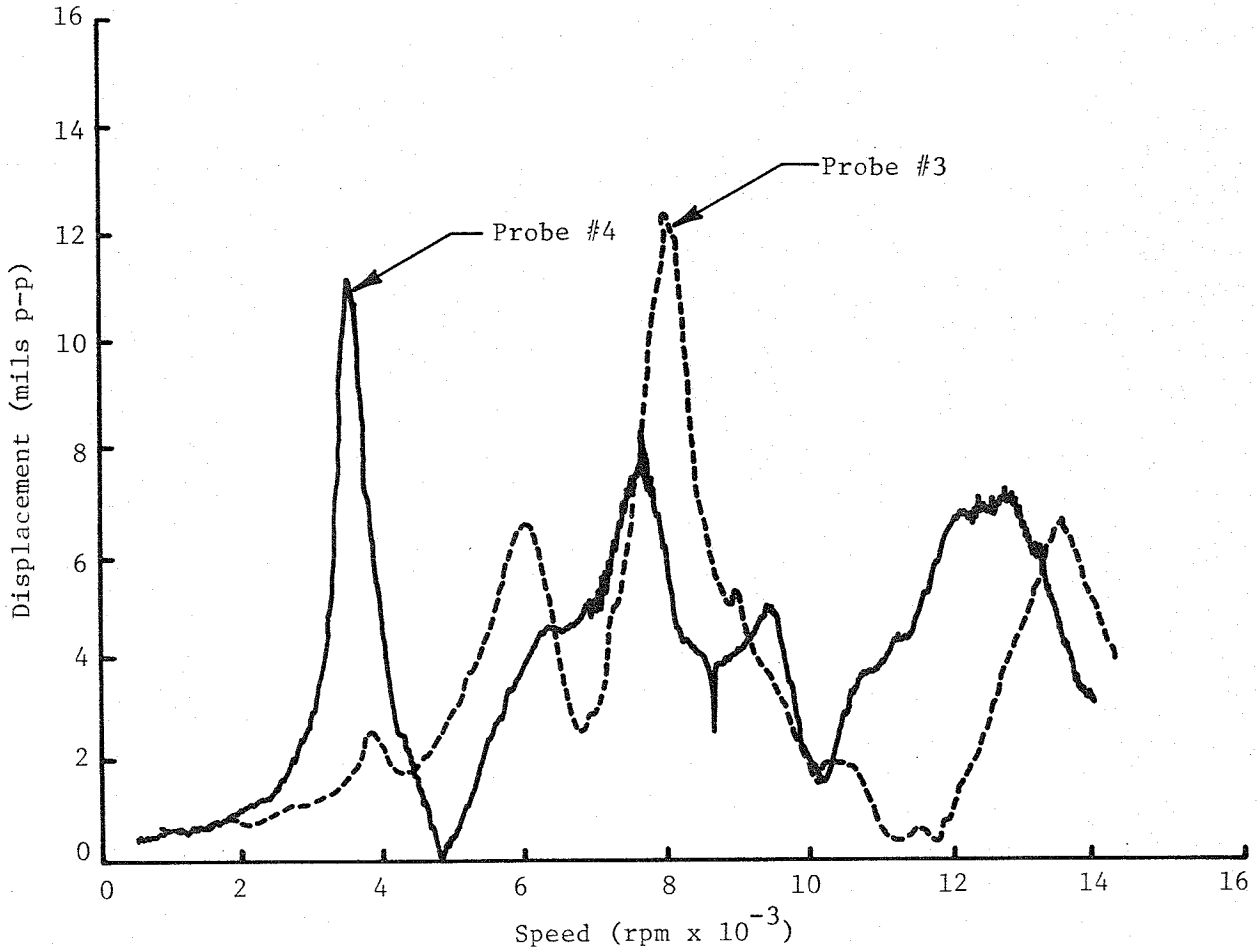

Fig. 46 T-55 Elastomer Damped; 3 gm @ 300° Plane #2

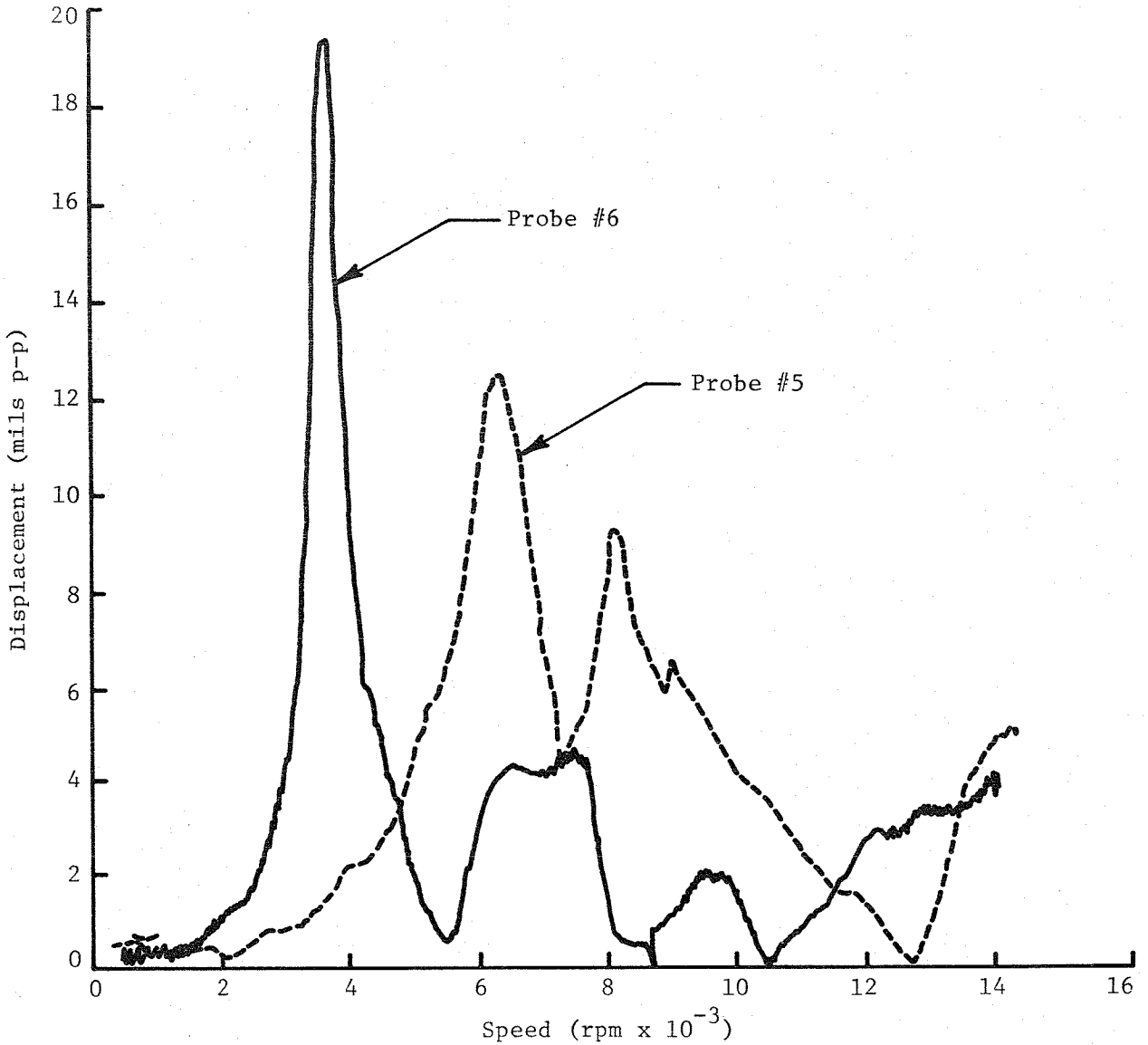

Fig. 47 T-55 Elastomer Damped; 3 gm @ 300° Plane #2

802333

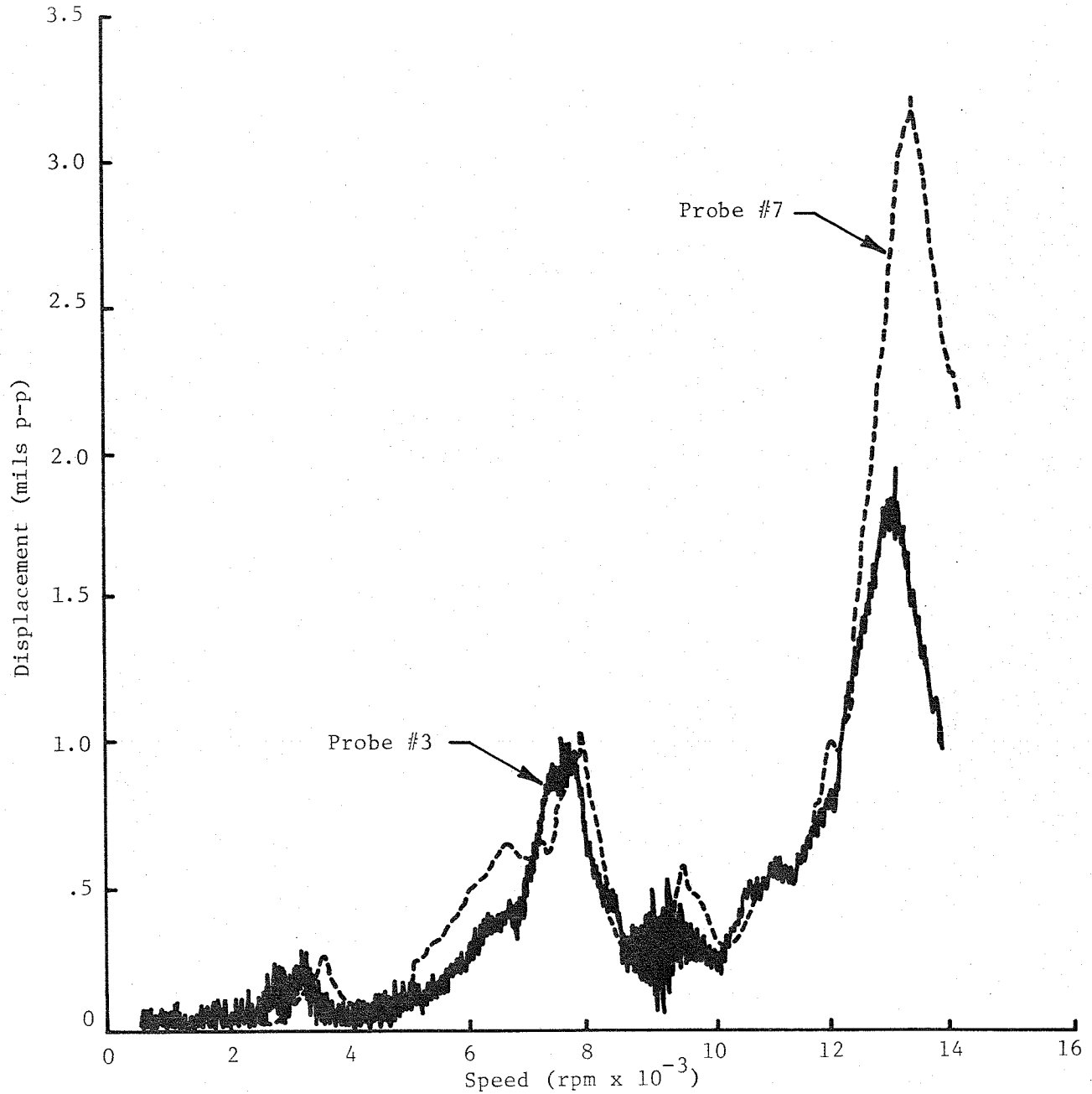

802334

Fig. 48 T-55 Elastomer Damped; 3 gm @ 300° Plane #2

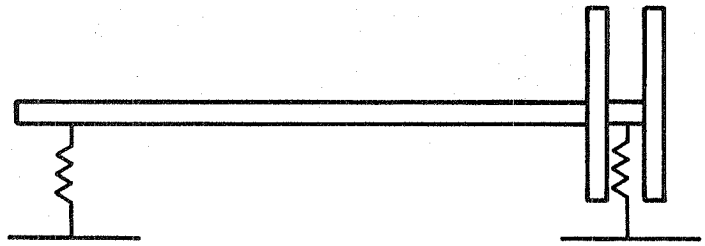

T-55 Schematic

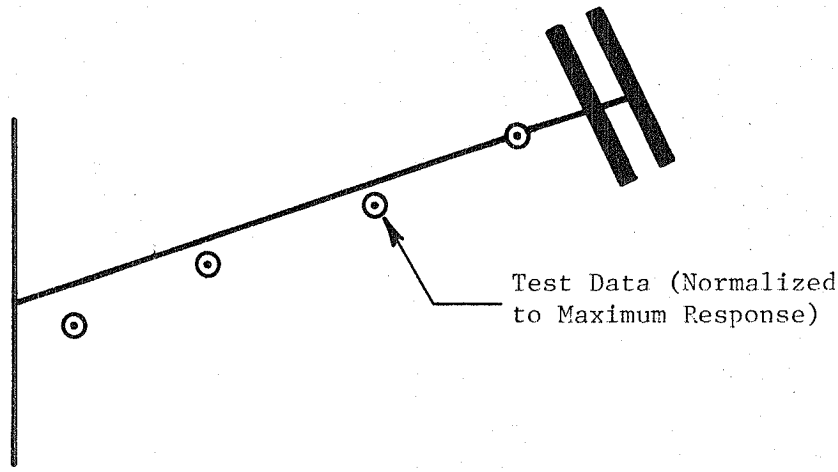

First Critical

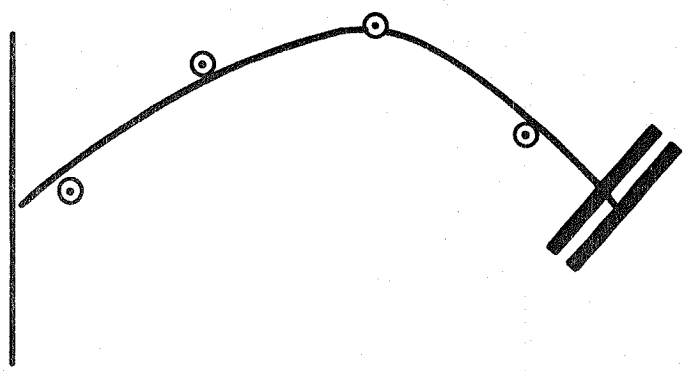

Second Critical

Fig. 49 Comparison of Test Data with Analytic Predicted Modes

802353

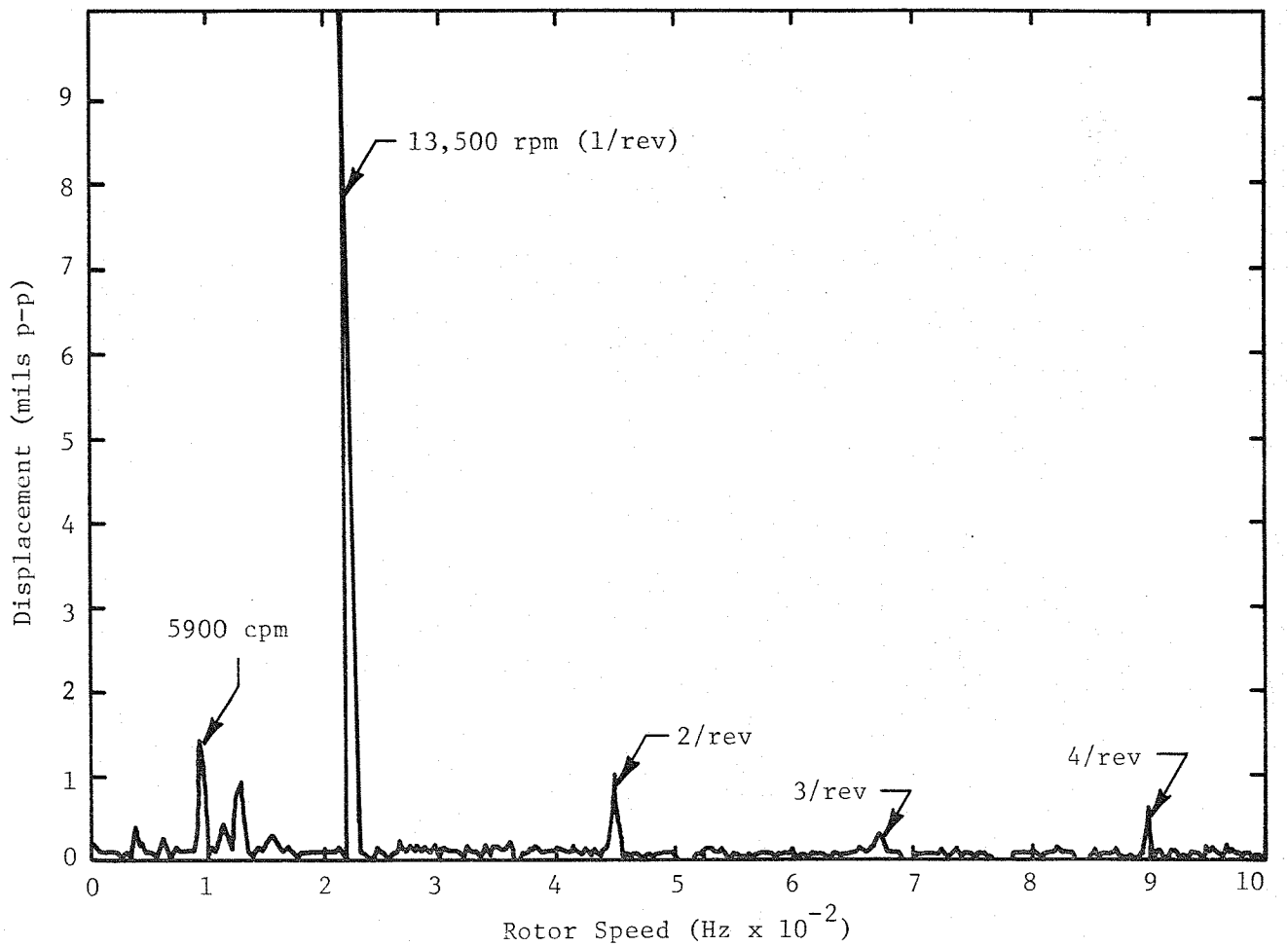

Fig. 50 Spectrum Plot on Elastomer Probe #5; 3 gm @ 300° Plane 1

REFERENCES

1. Tecza, J. A.; Darlow, M. S.; and Smalley, A. J. "Development of Procedures for Calculating Stiffness and Damping of Elastomers in Engineering Applications - Part V." NAS3-18546, February 1979.

2. Chiang, T.; Tessarzik, J. M.; and Badgley, R. H. "Development of Procedures for Calculating Stiffness and Damping Properties of Elastomers in Engineering Applications - Part I: Verification of Basic Methods." NASA Report CR-120905, March 1972.

3. Gupta, P. K.; Tessarzik, J. M.; and Cziglenyi, L. "Development of Procedures for Calculating Stiffness and Damping Properties of Elastomers in Engineering Application, Part II: Elastomer Characteristics at Constant Temperature." NASA Report CR-134704, April 1974.

4. Darlow, M. S., and Smalley, A. J. "Development of Prodcedures for Calculating Stiffness and Damping Properties of Elastomers in Engineering Application, Part IV: Testing of Elastomers Under a Rotating Load." NASA Report CR-135355, November 1977.

5. Rieger, A.; Burgess, G.; and Zorzi, E. "Development of Procedures for Calculating Stiffness and Damping Properties of Elastomers in Engineering Applications, Part VI." NASA Report CR-159838, April 1980.

August 11, 1980

DISTRIBUTION LIST

CR-165138 NAS 3-21263

Recipient	Number of Copies
NASA/Lewis Research Center 21000 Brookpark Road Cleveland, OH 55135	
Attn: R. E. Cunningham, MS 6-1	(15 + reproducible)
J. A. Ziemianski, MS 49-6	1
W. J. Anderson, MS 23-2	1
H. W. Scibbe, MS 23-2	1
L. P. Ludwig, MS 23-2	1
D. Drier, MS 21-4	1
D. Thomas, MS 501-11	1
N. Musial, MS 500-311	1
Report Control Office, MS 5-5	1
Library, MS 60-3	1
Reliability & Quality Assurance Office, MS 500-211	1
Technology Utilization Office, MS 7-3	1
Resources Management Office, MS 3-10	1
NASA Scientific and Technical Information Facility P. O. Box 8757 Balt/Wash Interntaional Airport Maryland 21240 Attn: Accessioning Department	10
NASA Headquarters Attn: REC-1/J. E. Slmomska Washington, DC 20546	1
NASA Headquarters Attn: RF-14/J. Anderson, Program Manager, OEP Washington, DC 20546	1
NASA/Ames Research Center Attn: Library Moffett Field, CA 94035	1
NASA/Hugh L. Dryden Research Center P. O. Box 273 Edwards, CA 93523 Attn: Library	1
NASA/Goddard Space Flight Center Greenbelt, MD 20771 Attn: Library	1
Jet Propulsion Laboratory 4800 Oak Grove Drive Pasadena, CA 91103 Attn: Library	1

Recipient	No. of Copies
NASA/Langley Research Center Langley Station Hampton, VA 23365 Attn: Library	1
NASA/Lyndon B. Johnson Space Center Houston, TX 77058 Attn: Library	1
NASA/Marshall Space Flight Center Marshall Space Flight Center, AL 35812 Attn: Library	1
NASA National Space Technology Laboratories NSTL Station, MS 39529	1
Aerospace Corporation P. O. Box 95085 Los Angeles, CA 91745 Attn: Library	1
AiResearch Manufacturing Co. Phoenix, AZ 85034 Attn: Library	1
AiResearch Manufacturing Co. 9851 Sepulveda Blvd. Los Angeles, CA 90009 Attn: Library	1
Air Force Aero Propulsion Laboratory Wright Patterson AFB, OH 45433 Attn: H. F. Jones R. Dayton	1
Battelle Columbus Labs 505 King Avenue Columbus, OH 43201 Attn: Library	1
Bendix Research Labs Division Detroit, MI 48232 Attn: Library	1
Boeing Co. Aerospace Division P. O. Box 3707 Seattle, WA 98124 Attn: Library	1

Recipient	No. of Copies
Boeing Company Vertol Division P. O. Box 16858 Philadelphia, PA 19142 Attn: Library	1
Continental Aviation and Engineering Corp. 12700 Kercheval Ave. Detroit, MI 48215 Attn: Library	1
Curtiss Wright Corporation Wright Aero Division Main & Passaic Streets Woodridge, NJ 07075 Attn: Library	1
Fafnir Bearing Co. 37 Booth St. New Britain, CT 06050 Attn: R. J. Matt	1
General Electric Company Aircraft Engine Technical Division Bearings, Fuels and Lubricants Evendale, OH 45215 Attn: E. N. Bamberger	1
General Electric Co. Gas Turbine Division Bldg. 53-330 Schenectady, NY 12345 Attn: C. C. Moore	1
General Electric Company Mechanical Technology Laboratory R&D Center Schenectady, NY 12301 Attn: Library	1
General Motors Corporation Allison Division Indianapolis, IN 46206 Attn: Library	1

Recipient	No. of Copies
Hughes Aircraft Corporation Centinda & Teale Avenue Culver City, CA 90230 Attn: Library	1
Industrial Tectonics, Inc. 18301 Santa Fe Avenue Compton, CA 90024 Attn: H. Signer	1
Institute for Defense Analyses 400 Army-Navy Drive Arlington, VA 22202 Attn: Library	1
Lockheed Missiles & Space Co. P. O. Box 504 Sunnyvale, CA 94088 Attn: Library	1
Massachusetts Institute of Technology Cambridge, MA 02139 Attn: Library	1
Mechanical Technology, Inc. 968 Albany-Shaker Rd. Latham, NY 12110 Attn: Library	1
National Science Foundation Engineering Division 1800 G Street, NW Washington, DC 20540 Attn: Library	1
Naval Air Systems Command Washington, DC 20360 Attn: Library	1
Naval Ship Engineering Center Washington, DC 20360 Attn: W. C. Lindstrom (NSC 613D4B)	1
David W. Taylor Naval Ship R&D Center Annapolis Division Annapolis, MD 21402 Attn: Library	1

Recipient	No of Copies
Naval Ship Systems Command Washington, DC 20360 Attn: J. E. Dray SNHIP 6148	1
Rockwell International 6633 Canoga Ave. Canoga Park, CA 91304 Attn: Library	1
Office of Naval Research Arlington, VA 22217 Sttn: S. W. Doroff (Code 438)	1
SKF Industries, Inc. Engineering & Research Ctr. 1100 First Ave. King of Prussia, PA 19406	
Attn: T. Tallian	1
L. Sibley	1
Sundstrand, Denver 2480 W. 70 Avenue Denver, CO 80221 Attn: Library	1
TRW, Inc. 23555 Euclid Avenue Cleveland, OH 44117 Attn: Library	1
TRW Marlin Rockwell Division 402 Chandler St. Jamestown, NY 14701 Attn: Library	1
U. S. Army Engineering R&D Labs Gas Turbine Test Facility Fort Belvoir, VA 22060 Attn: W. Crim	1
Pratt & Whitney Aircraft Division 400 Main St. East Hartford, CT 06108	
Attn: R. Shevchenko	1
P. Brown	1
Dr. F. C.Hsing	1
Library	1

Recipient	No. of Copies
United Aircraft Corporation Sikorsky Aircraft Division Stratford, CT 06497 Attn: L. Burroughs	1
U. S. Army Research & Technology Labs Applied Technology Laboratory Fort Eustis, VA 23604 Attn: Library	1
Rensselaer Polytechnic Institute Mechanics Division Troy, NY 12181 Attn: F. F. Ling	1
Southwest Research Institute P. O. Drawer 28510 San Antonio, TX 78284 Attn: Library	1
Tribon Bearing Co. Division of Pure Carbon Co. 5581 W. 164th St. Brookpark, OH 44132 Attn: D. W. Moyer	1
Materials Science Corp. Blue Bell Office Campus Merion Towel Bldg. Blue Bell, PA 19422 Attn: Library	1
Shaker Research Corp. Northway 10 Executive Park Ballston Lake, NY 12019 Attn: Dr. C. H. T. Pan	1
General Electric Co. P. O. Box 8, Malta Site Schenectady, NY 12301 Attn: Dr. A. J. Martenson	1
Northwestern University Department of Mechanical Engineering & Astronautical Science Evanston, IL 60201 Attn: Dr. R. Burton Dr. H. S. Cheng	1 1

Recipient	No. of Copies
Thiokol Corporation P. O. Box 524 Brigham City, UT 84302 Attn: Bliss Law, MS 308	1
Teledyne CAE, Turbine Engines 1330 Laskey Rd. Toledo, OH 43697 Attn: R. Beck	1
Ingersoll-Rand Corp. Phillipsburg, NJ 08865 Attn: R. G. Kirk	1
Deposits & Composites, Inc. 318 Victory Dr. Herndon Industrial Park Herndon, VA 22070 Attn: R. E. Engdohl	1
Williams Research Corporation 2280 W. Maple Rd. Walled Lake, MI 48088 Attn: G. Rourk	1
University of Virginia School of Engineering & Applied Science Charlottesville, VA 22901 Attn: Dr. E. J. Gunter	1
Chalk River Nuclear Labs Chalk, Ontario, Canada KOJIJO Attn: Dr. R. Metcalf	1

End of Document